Theoretical and Spectroscopic Studies of the Structure-Property Relationships in the Mono-substituted (η^6-Arene)chromiumtricarbonyl Complexes

by

John L. Payton

Submitted in Partial Fulfillment of the Requirements

for the Degree of

Master of Science

in the

Chemistry

Program

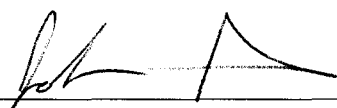YOUNGSTOWN STATE UNIVERSITY

December, 2004

Theoretical and Spectroscopic Studies of the Structure-Property Relationships in the Mono-substituted (η^6-Arene)chromiumtricarbonyl Complexes
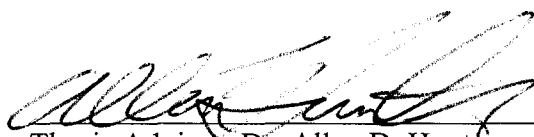
by

John L. Payton

I hereby release this thesis to the public. I understand this thesis will be housed at the Circulation Desk of the University library and will be available for public access. I also authorize the University or other individuals to make copies of this thesis as needed for scholarly research.

Signature:

_____   12/4/04
Student, John L. Payton   Date

Approvals:

_____   12/1/04
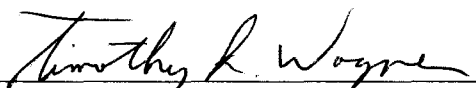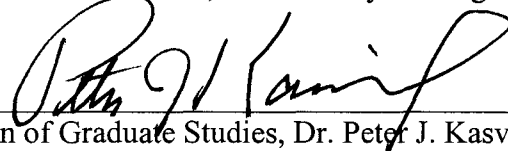Thesis Advisor, Dr. Allen D. Hunter   Date

_____   12/1/04
Committee Member, Dr. Howard D. Mettee   Date

_____   12/1/04
Committee Member, Dr. Timothy R. Wagner   Date

_____   12/3/04
Dean of Graduate Studies, Dr. Peter J. Kasvinsky   Date

Abstract

Over the decades there have been many classical studies done on the "three legged piano stool" complexes (η^6-arene)Cr(CO)$_3$. However, these complexes still have a number of questions to be answered in the matter of their structure-property relationships. One of these problems is the underlying reason for observed structural distortions in the planarity of the chromium tricarbonyl substituted arenes complexes. It has been shown that these distortions are correlated to the π-donor/acceptor abilities of the substituent(s) on the arene. We have continued these studies for a series of model mono-substituted (η^6-arene)Cr(CO)$_3$ complexes via their photoelectron spectral and molecular orbital characterizations. Our results are in general agreement with past qualitative reports. In particular, the arene-chromium bond seems to be strengthened by π-acceptors and weakened by π-donors which is in agreement with the elementary valence bond arguments.

Acknowledgments

First, I dedicate this thesis to my grandmother, Virginia Paisley, who past away during my studies for my masters degree. I also dedicate this thesis to my fiancée, Evelyn Lazich, and to my father and mother, Ray and Joan Payton.

I would like to thank my advisor, Dr. Allen D. Hunter, for his guidance and assistance throughout my studies and research at Youngstown State University. I would also like to thank our collaborators, Dr. Nadine E. Gruhn and Dr. Barry L. Westcott, for their editorial comments and assistance with the data contained in this thesis. In addition, I would like to thank my thesis committee, Dr. Howard D. Mettee and Dr. Timothy R. Wagner, for their editorial comments on this thesis and assistance throughout my studies at Youngstown State University. I am also grateful for all the help I have received from the Hunter Group, and a thanks to Dr. Matthias Zeller and Cynthia Perrine for the crystallographic structures.

Finally, I would like to thank God, my family, and my friends for their support and guidance. A very special thanks to my fiancée whose love, affection, and support have helped me in ways I can't describe.

Table of Contents

List of Figures

List of Tables

List of Equations

List of Abbreviations

A	π-acceptor substituent
Å	Angstrom
arene	C_6H_6, C_6Me_6, and C_6H_5X where X = CF_3, F, CO_2Me, Me, OMe, NMe_2
aryl	Arene
AM1	Austin Model
B3LYP	Becke Three Parameter Hybrid Functionals and Lee, Yang, and, Parr Correlation Functional
°C	Degrees Celsius
CF_3	Trifluoromethyl substituent
cm	Centimeters
cm^{-1}	Reciprocal centimeters, wavenumbers
CO	Carbonyl ligand
CO_2Me	Carbomethoxy substituent
Corrl	Correlation Coefficient
COD	Coefficient of determination
CPU	Central Processing Unit
D	π-donor substituent
DFT	Density Functional Theory
d_{Cr-CO}	Chromium-Carbonyl Bond Length
d_{CrC-O}	Carbon-Oxygen Bond Length

δ	Delta Bond
δ	Chemical shift (as in NMR spectroscopy)
δ_{ipso}	Chemical shift for *ipso*-carbon
δ_{ortho}	Chemical shift for *ortho*-carbon
δ_{meta}	Chemical shift for *meta*-carbon
δ_{para}	Chemical shift for *para*-carbon
δ_{CO}	Chemical shift for carbonyl ligands
$\Delta\pi$	Net π-Donor/Acceptor Parameter
ε	Eigenvalue
E	Energy of an orbital
$E^{o'}$	Formal Redox Potential
eV	Electron Volts
$E[\rho]$	Exact ground-state electron energy
$E_T[\rho]$	Kinetic energy term
$E_V[\rho]$	Potential energy term
$E_J[\rho]$	Coulomb energy term
$E_{XC}[\rho]$	Electron exchange-correlation energy term
E_x	Exchange Functionals
E_c	Correlation Functionals
F	Fluoro substituent
f_i	Fock operator
ϕ	Spinorbital

Fp	$(\eta^5 C_5 H_5)Fe(CO)_2$
FTIR	Fourier transform infrared
FW	Formula weight
g	Grams
GTO	Gaussian-type orbitals
H	Hamiltonian
h_i	Core hamiltonian
HF	Hartree-Fock
HOMO	Highest occupied MO
$h\nu$	Photon Energy
Hz	Hertz
IE	Ionization energy
IR	Infrared (as in spectroscopy)
$J_u(i)$	Exchange operator
K^i_{CO}	Interaction stretching force constant
K_{CO}	Stretching force constant
$K_u(i)$	Coulomb operator
L	Ligand
LUMO	Lowest unoccupied MO
LYP	Lee, Yang, and, Parr
μ	Mu
M	Metal atom (Cr, Mo, W) or Molecule
Mb	Megabytes

Me	Methyl substituent
Me$_6$	Hexamethyl substituent
MHz	Megahertz
mL	Milliliters
mmol	Millimoles
M$_n$	Molecular weight
MO	Molecular orbital
mol	Mole
MPPT	Møller-Plesset perturbation theory
MP2	Second order Møller-Plesset
MP4	Fouth order Møller-Plesset
NMe$_2$	Dimethylamine substituent
η	Eta
NMR	Nuclear magnetic resonance
OMe	Methoxy substituent
π	Bonding pi orbital
π^*	Anti-bonding pi orbital
ψ^o	Approximate wavefunction
ψ	True wavefunction
p	*Para*
PES	Photoelectron spectroscopy
ppm	Parts per million
PR$_3$	Phosphine or Phosphite

PM3	Parameterization Method Three
ρ	Charge Density
R	Alkyl or aryl group
RAM	Random Access Memory
rt	Room temperature
σ	Bonding sigma orbital
σ_i	Inductive Parameter
SCF	Self-constant field
SE	Semiempirical methods
SEC	Standard Calomel Electrode
STO	Slater-type orbitals
Σ	Sum of
T	Temperature
THF	Tetrahydrofuran
V	Volts
V_{XC}	Electron exchange-correlation potential
VMN	Vosko, Wilk, and, Nusair correlation functional III
ν	Stretching frequency (as in IR spectroscopy)
ν''	Ground Vibrational State
ν'	Excited Vibrational State
ν_{as}	Asymmetric stretching frequency (as in IR spectroscopy)
ν_{sy}	Symmetric stretching frequency (as in IR spectroscopy)

ν_{CO} (E)	Carbonyl stretching frequency of E symmetry
ν_{CO} (A$_1$)	Carbonyl stretching frequency of A$_1$ symmetry
in vacuo	High vacuum manifold
X	Halogen

Chapter One - Introduction

Section One

Structure and Properties of (η^6-arene)Cr(CO)$_3$ Complexes

There have been many classical studies done on (η^6-arene)Cr(CO)$_3$ complexes that have produced a wealth of information about their reactivity, bonding, spectra, and structure.[1-32] However, many questions still remain about the (η^6-arene)Cr(CO)$_3$ complex and its derivatives, particularly relating to a quantitative understanding of their structure-property relationships. One example of this is the fundamental reason for observed structural distortions in the substituted arene (η^6-arene)Cr(CO)$_3$ complexes. It has been empirically demonstrated that these distortions are strongly correlated to the π-donor/acceptor abilities of the substituent(s).[1] We hope to gain quantitative insight into the origins of these structural distortions by studying the photoelectron spectra and calculated electronic structures of a series model mono-substituted (η^6-arene)Cr(CO)$_3$ complexes.

1. Synthesis of (η^6-arene)Cr(CO)$_3$ complexes

A wide variety of different routes have been employed for the synthesis of the congeneric (η^6-arene)M(CO)$_3$ (where M = Cr, Mo, and W) complexes.[1-4,6] The greatest range of different synthetic routes and different arenes have been used for chromium. In contrast, the molybdenum and tungsten complexes are mainly restricted to arenes having

no heteroatom substituents. Some of these syntheses involve the direct reaction of the M(CO)$_6$ starting materials with the appropriate arene, *i.e.*,

$$\text{arene} + \text{M(CO)}_6 \longrightarrow (\eta^6\text{-arene})\text{M(CO)}_3$$
$$\text{M = Cr, Mo, W}$$
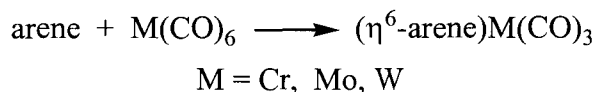
Equation 1.1.1 First general synthetic pathway for (η^6-arene)M(CO)$_3$ complexes.

These reactions involve a rate-determining dissociation of a carbonyl ligand from the metal followed by rapid initial arene coordination (i.e. in an η^2-fashion). [Note: the symbol η^n implies that n atoms on the ligand are coordinated to the metal center.] The subsequent loss of two additional carbonyl ligands and the concomitant slippage of the arene to first η^4- and then η^6-coordination give the observed products. To obtain acceptable overall reaction rates, this rate-determining step must have its rate accelerated. This can be done by several methods, including: heating these reactions to temperatures around or above 100 °C, irradiating the reaction mixtures with ultra violet light, or treating the reaction mixtures with ultrasonic energy. The thermal reactions can be carried out in neat arene solvents for inexpensive liquid aromatics,[2d] but, more commonly, they are carried out in a high boiling "inert" solvent. Although high boiling alkanes have been used, ethers such as di-*n*-butyl ether (often containing about 10% THF, see below), diglyme, and dioxane generally appear to be superior for chromium

complexes. They give cleaner reactions and shorter reaction times. For this reason pure or mixed ether solvents have been most widely employed.

A related route involves the displacement (generally thermal) of three equivalents of a ligand more weakly bound than the carbonyl group from the $M(CO)_3(ligand)_3$ complexes, *i.e.*,

$$arene \ + \ M(CO)_3(ligand)_3 \ \longrightarrow \ (\eta^6\text{-arene})M(CO)_3$$
$$M = Cr, \ Mo, \ W$$
$$ligand = NH_3, \ pyridine, \ arene, \ etc.$$
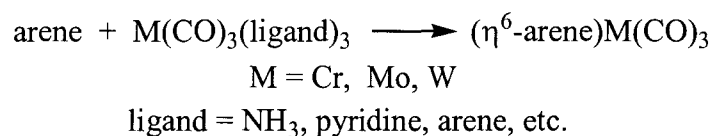
Equation 1.1.2 Second general synthetic pathway for $(\eta^6\text{-arene})M(CO)_3$ complexes.

Examples of the displaced ligands include nitriles, amines, and more weakly bound arenes (especially naphthalene).

For chromium, an especially widely used variant of these reactions is to combine the *in situ* generation of the $M(CO)_3(solvate)_3$ complexes with the arene complexation step, *i.e.*,

$$arene \ + \ active \ solvent \ + \ Cr(CO)_6 \ \longrightarrow \ (\eta^6\text{-arene})Cr(CO)_3$$
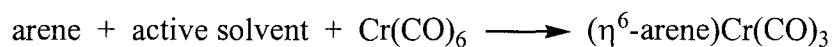
Equation 1.1.3 Third general synthetic pathway for $(\eta^6\text{-arene})Cr(CO)_3$ complexes.

The reaction with a solvent mixture of di-*n*-butyl ether and about 10% THF has proven to be particularly useful. The di-*n*-butyl ether provides a high boiling (*i.e.* 141°C) inert solvent from which almost all of the derivatives readily precipitate at room temperature. The THF provides the transient coordinating ligands, increases the reactant and product solubilities, decreases the reaction temperature enough to minimize thermal decomposition, and washes the sublimed $Cr(CO)_6$ back into the reaction flask. Another particularly useful ether solvent is dioxane which fulfills both functions simultaneously. Other commonly used ether solvents such as diglyme and tetraglyme can also be used. Indeed, this hybrid route has been used to prepare over 100 different (η^6-arene)$Cr(CO)_3$ derivatives.[1,6]

Whichever the route chosen for the synthesis, the reaction progress needs to be monitored to determine when it is completed. This is usually best done by monitoring the reactions by IR where one can observe the carbonyl band due to $M(CO)_6$ at about 1980 cm^{-1} being replaced by the two or three carbonyl bands characteristic of the target (η^6-arene)$Cr(CO)_3$ complexes.

2.   Reactions of (η^6-arene)Cr(CO)₃ complexes

The reactions of (η^6-arene)$Cr(CO)_3$ complexes can be divided into several broad categories, including the following: reactions which break the arene-chromium bond, reactions which break chromium-carbonyl bonds, and reactions which change the structure of the coordinated arenes. Heating these complexes or treating them with strong oxidants (e.g. O_2, I_2, or Ce^{IV} salts) in solution results in the release of the arene ligand, *i.e.*

$$(\eta^6\text{-arene})Cr(CO)_3 + \text{oxidant} \longrightarrow \text{arene} + \text{inorganic residues}$$
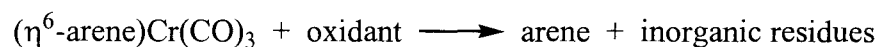
Equation 1.1.4 Oxidation reaction for $(\eta^6\text{-arene})Cr(CO)_3$ complexes.

Similarly, the addition of strongly Lewis basic ligands like phosphines or pyridines releases the arene and produces new organometallic complexes, *i.e.*,

$$(\eta^6\text{-arene})Cr(CO)_3 + 3\,PR_3 \longrightarrow Cr(CO)_3(PR_3)_3$$
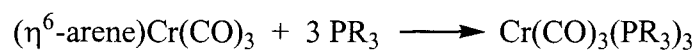
Equation 1.1.5 Phosphine substitution reaction for $(\eta^6\text{-arene})Cr(CO)_3$ complexes.

Photolysis of these complexes in the presence of Lewis bases such as olefins or phosphines results in the replacement of a carbonyl ligand, *e.g.*,

$$(\eta^6\text{-arene})Cr(CO)_3 + PR_3 + h\nu \longrightarrow (\eta^6\text{-arene})Cr(CO)_2(PR_3) + \text{arene}$$
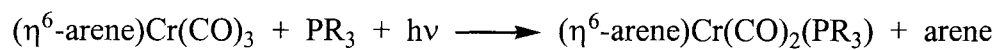
Equation 1.1.6 Photolysis reaction for $(\eta^6\text{-arene})Cr(CO)_3$ complexes.

Finally, the coordinated ligands are susceptible to the common organic reactions observed for their uncomplexed analogues, including: Friedel Crafts alkylation and acylation, acylation of amine substituents, alkylation of phenol hydroxy substituents, and deprotonation by strong bases, *e.g.*,

$$(\eta^6\text{-aryl-H})Cr(CO)_3 + R\text{-}X + AlX_3 \longrightarrow (\eta^6\text{-aryl-R})Cr(CO)_3$$

$$(\eta^6\text{-aryl-H})Cr(CO)_3 + R\text{-}C(O)Cl + AlCl_3 \longrightarrow (\eta^6\text{-aryl-C(O)R})Cr(CO)_3$$

$$(\eta^6\text{-aryl-NH}_2)Cr(CO)_3 + CH_3C(O)Cl + base \longrightarrow (\eta^6\text{-aryl-NH-C(O)CH}_3)Cr(CO)_3$$

$$(\eta^6\text{-aryl-OH})Cr(CO)_3 + RX + base \longrightarrow (\eta^6\text{-aryl-OR})Cr(CO)_3$$

$$(\eta^6\text{-aryl-H})Cr(CO)_3 + \text{strong lithium base} \longrightarrow (\eta^6\text{-aryl-Li})Cr(CO)_3$$
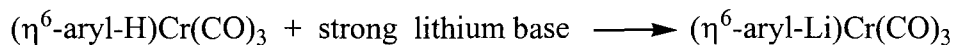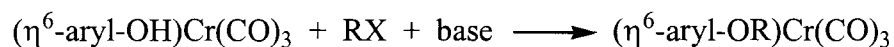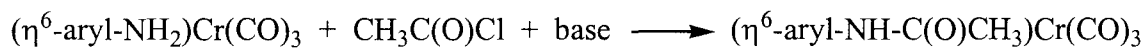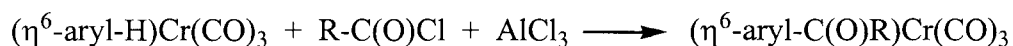
Equations 1.1.7 - 11 Reactions with the arene ligands of $(\eta^6\text{-arene})Cr(CO)_3$ complexes.

The latter organochromium/organolithium reagents can then react with a wide range of electrophiles, i.e.

$$(\eta^6\text{-aryl-Li})Cr(CO)_3 + CO_2 \longrightarrow (\eta^6\text{-aryl-}(CO_2Li))Cr(CO)_3$$

$$(\eta^6\text{-aryl-Li})Cr(CO)_3 + RX \longrightarrow (\eta^6\text{-aryl-R})Cr(CO)_3$$

$$(\eta^6\text{-aryl-Li})Cr(CO)_3 + R_2CO \longrightarrow (\eta^6\text{-aryl-}(CR_2OLi))Cr(CO)_3$$
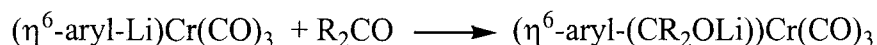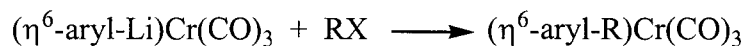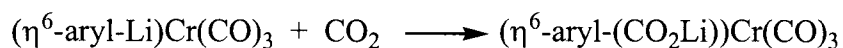
Equation 1.1.12 - 14 Reactions of organolithium derivatives of $(\eta^6\text{-arene})Cr(CO)_3$ complexes with electrophiles.

These complexes are also prone to reactions involving the replacement of halide substituents by nucleophiles in nucleophilic aromatic substitution, NAS, and hydrogen substituents by electrophiles in electrophilic aromatic substitution, EAS, reactions, i.e.

$$(\eta^6\text{-aryl-X})Cr(CO)_3 + \text{nucleophile}^- \longrightarrow (\eta^6\text{-aryl-nucleophile})Cr(CO)_3$$

$$(\eta^6\text{-aryl-H})Cr(CO)_3 + \text{electrophile}^+ \longrightarrow (\eta^6\text{-aryl-electrophile})Cr(CO)_3$$
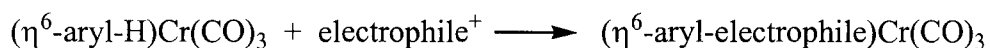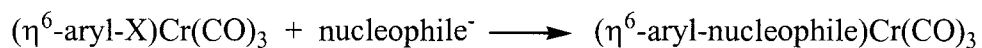
Equation 1.1.15 Nucleophilic and electrophilic aromatic substitution reactions.

Since the $Cr(CO)_3$ group is a net electron withdrawing group similar in electron withdrawing ability to a NO_2 group, the $Cr(CO)_3$ group on the ring enhances NAS and inhibits EAS. These reactions often occur with greater stereo control than is possible on uncomplexed arenes. This is partially due to the fact that complexation of a pro-chiral

arene to a $Cr(CO)_3$ group makes the molecule chiral and partially due to the fact that the $Cr(CO)_3$ group blocks one face of the arene. Using combinations of these methods, organic chemists can coordinate an arene to the $Cr(CO)_3$ group, chemically modify its structure in unusual and useful ways, and then cleave it from the chromium center to give a new aromatic compound.

3.   Physical Properties of (η^6-arene)$Cr(CO)_3$ Complexes

The physical properties of these complexes have been thoroughly documented in the literature. They range in color from pale yellow through orange to almost red with the most electron poor arenes generally giving the most highly orange/red colored materials. Interestingly, solutions of some of these complexes are thermochromic. That is, they reversibly change color as a function of temperature. The most common color change seen is from yellow or pale orange solutions at room temperature to dark orange or even red solutions at elevated temperatures. These compounds are all solids at ambient temperatures and generally have sufficiently high vapor pressures that they can be sublimed under a good vacuum. Under an inert atmosphere, many display reversible melting points in addition to the thermal decomposition observed at higher temperatures. At ambient temperatures, the derivatives of benzene are all thermally stable for an indefinite period if they are sufficiently pure. As noted above, the derivatives of fused ring aromatics are substantially less thermally stable. For examples of transition metal organometallic complexes, which are famous for their air sensitivity, this class of complexes is remarkably air stable in the solid state. Thus, pure single crystalline samples are normally stable in air for months or years while powdered samples are air

stable for hours, days, or, often, years. As one would expect, these materials are much less air stable in solution. Never-the-less, most derivatives are air stable in solution for minutes or hours. Because of this, much of their purification can often be carried out in air, and their IR and NMR spectra can routinely be collected in air if one moves quickly. [Note: These class of complexes are quite air sensitive at elevated temperatures, and therefore their syntheses need to be carried out under anaerobic conditions.] The $Cr(CO)_3$ group in these complexes strongly increases the polarities of complexes derived from non- or weakly-polar arenes (*e.g.*, for alkyl and siloxy aromatics). In general, these complexes are most soluble in polar organic solvents such as dichloromethane, acetone, and tetrahydrofuran, and are less soluble in non-polar organic solvents and in strongly hydrogen-bonding solvents such as methanol and water. In this context, it is noteworthy that these complexes don't appear to be particularly water sensitive. Therefore, rigorous drying of solvents used to prepare, chromatograph, and crystallize these materials is generally not required.

4.   Bonding in (η^6-arene)Cr(CO)$_3$ Complexes

Organometallic complexes have been prepared for all of the transition metals and for a large variety of ligands.[1-7] For "well behaved" organometallics (e.g. those of the mid-transition series in low oxidation states), the metal-ligand interactions can be understood in terms of several elementary approaches, including the following: Lewis acid-base interactions, the eighteen electron rule, valence bond theory, and localized molecular orbital approaches (e.g. the Dewar/Chatt/Duncanson model). Each of these models has advantages and disadvantages as tools for rationalizing aspects of the

observed structures and properties. Even though these descriptions are not as rigorously correct as the results of full molecular orbital analyses, their simplicity and surprisingly good explanatory powers have resulted in their being the most widely employed bonding descriptions used by practicing organometallic chemists.

The structures of organometallics have been established by a variety of different techniques ranging from elementary isomer number ideas through indirect spectroscopic means to direct methods such as X-ray crystallography. It is to these experimental three-dimensional structures that one tries to fit a bonding model. Remember, it is the observed numbers of ligands, bond angles, bond lengths, spectra, etc., which remain constant while we jump back and forth between different bonding models trying to find a satisfactory answer to our structural questions.

The most elementary bonding model is derived from Lewis acid-base theory. In this model, the metal-ligand bond is considered to arise from dative interactions between pair(s) of electrons on the ligand(s) and Lewis acid sites on the central metal atom. In terms of this model, the $(\eta^6$-arene$)Cr(CO)_3$ complex has six such dative interactions. The first three take the form of single lone pairs being donated from the carbon atoms of the carbonyl ligands to chromium. The final three take the form of the three pairs of electrons in the three π-bonds of the arene being donated to chromium.

The eighteen electron rule is an empirical observation that states that complexes of the mid-transition elements in low formal oxidation states will be most stable when they have a total of eighteen valence electrons associated with the central metal atom. This empirical rule is related to the fact that such organometallics have a stable closed shell noble gas configuration. An η^6-bonded arene can donate a total of six electrons to

chromium while each carbonyl can donate two. Since this chromium atom is in the neutral oxidation state, it is said to have a d^6 configuration and is, therefore, said to contribute six electrons to the valence electron count. Thus, the $(\eta^6\text{-arene})Cr(CO)_3$ complex has an eighteen electron configuration $(6 + 3(2) + 6 = 18)$ and is expected to be relatively stable.
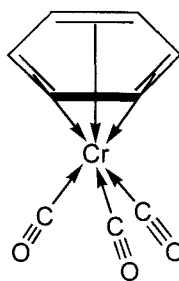
Figure 1.1.1 The electron count for the chromium complex.

The bonding between the carbonyl ligands and the chromium center can better be described in terms of complementary valence bond and molecular orbital bonding models. In the valence bond model, the metal-carbonyl interaction is explained in terms of two resonance forms, *i.e.*, (**Figure 1.1.2**)

Cr—C≡O: ⟷ Cr=C=O:

Resonance Form I   Resonance Form II
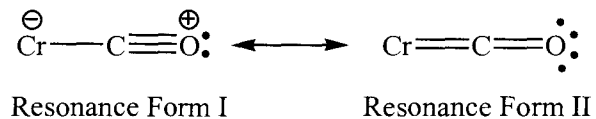
Figure 1.1.2 Resonance forms of Cr-C-O Bonds.

With electron rich metal centers, the second resonance form predominates, and the observed Cr-C bond order is relatively high (*i.e.,* approaching two), and the C-O bond order is relatively low (*i.e.,* approaching two) corresponding to relatively short Cr-C bonds and long C-O bonds. With electron poor metal centers, the first resonance form predominates, and the observed Cr-C bond order is relatively low (*i.e.,* nearer to one), and the C-O bond order is relatively high (*i.e.,* nearer to three) corresponding to relatively long Cr-C bonds and short C-O bonds.

From a molecular orbital perspective, this chromium-carbonyl interaction is explained as having two components, *i.e.,* (**Figure 1.1.3**)

σ-Symmetry Interaction: σ-Donation

π-Symmetry Interaction: π-Back Donation

Figure 1.1.3 Chromium-carbonyl interaction: σ-Donation and π-Back Donation.
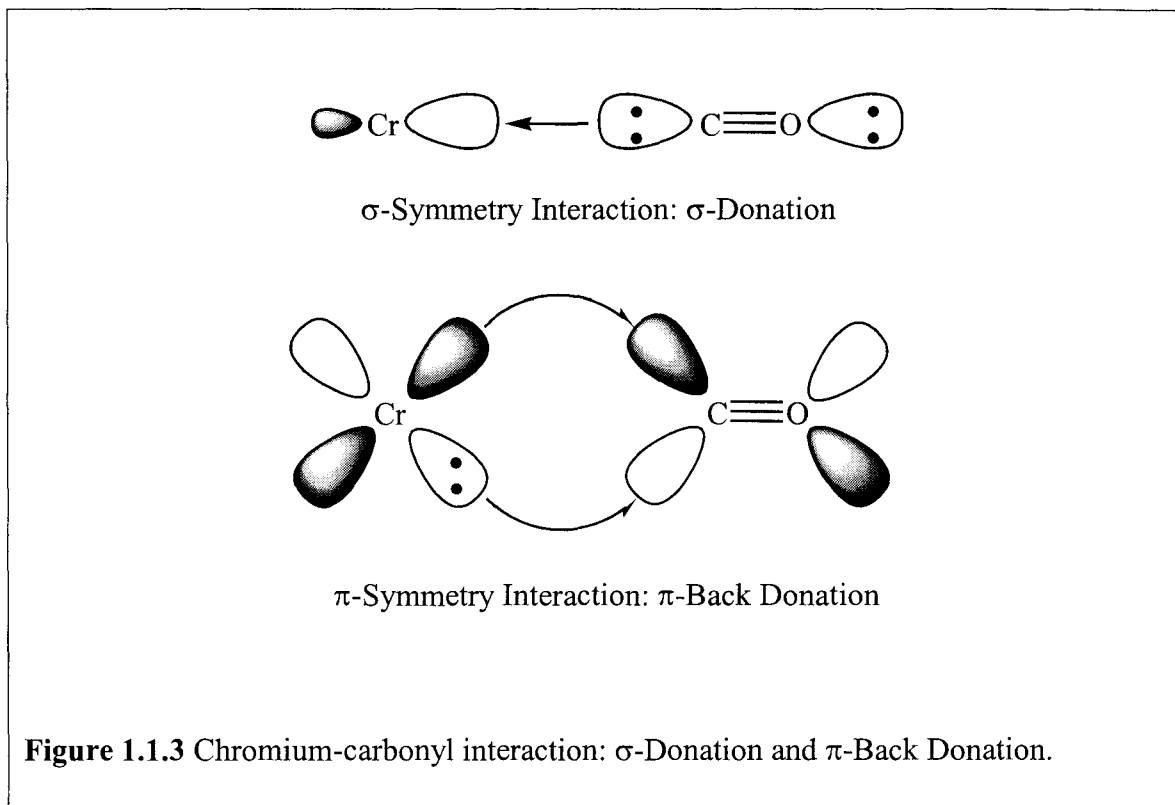
In the σ-symmetry component, there is σ-donation from a filled σ-symmetry orbital on the carbonyl (*i.e.*, approximately carbon sp in character) to a vacant σ-symmetry orbital on the chromium (*i.e.*, approximately metal d^2sp^3 in character). In the two π-symmetry components (one in the xz and one in the yz plane), there is π-back donation from two filled π-symmetry orbitals on the chromium (*i.e.*, approximately metal d_{xz} or d_{yz} in character) to a pair of vacant π-symmetry orbitals on the carbonyl (*i.e.*, approximately the pair of CO π* anti-bonding orbitals in the xz and yz planes, respectively). These σ-bonding and π-back bonding interactions are synergic. By this we mean that they mutually reinforce one another (*i.e.*, the whole being greater than the sum of the parts). With electron rich metal centers, σ-donation is mildly reduced, and π-back donation is strongly enhanced. This makes the net Cr-C bond order relatively high (*i.e.*, nearing two)

and the C-O bond order relatively low (*i.e.,* nearing two) corresponding to relatively short Cr-C bonds and long C-O bonds (**Figure 1.1.2 Resonance Form II**). With electron poor metal centers, σ-donation is mildly enhanced, and π-back donation is strongly reduced. As a result, the net Cr-C bond order is relatively low (*i.e.,* closer to one), and the C-O bond order is relatively high (*i.e.,* closer to three) corresponding to relatively long Cr-C bonds and short C-O bonds (**Figure 1.1.2 Resonance Form I**). Overall, the direction of net electron transfer is from the chromium center to the carbonyl ligand. Carbonyl ligands are therefore referred to as π-acid ligands.

The bonding between the arene ligands and the chromium center can also be described in terms of complementary valence bond and molecular orbital bonding models. Because of the presence of six bonding atoms and six donor electrons on the arene, these models are significantly more complex than those for carbonyls. However, they are qualitatively similar to those for alkene-metal interactions, which are much simpler to understand in detail. For alkenes, the valence bond model describes the bonding in terms of two resonance components, *i.e.,* (**Figure 1.1.4**)

Resonance Form I   Resonance Form II

"Alkene Like"   "Metallo-Cyclopropane Like"

Figure 1.1.4 Metal-alkene interaction in Valence Bond terms.
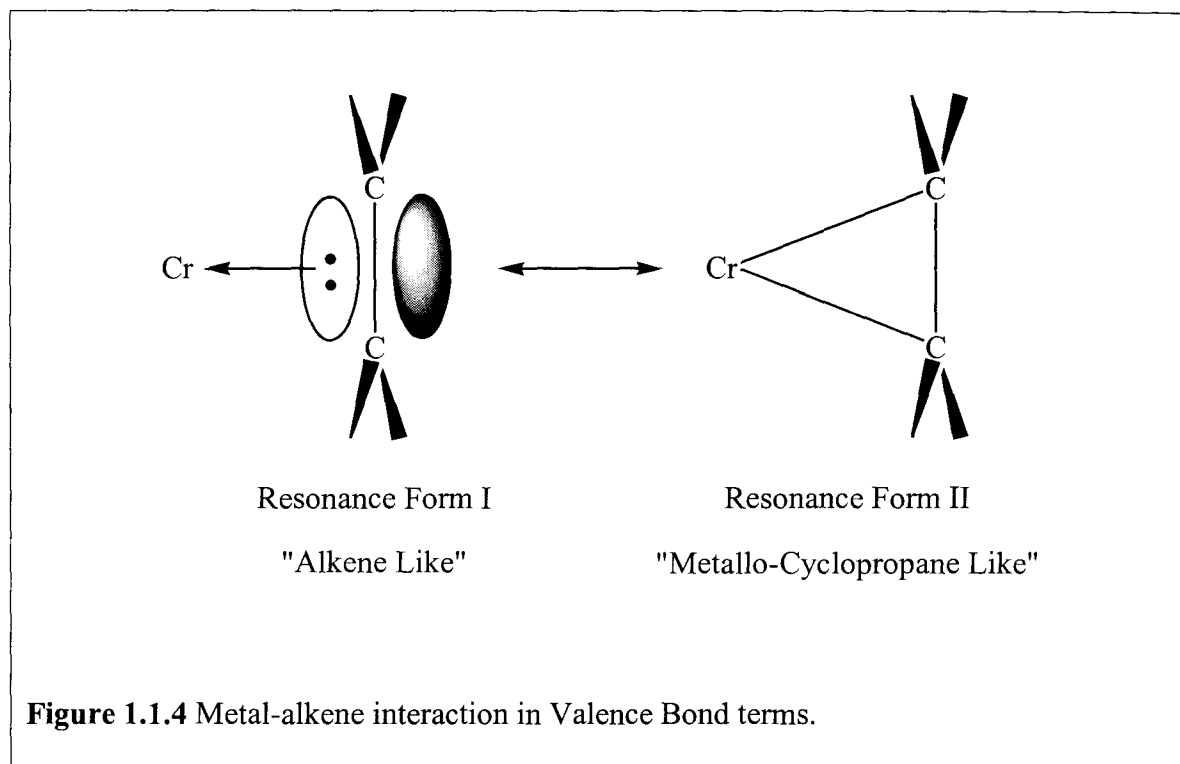
In the "alkene like" resonance form, the alkene carbons are sp^2 hybridized; while in the "metallo-cyclopropane like" resonance form, the alkene carbons move towards a sp^3 hybridization. Therefore, if the actual electronic structure contains a substantial resonance contribution from the second resonance form, the alkene substituents bend away from the metal due to this rehybridization. For alkenes, increased electron richness on the metal or decreased electron richness on the alkene favor contributions from the second resonance form, while decreased electron richness on the metal or increased electron richness on the alkene favor increased contributions from the first resonance form.

In localized molecular orbital terms (*i.e.,* the Dewar/Chatt/Duncanson model), the bonding is described as a synergistic combination of σ-donation and π-back donation, *i.e.,* (**Figure 1.1.5**)

The σ-Symmetry Interaction

σ-Donation

The π-Symmetry Interaction

π-Back Donation

Figure 1.1.5 Metal-alkene interactions: σ-donation and π-back donation.
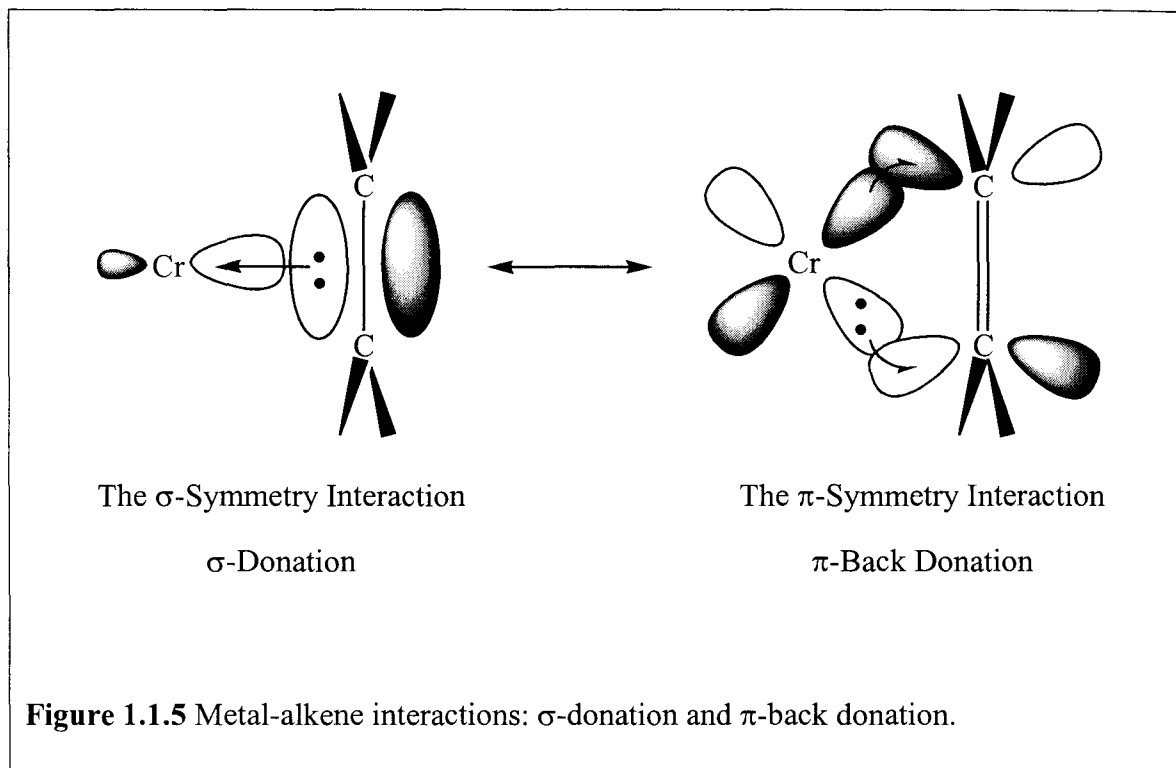
For alkenes, the σ-donation is from a filled σ-symmetry orbital on the alkene (*i.e.,* the alkene π-bonding orbital which is approximately σ-symmetry with respect to the metal) to a vacant σ-symmetry orbital on the chromium (*i.e.,* approximately metal d^2sp^3 in character). In the π-symmetry component, there is π-back donation from a filled π-symmetry orbitals on the chromium (*i.e.,* approximately metal d_{xz}, d_{yz}, or d_{xy} in character) to a vacant π-symmetry orbital on the alkene (*i.e.,* the alkene π* anti-bonding orbital which is π-symmetry with respect to the metal). Again, increased electron richness on the metal or decreased electron richness on the alkene favor somewhat decreased σ-donation and substantially increased π-back donation, while decreased electron richness on the metal or increased electron richness on the alkene favor somewhat increased σ-donation and substantially decreased π-back donation.

The net effect predicted for either bonding model is that increased contributions from the second resonance form, or increased π-back donation, will strengthen the chromium-carbon bond, weaken the alkene carbon-carbon bond, and bend the alkene substituents away from the metal. As with carbonyls, these two interactions are synergic. However, because the alkene is both a better σ-donor and a poorer π-acceptor than is a carbonyl, the direction of net electron density transfer is now typically from the alkene to the metal.

Although more complex,[2b,2c] the basic nature of the chromium-arene bond is analogous to that described above for alkenes with arene to chromium donation and chromium to arene back donation. Thus, arenes are strong net electron donors to the chromium centers, and their bonding has both arene to metal donation and metal to arene back donation, qualitatively similar to that observed for alkenes.

5.   Structures of (η^6-arene)Cr(CO)$_3$ Complexes

Arenes can coordinate to one or more metals in a wide variety of fashions.[2a] In the η^2 and η^4 bonding modes there are two and four, respectively, arene carbons within covalent bonding distance of the metal. Thus, they are structurally analogous to coordinated η^2-cycloalkenes and η^4-1,3-cyclohexadienes. The η^2 and η^4 bonding modes of arenes are relatively unstable for most complexes due to the partial loss of their aromatic character upon partial coordination to the metal center. Consequently, they are not usually observed in stable complexes. However, they are commonly invoked as reaction intermediates in organometallic arene chemistry. When they are isolated or suspected as intermediates, they display a strong tendency to expel other ligands from the

metal's coordination sphere and so change their coordination mode from η^2 through η^4 to the most stable η^6 form. As would be expected from this argument, by far the most common arene coordination mode in stable complexes is the η^6 bonding mode in which all six of the arene carbons are within covalent bonding distance to the metal. These three bonding modes donate a total of two, four, and six electrons, respectively, to the metal's eighteen electron count and formally occupy one, two, and three coordination positions about the metal, respectively.
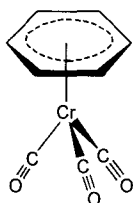
Figure 1.1.6 The "three legged piano stool" structure of $(\eta^6$-arene)Cr(CO)$_3$ complex.

The $(\eta^6$-arene)Cr(CO)$_3$ complexes were among the first classes of organometallics to receive intensive study during the golden years of explosive growth for transition metal organometallic chemistry (*i.e.*, during the 1950's and early 1960's). It was quickly realized that these complexes had the so called "three-legged piano stool" structures. In these structures, the carbonyl ligands are attached at approximately 90° angles to one another forming the three legs of a tripod while the arene is centered over the metal forming the flat top of the stool (*i.e.*, η^6 bonding). Overall, these complexes have approximately C_{3v} symmetry in the solid state.

These complexes have linear carbonyl groups and nearly planar arenes, three very similar Cr-C(carbonyl) bond distances of about 1.85 Å, three very similar C-O(carbonyl) bond distances of about 1.15 Å, six very similar Cr-C(arene) distances of about 2.25 Å, and six normal aromatic C-C distances.[1b] The observed deviations from equality are normally explained as arising from the effects of the arene substituents on the complexes' electronic structures, the effects of the carbonyls on eclipsed carbons, and crystal packing effects.

In the solid state, the arenes tend to adopt an eclipsed conformation with respect to the carbonyl ligands for arenes having π-donor substituents and staggered conformations for arenes having π-acceptor substituents. In solution, the arene rings rotate rapidly with respect to the carbonyl tripod largely averaging out the effects of the carbonyl ligands on the different parts of the ring, i.e.,

Eclipsed Conformation   Staggered Conformation

Figure 1.1.7 Eclipsed and staggered conformation of (η^6-arene)Cr(CO)$_3$ complexes. (Bottom view of complex showing arene rotation with respect to the carbonyl ligands).
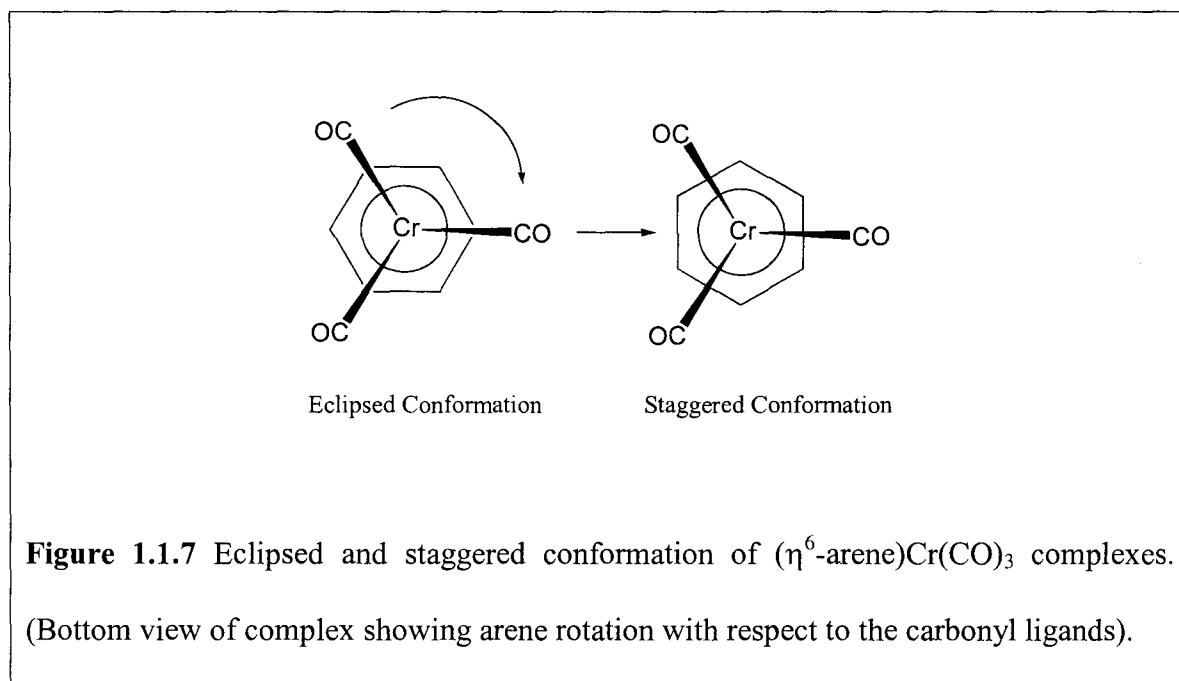
Similarly, most arene substituents retain the abilities they had in the uncomplexed arenes to rapidly rotate around the arene-substituent bond. For example, methoxy, amino, and methyl groups still typically freely rotate around their single bonds to the arene rings.

6. Arenes Distortions in the (η^6-arene)Cr(CO)$_3$ Complexes

The study of the interactions between substituents and arenes has been a central theme in physical organic chemistry.[8] Thus, the importance of π-symmetry interactions, e.g.,

Figure 1.1.8 π-Symmetry interactions of a substituent on the complexed arene (where D = a π-donor substituent such as NMe$_2$ and A = a π-acceptor substituent such as NO$_2$).
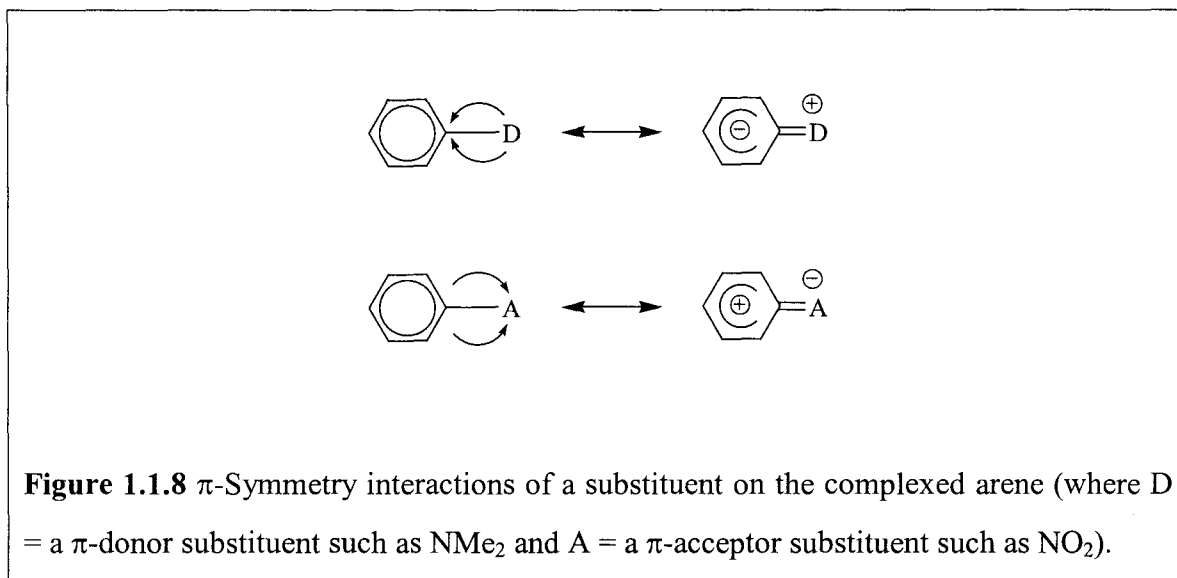
is well recognized and they are known to give rise to a variety of changes in the reactivity,[9] spectroscopic properties,[10] bonding[11] and structures[12] of these species which can be used to detect and quantify these interactions.[8-12] However, for arenes bonded in an η^6-fashion to transition-metal centers in complexes such as (η^6-arene)Cr(CO)$_3$,[13] the spectroscopic,[14,15] electrochemical,[16] electronic[17] and especially structural[18] consequences

of the analogous π-symmetry interactions are more poorly understood. Therefore, when Hunter *et al.* observed that the arene rings in (η^6-arene)Cr(CO)$_3$ complexes having organometallic substituents (e.g. (η^6-1,3,5-C$_6$H$_3$Fp$_3$)Cr(CO)$_3$ where Fp = (η^5-C$_5$H$_5$)Fe(CO)$_2$)[18] were very non-planar.[20] They were not initially sure if this was due to some unique aspect of the Fe-Cr interaction[19a] or whether it was simply a manifestation of the π-donor character of the Fe-aryl bond.[19b-19d,22] The nature of various anomalies in the spectroscopic and electrochemical data for these complexes,[19b-19d] along with the close relationship between the effects of NO$_2$ and Cr(CO)$_3$ groups on the chemistry of arenes,[13b] suggested to the Hunter group that the latter explanation was the correct one.[23] To confirm this hypothesis, they decided to carry out a systematic investigation to quantify the effects of main-group π-donor and π-acceptor substituents[24] on the planarity of the arene rings in (η^6-arene)Cr(CO)$_3$ complexes. The results from such a study were also expected to add an additional novel measure of the magnitudes of these π-symmetry interactions to the physical organic repertoire.

The molecular orbital calculations which have been reported for (η^6-arene)Cr(CO)$_3$ complexes have not generally addressed the origins or consequences of arene nonplanarity or its relationship to substituent π-donor and π-acceptor interactions.[17,25] Fortunately, the qualitative effects of any significant degree of π-donation or π-acceptance in these complexes are readily predictable in elementary valence bond terms, as they are for the uncomplexed arenes. Thus, π-donation from a π-donor substituent, D, would be expected to result in the contribution of the second resonance form (*i.e.*, **Figure 1.1.9** Resonance Form II) to the electronic structures of these complexes, *i.e.*,

Figure 1.1.9 Resonance forms for the π-Donor substituent (D = a π-donor, *e.g.* NMe₂, OMe, or F).
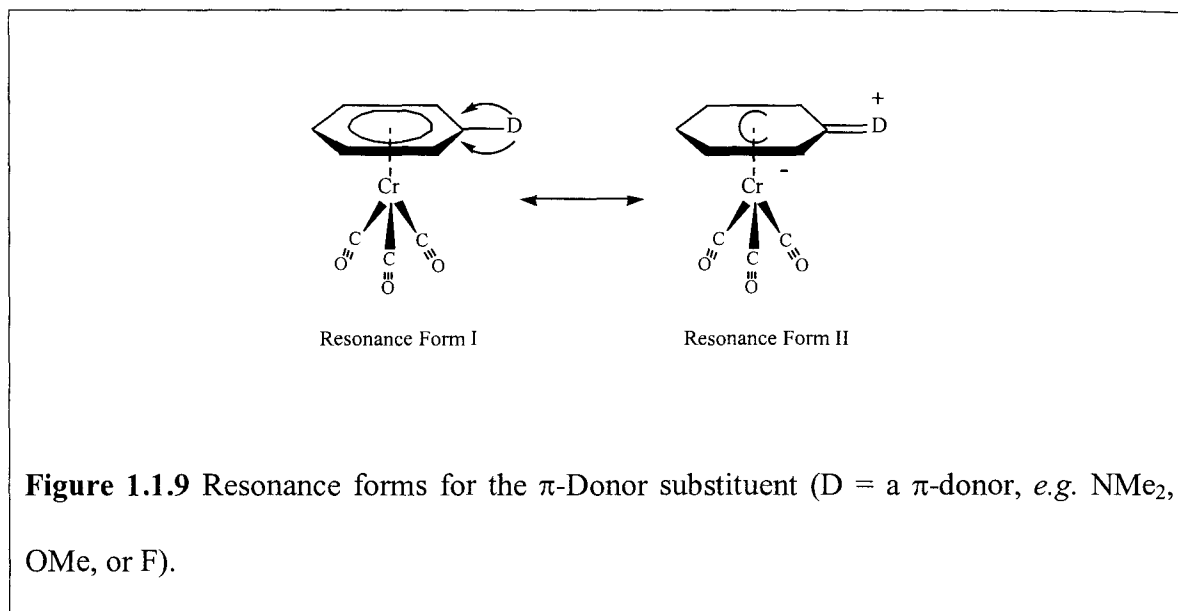
having an exocyclic double bond, a positive charge localized on D and a negative charge localized on the Cr(CO)₃ fragment.[26] The anionic Cr(CO)₃ center in the charge-separated zwitterionic (cyclohexadienyl)Cr(CO)₃ resonance form would have an 18-electron configuration and would therefore be expected to repel the electron density of the exocyclic double bond. Hence, the π-donor substituent and its *ipso*-carbon atom would be expected to bend away from the Cr(CO)₃ center. This would result in the loss of arene planarity as the contribution from resonance form Resonance Form II **(Figure 1.1.9)** to the electronic structure of the complex was increased, *i.e.*,

Figure 1.1.10 Distortion for the arene with a π-Donor substituent (D = a π-donor, *e.g.* NMe$_2$, OMe, or F).
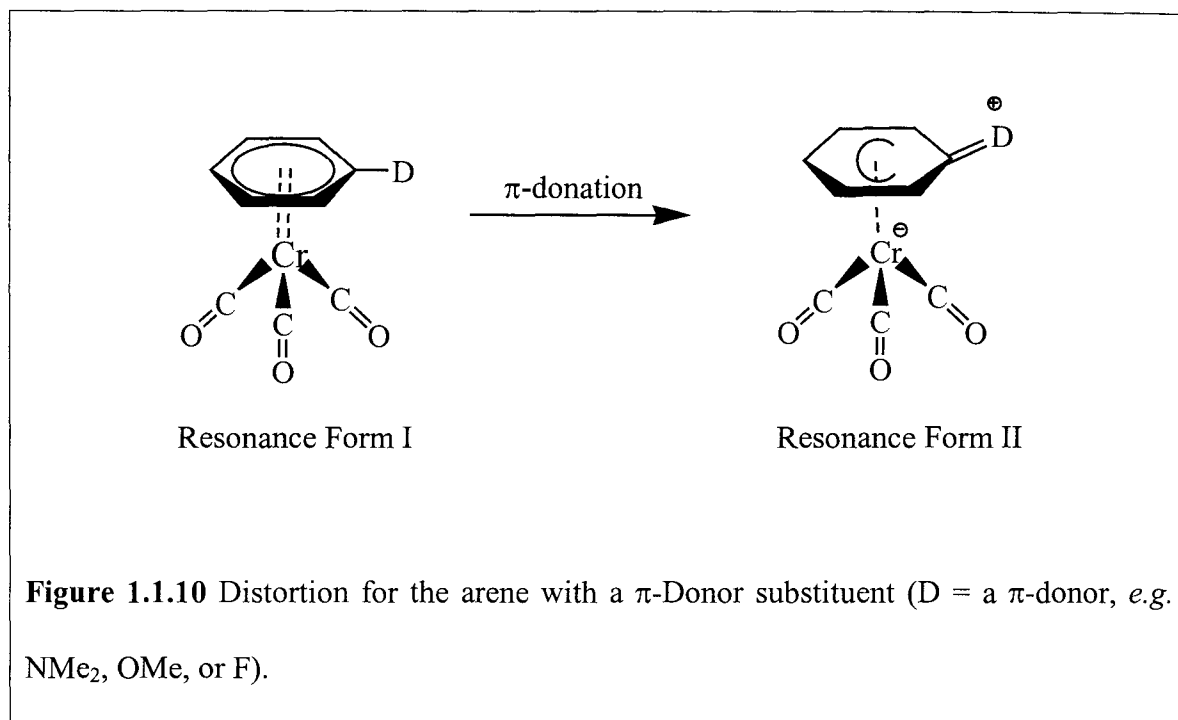
In the extreme, such a π-donor interaction would produce a cyclohexadienyl complex in which the exocyclic double bond was completely nonbonding with respect to, and bent away from, Cr(CO)$_3$.[27] Indeed, this hypothesis corresponds to the calculated structure for the hypothetical species [(η^5-C$_6$H$_5$=CR$_2$)Cr(CO)$_3$]$^-$.[28] With π-acceptor substituents, an analogous π-symmetry interaction might be expected, *i.e.*, (**Figure 1.1.11**)
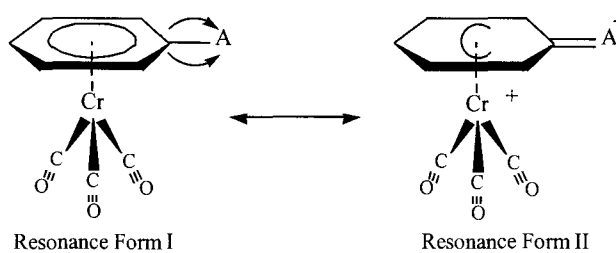
Figure 1.1.11 Resonance forms for the π-Acceptor substituent (A = a π-acceptor, *e.g.* CO_2Me or CF_3).

However, here the exocyclic double bond would be expected to bend towards, and thus bond to, the 16-electron cationic $Cr(CO)_3$ (reestablishing the favored 18-electron count), *i.e.*,
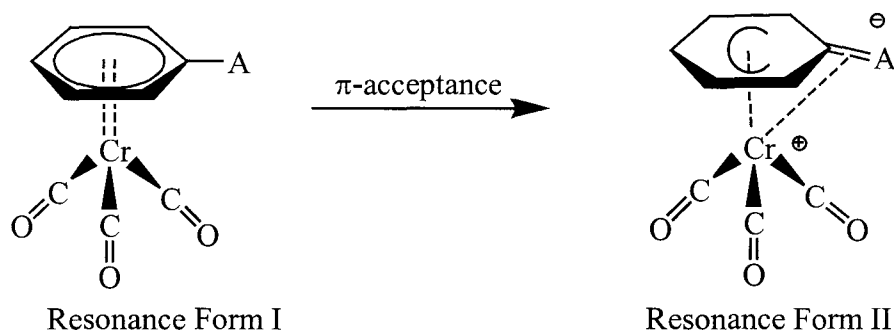
Figure 1.1.12 Distortion for the arene with a π-Acceptor substituent (A = a π-acceptor, *e.g.* CO_2Me or CF_3).

as has been predicted for the related species $[(\eta^7\text{-}C_6H_5\text{=}CR_2)Cr(CO)_3]^+$.[28] However, any contribution from Resonance Form II **(Figure 1.1.11)** to the overall bonding of the complex, and hence any structural distortion of the arene towards $Cr(CO)_3$, would be expected to be relatively small compared to the π-donor case (for conventional (η^6-arene)$Cr(CO)_3$ complexes) both for the obvious steric reasons and because such bending would be expected to result in decreased electron-density on the already relatively electron-poor $Cr(CO)_3$ center.[26,29-31]

7.   **Previous Studies of the Bonding in (η^6-arene)Cr(CO)₃ Complexes**

Elementary treatments of the bonding in these complexes have been presented above. They agree qualitatively with the results of more rigorous molecular orbital calculations. These calculations predict substantial net transfer of electron density from the arene rings through the chromium centers and onto the carbonyl ligands. The greatest net electron transfer is expected to occur for the most electron rich arenes. Indeed, it has been shown that the electron richness of uncomplexed arenes is strongly and linearly correlated with the electron richness of the corresponding (η^6-arene)$Cr(CO)_3$ complexes. In addition, these results have consistently shown that the highest occupied molecular orbital, HOMO, of these complexes is metal-carbonyl bonding in character while the lowest unoccupied molecular orbital, LUMO, of these complexes is metal-carbonyl anti-bonding in character.

8. Electrochemical Properties of (η^6-arene)Cr(CO)$_3$ Complexes

Cyclic voltammetry measures the relative ease and reversibility with which electrons can be added to or removed from a complex in solution. In non-donor solvents (e.g. dichloromethane with tetra-n-butylammonium hexafluorophosphate as the support electrolyte), most (η^6-arene)Cr(CO)$_3$ complexes are reversibly oxidized at potentials of between 0.4 and 1.4 volts with respect to a ferrocene standard,[1a] $i.e.$,

$$(\eta^6\text{-arene})Cr(CO)_3 \; \underset{+\,e^-}{\overset{-\,e^-}{\rightleftharpoons}} \; [(\eta^6\text{-arene})Cr(CO)_3]\overset{+}{\cdot}$$
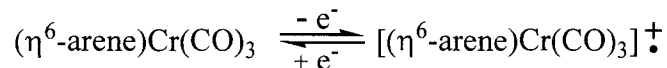
Equation 1.1.16 Electrochemical Oxidation.

Since the energy of the HOMO of these complexes reflects the electron richness of the complexes, it is not surprising that the most electron rich arenes produce the most electron rich complexes displaying the lowest oxidation potentials. The reversibility of these oxidations are also found to be strongly correlated with arene structure. Thus, the most electron rich arenes having the most steric congestion give $[(\eta^6\text{-arene})Cr(CO)_3]\overset{+}{\cdot}$ radical cations that have the highest thermal stabilities and greatest resistance to decomposition by nucleophiles.[32]

Section Two

Photoelectron Spectroscopy

1.   General Background of Photoelectron Spectroscopy

Photoelectron Spectroscopy (PES) is the most common method for finding the ionizations energies of atoms or molecules.[33] The origin of PES is found in Einstein's photoelectric effect which states that there is a threshold in energy which a photon must over come to allow any ionization of a substance.[34] PES employs this effect by having a photon hit a sample inducing an ionization. The energy of this photon is translated to the ejected electrons' kinetic energy, which can be measured, and the ionization energy for that electron. Since the photon energy is known and that the kinetic energy of the electron can be measured, the ionization energy can be calculated as show below in **Equation 1.2.1** and **Figure 1.2.1**.

Ionization Energy = Photons Energy ($h\nu$) - Kinetic Energy of the photo ejected electron

Equation 1.2.1 General equation for ionization energies in PES.

Figure 1.2.1 An illustration for general equation for ionization energies.
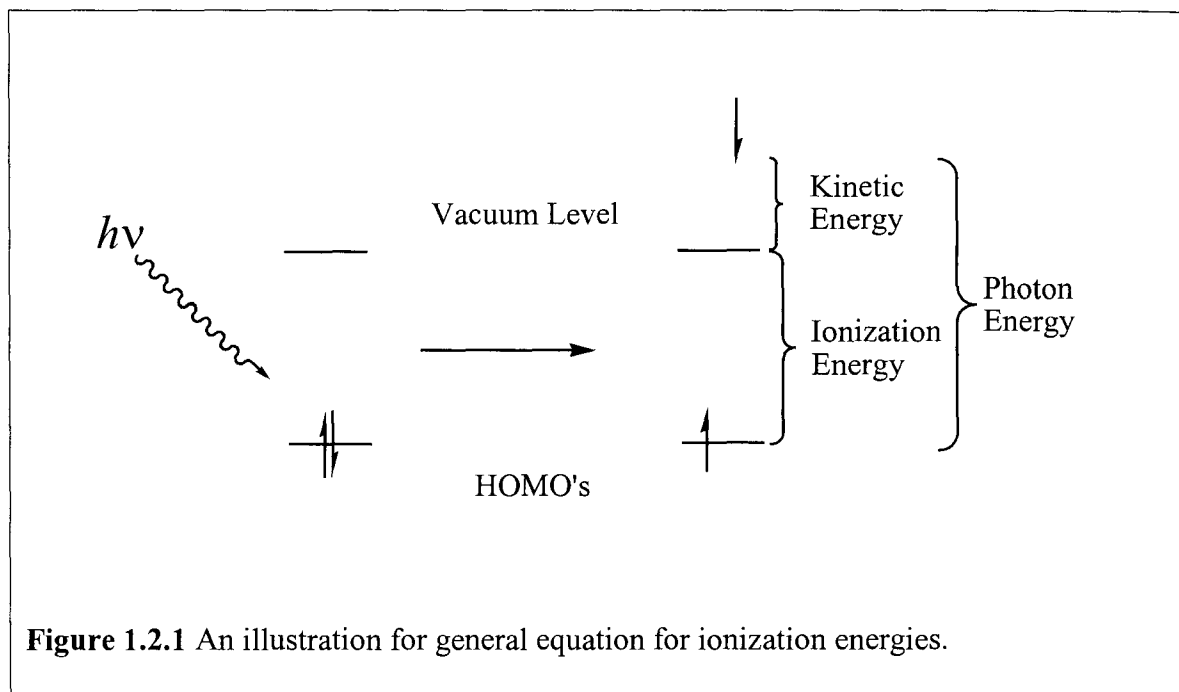
The basic process that goes on when you are colleting PES data is typically that a neutral molecule in the gas phase is bombarded with the photons which results in the formation of a cation in conjuction with a loss of an electron as seen in **Equation 1.2.2**.

$$\text{Molecule} + \text{Photon} (h\nu) \longrightarrow \text{Molecule}^{+} + e^{-}$$
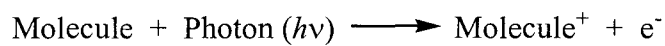
Equation 1.2.2 Reaction that occurs in a photoelectron spectrometer.

From **Equation 1.2.2,** it can be noted that the first ionization is the difference between the energy of the neutral molecule and the energy of the singly charged cation.[33]

2.   Koopmans' Theorem

Koopmans' Theorem is one of the main assumptions in photoelectron spectroscopy. This theorem states that the negative of an eigenvalue calculated for a single electron orbital from the Hartee-Fock method is the ionization energy for that orbital (**Equation 1.2.3**). [35]

$$IE = -\varepsilon_{HF}$$

Equation 1.2.3 Koopmans' Theorem.

One reason this theorem is valid is that its errors tend to cancel each other out. This cancellation occurs because a HF calculation lacks electron correlation effects and the gain in relaxation energy is usually about the same size as this correlation and thus these two errors cancels each other out. [35] This theorem is based on the fact that the ionization is relatively fast and that the electronic relaxation is relatively slow; thus electron structure can be crudely looked at as a static system. [33] The theorem tends to be least reliable when the relaxation energy is much larger than usual such as the case of the d orbitals of complexes containing transition metal. However, it works relatively well for assigning the ionization bands in the spectum when suitable calculations are conducted for the system (*i.e.*, HF for simple organic system and DFT for transition metal complexes).

3.   Ionization Band Profile

In the past, there has been the various ways to fit data such as PES, and most of used symmetric guassians.[36,37] According to Lichtenberger *et al.*, representing PES data with symmetric guassians can cause major errors in the positions and half-widths of the peaks because the PES data typically exhibit vibrational broadening. This is due to the fact that a molecule has a vibrational structure which can be excited during ionzation.

Figure 1.2.2 Transitions for the vibrational structure of a molecule.
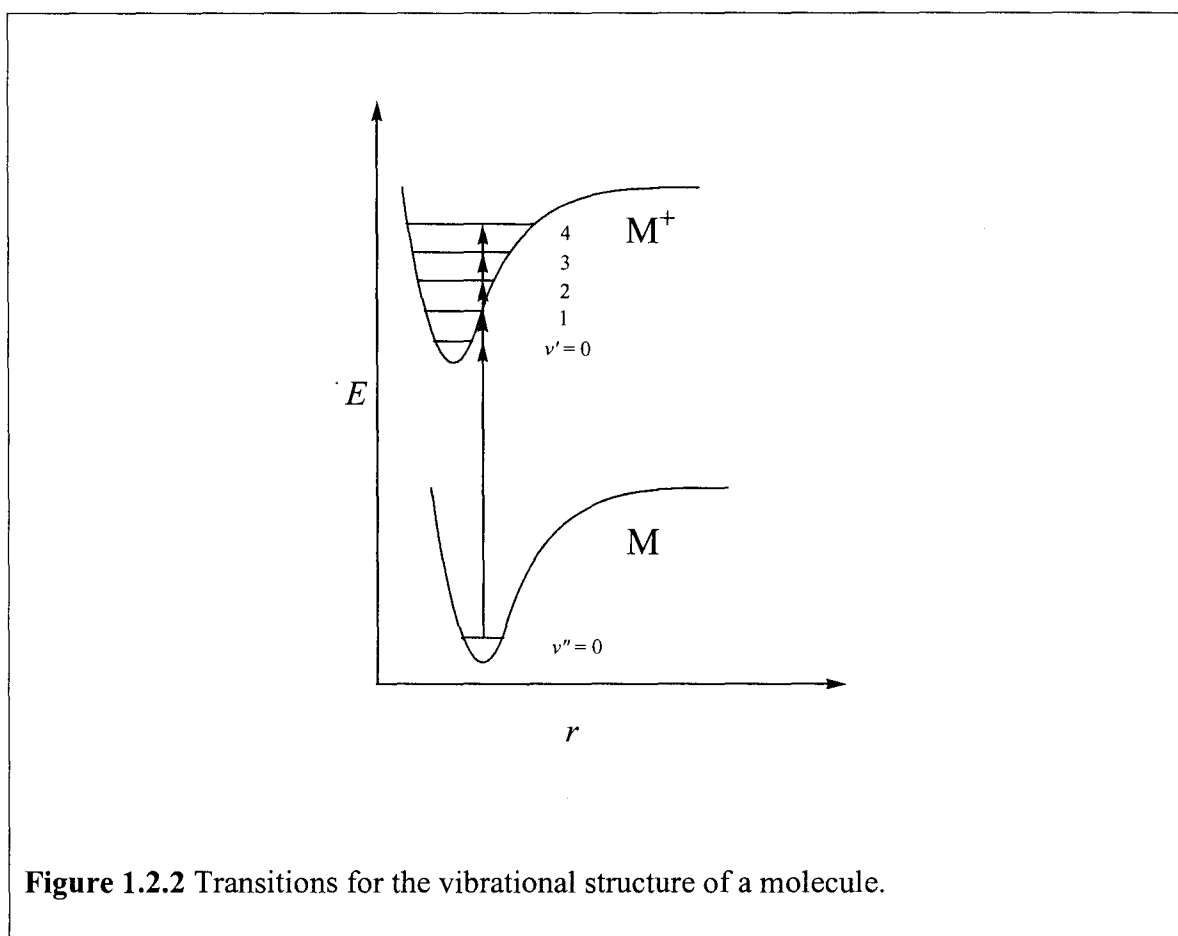
Thus, when the vibrational structure is unresolved we will then observer an ionization band with skewed gaussian. This is shaped because the vertical transition in the potential well does not have to have a symmetric distribution about it. For example, in **Figure**

1.2.2 we see that the vertical transition is 0→1 (v''→v') and therefore the top of the peak for the ionization band would be here. The 0→0 and 0→2 transitions should have the roughly the same intensity. There are no more transtions before the vertical transition. Thus the band would end on the lower energy side leading to a small contribution to half-width. However, on the higher energy side there are many more progressively weaker transtitions, leading to a longer contribution to haft-width. Thus, the low energy side has a short contribution to half-width and the high energy side with longer contribution to haft-width and the overall band would be best fit with an "asymmetric" Gaussian.[38]

0→1
Vertical Ionization

0→2

0→0

0→3

0→4

Ionization Energy

Figure 1.2.3 Example of how vibrational structures are seen in the PES. (Transition based on **Figure 1.2.2.** This is only illustration!)
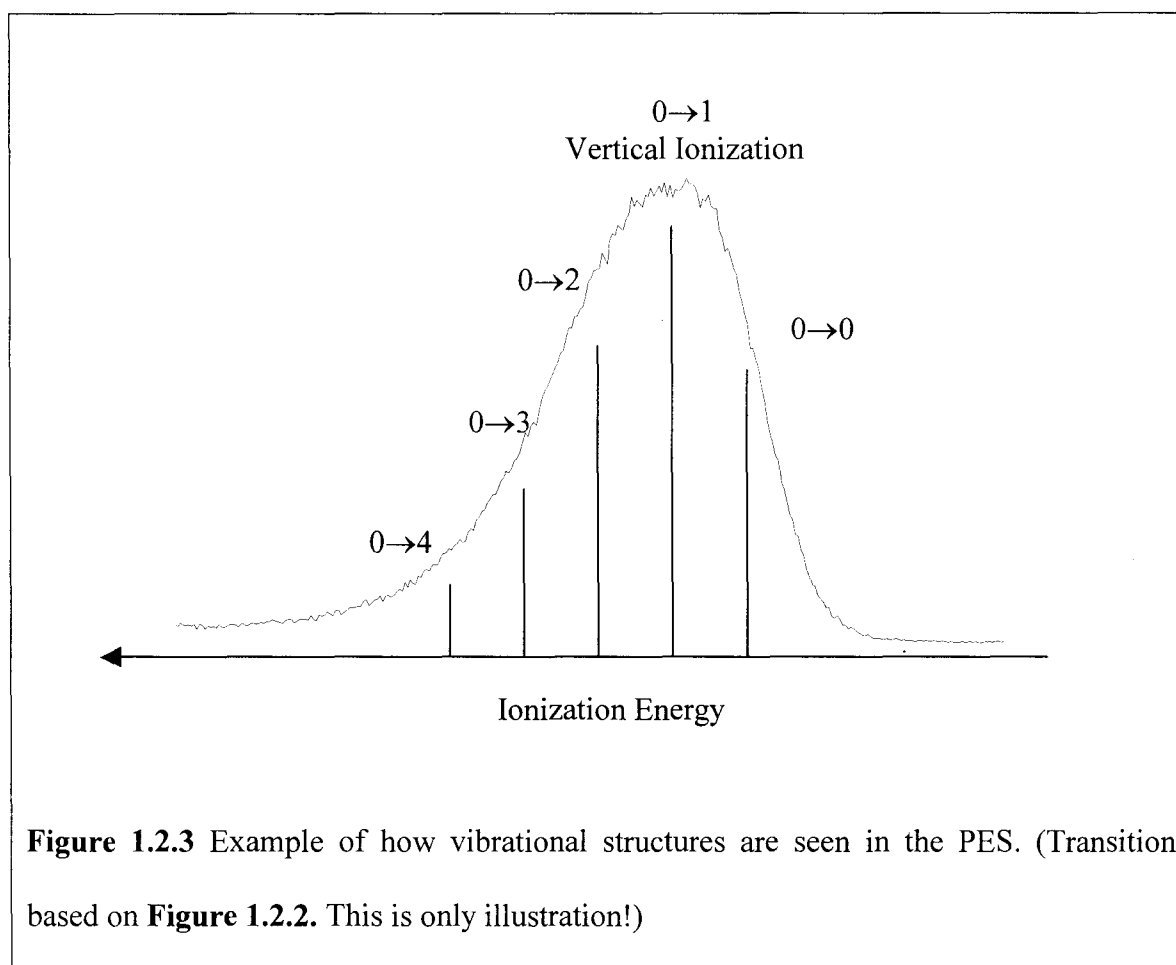
Section Three

Computational Chemistry

1.   General Background on Computational Chemistry

Over the last several decades, there has been a major interest into development of computational programs to aid in solving real world chemical problems (*e.g.,* for molecular geometries, spectroscopic values, transition states, and various thermodynamic properties). In the beginning, attempts to solve the time-independent Schrödinger equation for the electronic structure of a system were carried out through approximation techniques. One of the first methods used was called *ab initio*, "from the beginning," calculations. This method starts with the Schrödinger equation and makes approximations to construct Hamiltonians that can be solved. This gives approximate values from the selected wavefunctions when the Schrödinger equation has too many variables to be solved exactly (*i.e.,* for any system more complex than the hydrogen atom).[39]

Another method proposed in the 1960's was Density Functional Theory, DFT. This method states that a good approximation for the wavefunctions can be found by using a function that defines the electron density about the nucleus or nuclei of the system.[40,41] DFT was first used in the physics community and did not see much popularity with chemists until the late 1980's and early 1990's when computers became more powerful and easier to use and when "user friendly" computational software packages (*i.e.,* Gaussian, Spartan, etc.) became more readily available. As DFT method has developed there has been a trend to create hybrid functionals that use a mix of HF

and DFT (*i.e.*, B3LYP, BHandHLYP, TDDFT, etc.) to more properly describe both electron exchange and electron correlation effects.

Other methods have also been developed to find solutions for the wavefunctions. One class of methods that was used to handle computationally difficult cases was semiempirical methods. These methods used simplified Hamiltonians and employed empirical data to reduce the computational time spent in a calculation. Because of their reduced computational demands, semiempirical methods are a good starting point for a computational study of a new system.[39] Another method that helps reduce computational times is molecular mechanics. This method does not find the wavefunctions but finds molecular geometries using classical physics. Thus, all of the force constants for the molecular fragments are taken into consideration to predict an equilibrium geometry. Generally, experimental data for large set of compounds and quantum mechanical data for model systems are used to find reasonable values for the constants for each fragment. This approach is used in systems with large bulky groups (*e.g.*, dendrimers, polymers, and proteins) and where only one or a few sites in the molecule are of interest to the researcher. These sites are "targeted" by the high level quantum mechanical calculations with the geometries of the surrounding molecular fragments being determined by molecular mechanics.[43]

All of the methods used to solve various chemical problems "chemical accuracy," as 0.01 eV, is still very difficult to achieve.[39] The key to obtaining the best computational results is to have a detailed understanding of the assumptions made by the method you choose to study your system. For example, in a previous study of the photoelectron spectra with Hartree-Fock calculations for benzenechromiumtricarbonyl Hillier *et al.*,

expected, based on their calculations, to find the first two ionization bands (energies) to be fully resolved. However, they observed in the experimental spectra only one peak. They rationalized that the single peak contained two overlapping ionization bands. However, their Hartree-Fock calculations failed to take into account the major electron correlation effects which occurs more significantly in a complex containing transition metal(s).[42] When a DFT/B3LYP study, which does take into account electron correlation effects, was done on this system, it was found that the first two ionization bands are predicted to be close together and unresolved. **Table 1.3.1** summarizes the general advantages and disadvantages of the methods considered in our work.

Method	Advantage	Disadvantage
ab initio (HF, MPPT, etc.)	1. Pure Theoretical Method 2. Good accuracy when large basis sets are used	1. Long computational times 2. Poor handling of electron correlation effects in HF
DFT	1. Faster computational times than *ab initio* 2. Great treatment of electron correlation effects 3. Result comparable in accuracy to experimental data	1. Uses the electron density to find the electronic properties 2. Cannot calculate the precise electron density and therefore many approximations are made
Hybrid Functionals (*i.e.*, B3LYP)	1. Blend of HF and DFT 2. Good treatment of both electron exchange and correlation effects	1. Has approximations from both HF and DFT 2. Electron density is still an approximation
Semiempirical (*i.e.*, AM1, PM3, etc.)	1. Fast computational times even with large systems 2. Accuracy is good	1. Accurate and optimized experimental data to "standardize" most Semiempirical methods 2. Not a "pure" theoretical method
Fenske-Hall	1. Fast computational times (only a few minutes even with large systems) 2. Accuracy is good 3. Optimized for transition metal complexes	1. Simplified Hamiltonian 2. Does not compute optimized geometries

Table 1.3.1 Advantages and disadvantages of the main computational methods.

2.   *Ab initio* **Calculations**

2a.   **Principles of** *ab initio* **Calculations**

As stated above, *ab initio* calculations were one of first methods used to try to find solutions to the Schrödinger equation. However, one can't find exact solutions to Schrödinger equation for systems larger than the hydrogen atom so approximations are made to find a good solution. Due to those approximations, you will not find the true wavefunction, ψ, but instead will find a form of the wavefunction that is a close approximation and which will be denoted as ψ^o.

$$H^o \, \psi^o = E^o \, \psi^o \qquad\qquad H^o = \sum_{i=1}^{n} h_i$$

Equation 1.3.1 The Schrödinger equation and core hamiltonian, h_i. (Note: i is for electron i.)

The above equation shows the general Schrödinger equation and the core hamiltonian, h_i, for an n electron system which can be rewritten for a single electron in the n state. Thus, the wavefunction ψ^o would be rewritten as a wavefunction for a single electron of form $\psi^o_a(i)$. The wavefunction is dependent on all of the nuclear and electron coordinates. The E^o_a is the energy for electron (i) in orbital a.

$$h_i \, \psi^o_a(i) = E_a{}^o \, \psi^o_a(i)$$

Equation 1.3.2 The Schrödinger equation written for one electron in a frozen nuclear skeleton.

The calculation must take into account the spin of the electron and obey the Pauli principle. This is done with a Slater determinant which works with "spinorbitals." A spinorbital, ϕ_a (*i*), is the product of the orbital wavefunction (*i.e.*, s, p, d... orbitals) and the spin function (*i.e.*, α, β).

$$\psi^o(\mathbf{x};\mathbf{R}) = (n!)^{-1/2} \det |\phi_a(1)\phi_b(2)... \phi_z(n)|$$

Equation 1.3.3 Slater determinate.

One of the more common types of *ab initio* calculations are based on the Hartree-Fock method (HF). Hartree-Fock attempts to have **Equation 1.3.1** take into consideration electron-electron repulsion as an average. This method assumes that the electrons are moving in the electric field of the nuclei and the average fields of all the other electrons.

$$f_i = h_i + \sum_u \{J_u(i) - K_u(i)\}$$

Equation 1.3.4 Fock operator.

This method also employs the Fock operator, f_i, to find the spinorbitals, h_i is the core hamiltonian for electron i and the sum is over all spinorbitals $u = a, b... z$, and where $J_u(i)$ and $K_u(i)$ are the Coulomb operator and the exchange operator. The Coulomb operator takes into account the coulombic force between the electrons. The exchange operator recognizes the effects of spin correlation and is an average of the energy potential from a single electron in the presence of the other (n-1) electrons.

One interesting problem occurs in nearly all methods. This is that to find the spinorbital for one state the other spinorbitals for the other energy states are required to be known. Thus, the problem must have been solved before starting it. Of course, this is not the case, so generally most methods start out with a guess of the lower energy states and the higher states can be calculated form this initial guess. After that, the calculation is rerun with these newly calculated values and this is continuously done in a series of iterations until the values become constant. This is known as the self-consistant field (SCF) approach. The idea of a SCF is used throughout nearly all methods to find the lowest energy or most stable electronic structure.

As good as the HF method may seem, it still lacks electron correlation effects which results from instantaneous electron-electron repulsions. HF does include an

average electron-electron repulsion, but it does not include instantaneous repulsions. There have been many methods used to try to deal with this problem. One of the better approaches is perturbation theory which allows the final Hamiltonian to take into account single, double, triple, etc., excitations thus giving the calculation some additional terms to account for to electron correlation. A commonly used version of this the Møller-Plesset perturbation theory (MPPT). The most common forms of MPPT are second, MP2, and fourth order, MP4, MPPT. Higher order MPPT treatments are more accurate but are also the more computational intense and therefore, as usual, one trades off accuracy for computational accessibity.[39]

2b.   Basis Sets

To do any type of *ab initio* calculation a basis set is needed to represent the spinorbitals. To have the most accurate solution a complete level basis set is needed, but larger basis sets dramatically increase computational time. Thus, the goal in setting up a calculation is to strike a balance between a basis set that is large enough to be sufficiently accurate yet still small enough to be acceptably fast.

The most common type of basis set is Gaussian-type orbitals (GTO). Generally, GTOs are computationally easy but they do not have a cusp at the atomic nucleus. This results in the GTOs being less accurate than Slate-type orbitals (STO) which do have such a cusp. Unfortunately, STOs are rather cumbersome to compute. When GTOs have sufficiently large basis sets they become, in practical terms, as accurate as STOs. Thus, GTOs are generally employed in computational studies of real molecules because of their reduced computational requirements.

Gaussian-type orbital,
GTO, for n=1

The STO has a cusp at
the nucleus while the
GTO does not.

Slater-type orbital,
STO, for n=1

distances from nucleus

Figure 1.3.1 The exponential function for a hydrogenic s-orbital. (Graph is exaggerated!)
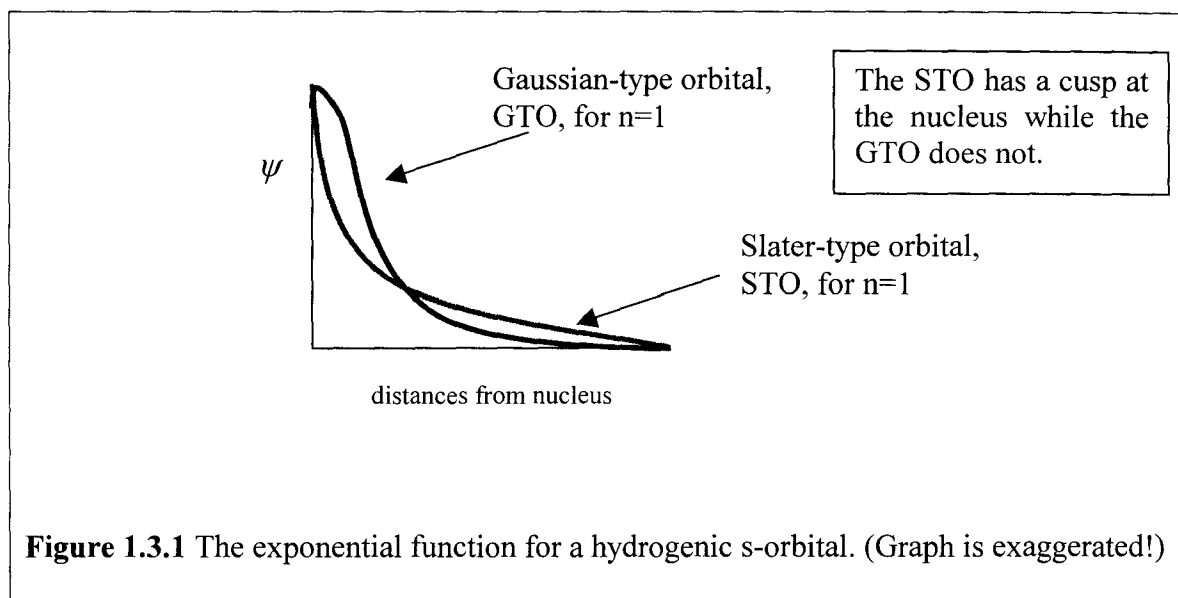
GTOs are simply a Cartesian Gaussian function that represents the usual atomic orbitals (*i.e.*, s, p, d, etc.) where r_c is the center of the Gaussian (x_c, y_c, z_c) and r_1 is the Cartesian coordinate for the electron (x_1, y_1, z_1). The variables i, j, and k are all non-negative integers and the exponent α is positive. The sum of i, j, and k determines the type of Gaussian (zero is an s-type, one is p-type, two is d-type, etc.).[39]

$$\theta_{ijk}(\mathbf{r}_1 - \mathbf{r}_c) = (x_1 - x_c)^i (y_1 - y_c)^j (z_1 - z_c)^k e^{-\alpha |\mathbf{r}_1 - \mathbf{r}_c|^2}$$

Equation 1.3.5 Cartesian Gaussian function.

2c. Advantages of *ab initio* Calculations

The main advantage of *ab initio* calculations is that they are closely related to the "pure" Schrödinger equation. Thus, they will, in the end, give a truer representation of the actual wavefuctions. This means that, in principle, *ab initio* calculations might be more accurate than others when better approximations are made and if sufficient computational resources are available.

2d. Disadvantages of *ab initio* Calculations

With large basis sets and high levels of theory, relatively accurate solution can be found from *ab initio* calculations. However, the computational time spent to achieve that can be extremely long and, in practice, can be impractical to do even with large super computers. Also, HF still lacks electron correlation effects which are very important in heavy atoms like transition metals. MPPT does take electron correlation effects into account but the computational time can agian be rather impractical.

3. Density Functional Theory

3a. Principles of Density Functional Theory

Density Functional Theory (DFT) is a type of *ab initio* calculation but, rather than starting with ideas that most other *ab initio* calculations do, DFT starts with the idea that the electron density, rather than the orbitals, can be described by a universal function to find the electronic structure and other electron properties. The fundamentals of DFT came from the work in the 1920's for the Thomas-Fermi model which stated that the electron density could be crudely looked at as a classical liquid. However, the first proof

for DFT wasn't seen until 1964 by Hohenberg and Kohn.[40,44] The next significant advancement for DFT was the derivations of the equations by Kohn and Sham.[41]

$$E[\rho] = E_T[\rho] + E_V[\rho] + E_J[\rho] + E_{XC}[\rho]$$

$$E[\rho] = [-(\hbar^2)/(2m_e)]\sum_{i=1}^{n}\int \psi^*_i(\mathbf{r}_1)\nabla^2_1 \psi_i(\mathbf{r}_1)d\mathbf{r}_1 - \sum_{I=1}^{N}\int [(Z_I e^2)/(4\pi\varepsilon_0 r_{I1})] \rho(\mathbf{r}_1)d\mathbf{r}_1 +$$

$$\tfrac{1}{2}\int [(\rho(\mathbf{r}_1)\rho(\mathbf{r}_2)e^2)/(4\pi\varepsilon_0 r_{12})]d\mathbf{r}_1 d\mathbf{r}_2 + E_{XC}[\rho]$$

Equation 1.3.6 The exact ground-state electron energy for a n-electron system in DFT.

The fundamental equation for DFT is the exact ground-state electron energy, $E[\rho]$, and it has four major components, which are: the kinetic energy (E_T), the potential energy (E_V), the coulomb energy (E_J), and the electron exchange-correlation energy (E_{XC}). The first three terms, kinetic, potential, and coulomb energy, are defined exactly and are relatively easy to compute. However, the electron exchange-correlation energy is relatively difficult to compute and this is the term that introduces the most error into a DFT calculation. Electron exchange-correlation energy is difficult to calculate because it cannot be obtained exactly and thus SCF and approximations are employed to find its value.

$$\rho(\mathbf{r}) = \sum_{i=1}^{n} \mid \psi_i(\mathbf{r}) \mid^2$$

Equation 1.3.7 The exact ground-state charge density, ρ, in DFT.

The Kohn-Sham orbitals, ψ_i, are used to solve the above equation. First, the Kohn-Sham orbitals must be computed and this is done by the Kohn-Sham equation which is derived from the $E[\rho]$. Then, the exact ground-state charge density, ρ, is used to find the exact ground-state electron energy, $E[\rho]$.

$$\{[-(\hbar^2)/(2m_e)]\nabla^2_1 - \sum_{I=1}^{N} [(Z_I e^2)/(4\pi\varepsilon_0 r_{I1})] + \int [(\rho(\mathbf{r}_2)e^2)/(4\pi\varepsilon_0 r_{12})]d\mathbf{r}_2 + V_{XC}(\mathbf{r}_1)\}\psi_i(\mathbf{r}_1) = \varepsilon_i\psi_i(\mathbf{r}_1)$$

Equation 1.3.8 The Kohn-Sham equation for one electron in DFT.

The Kohn-Sham equation has new terms. The ε_i is the energy value for the Kohn-Sham orbital and the V_{XC} is the exchange-correlation potential which is the derivative of the exchange-correlation energy, E_{XC}.

$$V_{XC}[\rho] = \frac{\delta E_{XC}[\rho]}{\delta \rho}$$

Equation 1.3.9 Equation for exchange-correlation potential in DFT.

After observing **Equation 1.3.8**, it is easy to understand that by knowing E_{xc} finding the values for the orbitals is relatively simple. Unfortunally, E_{xc} is not known. Thus, various methods are used to find a good approximation for E_{xc}. But what is common in all the methods is that a guess is made of the charge density, ρ, and then the Kohn-Sham equation can be solved with an SCF method.[39-41,44,45]

3b. Advantages of Density Functional Theory

The main advantage to DFT is that it is less computationally intensive than other *ab initio* calculations (*eg.,* HF and MPPT). One might expect faster calculations to be less accurate but DFT has been shown to predict values that are close to experimental values for a wide range of "real world" situations. Also, DFT takes electron correlation effects into account relatively well because the method is based on local electron density gradient.[39]

3c. Disadvantages of Density Functional Theory

The main disadvantage to DFT is that it is a rather an indirect method for finding electron properties though the electron density. Although it has proven successful in finding the electronic structure of many systems, theoreticians still remain unconvinced

that an electron density is the appropriate method to derive electron structure. The other disadvantage is that it is still not know how to actually calculate the complete electron density, and many approximations are neccessary.[40,41] Final DFT also has a weakness with electron exchange effects, however this issue has been improved by incorporating parts of the Hartree-Fock method into the DFT calculation (*i.e.*, hybrid functionals).[46]

4.   Principles of Hybrid Functionals

Hybrid functionals are a slight modification to a DFT calculation where E_{xc} contains a blend of the Hartree-Fock and Density Functional Theory approaches. This is done because, as Becke demonstrated,[46] the Kohn-Sham DFT formalism while producing results comparable in accuracy to experimental data and while accounting for electron correlation effects rather well. However, Kohn-Sham DFT formalism does not account very well for electron exchange effects. Therefor Becke and others have developed methods that incorporate parts of Hartree-Fock into the DFT calculation to more properly describe electron exchange effects which Hartree-Fock does a better job of accounting for this effect.

$$E_{xc} = aE_x^{\text{Slater}} + (1\text{-}a)E_x^{\text{HF}} + b\Delta E_x^{\text{Becke}} + E_c^{\text{VWN}} + c\Delta E_c^{\text{non-local}}$$

Becke Three Parameters
(Exchange Functionals, E_x)

DFT Parameters
(Correlation Functionals, E_c)

Equation 1.3.10 Equation for E_{xc} in a hybrid functional. (a, b, and, c are constants determined by Becke's work.)[46]

The above equation, **Equation 1.3.10**, expresses E_{xc} in a hybrid functional as devised by Becke in 1993. There have been many adaptations to Becke's early hybrid functional papers. One method used in our work is B3LYP (*i.e.*, Becke Three Parameter Hybrid Functionals and Lee, Yang, and, Parr Correlation Functional). B3LYP employs both the localized correlation of the VMN (Vosko, Wilk, and, Nusair correlation functional III) expression and the LYP (Lee, Yang, and, Parr) expression for the non-localized correlation.[46]

5. Principles of Semiempirical Methods[39]

Semiempirical methods are one of the fastest methods for finding electronic properties and they have been able to handle large systems while giving relatively accurate solutions. The main reason that these methods are fast is that they use empirical

data for the core atomic potentials and that they use simplified Hamiltonians. There are numerous semiempirical methods because different methods use different empirical data and also different approximations are used to simplify the calculation. Thus, it important to understand the method you want to use because it could lead to high error if a poor choice is made. AM1 (*i.e.*, Austin Model) and PM3 (*i.e.*, Parameterization Method Three) are commonly used in organic systems.

The main advantage to semiempirical methods is they are fast relative to *ab initio* calculations and they give fairly accurate solutions. Large systems that are just totally impractical using *ab initio* and even DFT calculations become possible. Indeed, not only are they possible but the solutions can be rather accurate.

A major problem with the semiempirical methods is that the empirical data in the calculation must be very accurate to obtain an accurate solution. Most methods have tried to optimize these parameters but this is still a difficult task. The main reasons for this is that not all experimental data is really accurate, a sufficient range of data may not be readily available, and/or that the simultaneous optimization of these parameters for a large data set can be impractical.[39]

6.   Principles of Fenske-Hall[47]

One method that has been optimized for organometallic system is Fenske-Hall. This method is not semiempirical because the basis sets were calculated. However, Fenske-Hall uses the calculated basis sets much like the predetermined empirical data is used in conventional semiempirical methods. Fenske-Hall produces results that are similar to DFT with small basis sets, and generates reasonable electronic and orbital

structures at very low computational cost. This method has been a great tool in constructing molecular orbital diagrams. However, it does not compute optimized geometries which can be major problem if an appropriate structure cannot be obtained from other sources.[47,48]

Section Four

References

1. For a detailed introduction to the chemistry of $(\eta^6\text{-arene})Cr(CO)_3$ complexes, see the following two papers and the extensive list of references cited therein: (a) Hunter, A. D.; Mozol, V.; Tsai, S. D. *Organometallics* **1992**, *11*, 2251-2262. (b) Hunter, A. D.; Shilliday, L. *Organometallics* **1992**, *11*, 1550-1560.

2. (a) Maslowsky, E. *J. Chem. Educ.* **1993**, *70*, 980-984. (b) Lukehart, C. *Fundamental Transition Metal Organometallics Chemistry*; Brooks/Cole Publishing Co.: Monterey California, 1985; pp 128-129. (c) Collman, J. P.; Hegedus, L. S.; Norton, J. R.; Finke, R. G. *Principles and Applications of Organotransition Metal Chemistry*; University Science Books: Mill Valley, California, 1987; pp 158-164, 253-255, 425-427, 546-549, 921-940. (d) King, R. B. Organometallic Syntheses, Volume 1, Transition-Metal Compounds; Academic Press: New York, 1965; pp 136-138.

3. Angelici, R. J. *Synthesis and Technique in Inorganic Chemistry*, 2nd Edition.; Mill Valley, California, 1986; pp 129-146.

4. Angelici, R. J. *J. Chem. Educ.* **1968**, *45*, 119.

5. For other reports of discovery based labs and cooperative learning experiences see, for example: (a) Jarret, R. M.; New, J.; Patraitis, C. *J. Chem. Educ.* **1995**, *72*, 457. (b) Burns, D. S.; Berka, L. H.; Kildahl, N. *J. Chem. Educ.* **1993**, *70*, A100. (c) Millikan, R. C. *J. Chem. Educ.* **1978**, *55*, 807. (d) Kharas, G. B. *J. Chem. Educ.* **1997**, *74*, 829. (e) Robinson, W. R. *J. Chem. Educ.* **1997**, *74*, 622.

(f) Nurrenbern, S. C.; Robinson, W. R. *J. Chem. Educ.* **1997**, *74*, 623. (g) Kogut, L. S. *J. Chem. Educ.* **1997**, *74*, 720. (h) Dougherty, R. C. *J. Chem. Educ.* **1997**, *74*, 722.

6. Mahaffy, C. A. L.; Pauson, P. L. *Inorg. Synth.* **1979**, *19*, 154-158.

7. (a) Schwan, A. L. *J. Chem. Educ.* **1993**, *70*, 1001. (b) Davis, W. H. Jr.; Pryor, W. A. *J. Chem. Educ.* **1976**, *53*, 285. (c) Maskill, H. *The Physical Basis of Organic Chemistry*; Oxford University Press: New York, 1985; pp 202-215, 442-473. (d) Exner, O. *Advances in Linear Free Energy Relationships*; Chapman, N. B., Shorter, J. Eds.; Plenum Press: New York, 1972; pp 1-69.

8. (a) Maskill, H. *The Physical Basis of Organic Chemistry*; Oxford University Press: New York, 1985; pp 202-215, 442-473. (b) Exner, O. In *Advances in Linear Free Energy Relationships*; Chapman, N. B., Shorter, J., Ed; Plenum Press: New York, 1972; pp 1-69. (c) Hind, J. *Physical Org. Chem.*; McGraw-Hill: New York, 1962; pp 81-103.

9. See, for example: (a) March, J. *Advanced Organic Chemistry, Reactions, Mechanisms, and Stru*cture, Third Edition, John Wiley and Sons: New York, 1985; pp 453-462. (b) Carey, F. A.; Sundberg, R. J. *Advanced Organic Chemistry, Part A: Structure and Mechanisms, Third Edition*, Plenum: New York, 1990; pp 196-209.

10. See, for example: (a) Levy, G. C.; Lichter, R. L.; Nelson, G. L. *Carbon-13 Nuclear Magnetic Resonance Spectroscopy*; John Wiley and Sons: New York, 1980. (b) Stothers, J. B. *Carbon-13 NMR Spectroscopy*; Academic: New York, 1972. (c) Memory, J. D.; Wilson, N. K. *NMR of Aromatic Compounds*, John

Wiley and Sons: New York, 1982. (d) Nelson, G. L.; Levy, G. C.; Cargioli, J. D. *J. Am. Chem. Soc.* **1972**, *94*, 3089-3094. (e) Ewing, D. F. *Org. Magn. Reson.* **1979**, *12*, 499-524. (f) Katritzky, A. R.; Topsom, R. D. *Angew. Chem., Int. Ed.* **1970**, *9*, 87-100. (g) Nelson, G. L.; Williams, E. A. *Prog. Phys. Org. Chem.* **1976**, *12*, 229-342. (i) Bromilow, J.; Brownlee, R. T. C.; Craik, D. J., Sadek, M.; Taft, R. W. *J. Org. Chem.* **1980**, *45*, 2429-2440. (j) Hugel, H. M.; Kelly, D. P.; Spear, R. J.; Bromilow, J.; Brownlee, R. T. C.; Craik, D. J. *Aust. J. Chem.* **1979**, *32*, 1511-1519. (k) Brownlee, R. T. C.; Sadek, M. *Aust. J. Chem.* **1981**, *34*, 1593-1602. (l) Bromilow, J.; Brownlee, R. T. C.; Topsom, R. D.; Taft, R. W. *J. Am. Chem. Soc.* **1976**, *98*, 2020-2022. (m) Maciel, G. E.; Natterstad, J. J. *J. Chem. Phys.* **1965**, *42*, 2427-2435.

11. (a) Dillow, G. W.; Kebarle, P. *J. Am. Chem. Soc.* **1989**, *111*, 5592-5596. (b) Chowdhury, S.; Kishi, H.; Dillow, G. W.; Kebarle, P. *Can. J. Chem.* **1989**, *67*, 603-610. (c) Gould, I. R.; Ege, D.; Moser, J. E.; Farid, S. *J. Am. Chem. Soc.* **1990**, *112*, 4290-4301. (d) Ferguson, G.; Robertson, J. M. *Adv. Phys. Org. Chem.* **1963**, *1*, 203-281. (e) Hehre, W. J.; Taft, R. W.; Topsom, R. D. *Prog. Phys. Org. Chem.* **1976**, *12*, 159-187. (f) Turner, D. W. *Adv. Phys. Org. Chem.* **1966**, *4*, 31-71. (g) Jug, K.; Koster, A. M. *J. Am. Chem. Soc.* **1990**, *112*, 6772-6777, and references cited therein

12. See, for example: (a) Allen, F. H.; Kennard, O.; Taylor, R. *Acc. Chem. Res.* **1983**, *16*, 146-153. (b) Domenicano, A.; Vaciago, A.; Coulson, C. A. *Acta Crystallogr., Sect. B* **1975**, *31*, 221-234. (c) Skancke, A. In *Fluorine-Containing*

Molecules; Liebman, J. F.; Greenberg, A.; Dolbier, W. R. Jr., Eds.; VCH Publishers: New York, 1988; pp 43-64.

13. For general reviews on (η^6-arene)Cr(CO)$_3$ chemistry see, for example: (a) Solladié-Cavallo, A. *Polyhedron*, **1985**, *4*, 901-927. (b) Muetterties, E. L.; Bleeke, J. R.; Wucherer, E. J.; Albright, T. A. *Chem. Rev.* **1982**, *82*, 499-525. (c) Silverthorn, W. E. *Adv. Organomet. Chem.* **1975**, *13*, 47-137. (d) Senoff, C. V. *Coord. Chem. Rev.* **1980**, *32*, 111-191.

14. For infrared spectroscopic studies on (η^6-arene)Cr(CO)$_3$ complexes see reference 1b and, for example: (a) Neuse, E. W. *J. Organomet. Chem.* **1975**, *99*, 287-295, and work cited therein.

15. For ^{13}C NMR studies on (η^6-arene)Cr(CO)$_3$ complexes see reference 1b and, for example: (a) Bodner, G. M.; Todd, L. J. *Inorg. Chem.* **1974**, *13*, 360-363. (b) Roques, B. P. *J. Organomet. Chem.* **1977**, *136*, 33-37, and work cited therein.

16. For electrochemical studies of (η^6-arene)Cr(CO)$_3$ complexes see, reference 1b and: (a) Connelly, N. G.; Geiger, W. E. *Adv. Organomet. Chem.* **1984**, *23*, 1-93, and references cited therein.

17. For molecular orbital studies on (η^6-arene)Cr(CO)$_3$ complexes see, references 8b, 12f and: (a) Albright, T. A.; Hofmann, P.; Hoffmann, R. *J. Am. Chem. Soc.* **1977**, *99*, 7546-7557. (b) Ono, I.; Mita, S.; Kondo, S.; Mori, N. *J. Organomet. Chem.* **1989**, *367*, 81-84. (c) Allen, G. C.; Butler, I. S.; Kirby, C. *Inorg. Chim. Acta.* **1987**, *134*, 289-292. (d) Modelli, A.; Distefano, G.; Guerra, M.; Jones, D. *J. Am. Chem. Soc.* **1987**, *109*, 4440-4443. (e) Byers, B. P.; Hall, M. B. *Organometallics* **1987**, *6*, 2319-2325. (f) Rogers, R. D.; Atwood, J. L.; Albright, T. A.; Lee, W.

A.; Rausch, M. D. *Organometallics* **1984**, *3*, 263-270. (g) Chinn, J. W.; Hall, M.

B. *J. Am. Chem. Soc.* **1983**, *105*, 4930-4941. (h) Albright, T. A.; Hofmann, P.;

Hoffmann, R.; Lillya, C. P.; Dobosh, P. A. *J. Am. Chem. Soc.* **1983**, *105*, 3396-

3341. (i) Semmelhack, M. F.; Garcia, J. L.; Cortes, D.; Farina, R.; Hong, R.;

Carpenter, B. K. *Organometallics* **1983**, *2*, 467-469. (j) Albright, T. A. *Acc.

Chem. Res.* **1982**, *15*, 149-155. (k) Aroney, M. J.; Copper, M. K.; Englert, P. A.;

Pierens, R. K. *J. Mol. Struct.* **1981**, *77*, 99-108. (l) Albright, T. A.; Carpenter, B.

K. *Inorg. Chem.* **1980**, *19*, 3092-3087. (m) Albright, T. A.; Hoffmann, R. *Chem.

Ber.* **1978**, *111*, 1578-1590. (n) Hoffmann, R.; Albright, T. A.; Thorn, P. L. *Pure

Appl Chem.* **1978**, *50*, 1-9. (o) Ceccon, A.; Gentiloni, M.; Romanin, A.; Venzo,

A. *J. Organomet. Chem.* **1977**, *127*, 315-324. (p) Elian, M.; Chen, M. M. L.;

Mingos, D. M. P.; Hoffmann, R. *Inorg. Chem.* **1976**, *15*, 1148-1155. (q) Elian,

M.; Hoffmann, R. *Inorg. Chem.* **1975**, *14*, 1058-1076. (r) Khandkarova, V. S.;

Gubin, S. P.; Kvasov, B. A. *J. Organomet. Chem.* **1970**, *23*, 509-515. (a) Müller,

J. *J. Organomet. Chem.* **1969**, *18*, 321-325. (t) Brown, D. A.; Rawlinson, R. M. *J.

Chem. Soc. A* **1969**, 1534-1537. (u) Carroll, D. G.; McGlynn, S. P. *Inorg. Chem.*

1968, *7*, 1285-1290. (v) Rooney, D.; Chaiken, J.; Driscoll, D. *Inorg. Chem.*

1987, *26*, 3939-3945. (w) Solladie-Cavallo, A.; Wipff, G. *Tetrahedron Lett.*

1980, 3047-3050.

18. For the crystallographic studies of the non-cyclic (η^6-arene)Cr(CO)$_3$ complexes

used in this work, see: (a) Bailey, M. Y.; Dahl, L. F. *Inorg. Chem.* **1965**, *4*,

1314-1319. (b) Rees, B.; Coppers, P. *Acta Crystallogr., Sect. B* **1973**, *29*, 2516-

2528. (c) Bailey, M. F.; Dahl, L. F. *Inorg. Chem.* **1965**, *4*, 1314-1319. (d) Rees,

B.; Coppens, P. *J. Organomet. Chem.* **1972**, *42*, C102-C104. (e) Le Maux, P.; Saillard, J. Y.; Grandjean, D.; Jaouen, G. *J. Org. Chem.* **1980**, *45*, 4526-4528. (f) Saillard, J. Y.; Grandjean, D.; Le Maux, P.; Jaouen, G. *Nouv. J. Chim.* **1981**, *5*, 153-160. (g) Dusausoy, Y.; Protas, J.; Besancon, J.; Tirouflet, J. *C.R. Acad. Sci., Ser. C* **1970**, *270*, 1792-1794. (h) Wasserman, H. J.; Wovkulich, M. J.; Atwood, J. D.; Churchill, M. R. *Inorg. Chem.* **1980**, *19*, 2831-2834. (i) Van Meurs, F.; Van Koningsveld, H. *J. Organomet. Chem.* **1976**, *118*, 295-303. (j) Fukui, M.; Ikeda, T.; Oishi, T. *Chem. Pharm. Bull.* **1983**, *31*, 466. (k) Van Meurs, F.; Van Koningsveld, H. *J. Organomet. Chem.* **1977**, *131*, 423-428. (l) Abraham, F.; Nowogrocki, G.; Brocard, J.; Lebibi, J.; Bremard, C. *Acta Crystallogr., Sect. C* **1984**, *40*, 1181-1183. (m) Van Der Helm, D.; Loghry, R. A.; Hanlon, D. J.; Hagen, A. P. *Cryst. Struct. Commun.* **1979**, *8*, 899-903. (n) Halet, J. F.; Saillard, J. Y.; Caro, B.; Le Bihan, J. Y.; Top, S.; Jaouen, G. *J. Organomet. Chem.* **1984**, *267*, C37-C40. (o) Le Bihan, J. Y.; Senechal-Tocquer, M. C.; Senechal, D.; Gentric. D.; Caro, B.; Halet, J. F.; Saillard, J. Y.; Jaouen, G.; Top, S. *Tetrahedron* **1988**, *44*, 3565-3574. (p) Schubert, U.; Hornig, H. *J. Organomet. Chem.* **1984**, *273*, C11-C16. (q) Carter, O. L.; McPhail, A. T.; Sim, G. A. *J. Chem. Soc., A* **1967**, 1619-1626. (r) Saillard, J. Y.; Grandjean, D. *Acta Crystallogr., Sect. B* **1976**, *32*, 2285-2289. (s) Ceccon, A.; Giacometti, G.; Venzo, A.; Ganis, P.; Zanotti, G. *J. Organomet. Chem.* **1981**, *205*, 61-69. (t) Schöllkopf, K.; Stezowski, J. J.; Effenberger, F. *Organometallics* **1985**, *4*, 922-929. (u) Xiaoguang, Y.; Jinshun, H.; Jinling, H. *J. Struct. Chem.* **1985**, *4*, 52. (v) Schubert, U.; Dötz, K.H.; *Cryst. Struct. Commun.* **1979**, *8*, 989-994. (w) Denise,

B.; Goumont, R.; Parlier, A.; Rudler, H.; *J. Organomet. Chem.* **1989**, *337*, 89-104.

(x) Chung, T. M.; Lee, Y. A.; Chung, Y. K.; Jung, I. N. *Organometallics* **1990**, *9*, 1976-1979. (y) Dusausoy, Y.; Protas, J. *J. Organomet. Chem.* **1975**, *94*, 47-53.

(z) Boutonnet, J. C.; Levisalles, J.; Rose-Munch, F.; Rose, E.; Precigoux, G.; Leroy, F. *J. Organomet. Chem.* **1985**, *290*, 153-164. (aa) Blagg, J.; Davies, S. G.; Goodfellow, C. L.; Sutton, K. H. *J. Chem. Soc. Perkin Trans., I* **1987**, 1805-1811. (bb) Dusausoy, Y.; Protas, J.; Besancon, J.; Tirouflet, J. *Acta Crystallogr., Sect. B* **1973**, *29*, 469-4476. (cc) Dusausoy, Y.; Protas, J.; Besancon, J.; Tirouflet, J. *Acta Crystallogr., Sect. B* **1972**, *28*, 3183-3188. (dd) Dusausoy, Y.; Protas, J.; Besancon, J. *J. Organomet. Chem.* **1973**, *59*, 281-292. (ee) Bush, M. A.; Dullforce, T. A.; Sim, G. A. *J. Chem. Soc., D* **1969**, 1491-1493. (ff) Dusausoy, Y.; Lecomte, C.; Protas, J.; Besancon, J. *J. Organomet. Chem.* **1973**, *63*, 321-327.

(gg) Carter, O. L.; McPhail, A. T.; Sim, G. A. *J. Chem. Soc., A* **1967**, 228-236. (hh) Dötz, K. H.; Tiriliomis, A.; Harms, K. *J. Chem. Soc., Chem. Commun.* **1989**, 788-790. (ii) Van Meurs, F.; Van Koningsveld, H. *J. Organomet. Chem.* **1974**, *78*, 229-235. (jj) Gilday, J. P.; Widdowson, D. A. *J. Chem. Soc., Chem. Commun.* **1986**, 1235-1237. (kk) Rose-Munch, F.; Rose, E.; Semra, A. *J. Organomet. Chem.* **1989**, *363*, 103-121. (ll) Wright, M. E. *J. Organomet. Chem.* **1989**, *376*, 353-358. (mm) Boutonnet, J. C.; Rose-Munch, F.; Rose, F.; Jeannin, Y.; Robert, F. *J. Organomet. Chem.* **1985**, *297*, 185-190. (nn) Levisalles, J.; Rose-Munch, F.; Rose, E.; Semra, A.; Oricain, J.G.; Jeannin, Y.; Robert, F. *J. Organomet. Chem.* **1983**, *328*, 109-122. (oo) Rose-Munch, F.; Rose, E.; Semra, A. *J. Organomet. Chem.* **1989**, *363*, 123-130. (pp) Rose-Munch, F.; Rose, E.;

Semra, A.; Mignon, L.; Garcia-Oricain, J. *J. Organomet. Chem.* **1989**, *363*, 297-309. (qq) Yoshifuji, M.; Inamoto, N.; Hirotsu, K.; Higuchi, T. *J. Chem. Soc., Chem. Commun.* **1985**, 1109-1111. (rr) Bailey, M. F.; Dahl, L. F. *Inorg. Chem.* **1965**, *4*, 1298-1306. (ss) Byers, B. P.; Hall, M. B. *Inorg. Chem.* **1987**, *26*, 2186-2188. (tt) Hunter, G.; Iverson, D. J.; Mislow, K.; Blount, J. F. *J. Am. Chem .Soc.* **1980**, *102*, 5942-5943. (uu) Iverson, D. J.; Hunter, G.; Blunt, J. F.; Damewood, J. R. Jr.; Mislow, K. *J. Am. Chem. Soc.* **1981**, *103*, 6073-6083. (vv) Downton, P. A.; Mailvaganam, B.; Frampton, C. S.; Sayer, B. G.; McGlinchey, M. J. *J. Am. Chem. Soc.* **1990**, *112*, 27-32.

19. (a) Hunter, A. D. *Organometallics* **1989**, *8*, 1118-1120.   (b) Hunter, A. D.; McLernon, J. L. *Organometallics* **1989**, *8*, 2679-2688.   (c) Richter-Addo, G. B.; Hunter, A.D. *Inorg. Chem.* **1989**, *28*, 4063-4065.   (d) Richter-Addo, G. B.; Hunter, A. D.; Wichrowska, N. *Can. J. Chem.* **1989**, *68*, 41-48.

20. In the X-ray crystal structures of the complexes $(\eta^6\text{-}1,3,5\text{-}C_6H_3Fp_3)Cr(CO)_3$,[14a,b] $(\eta^6\text{-}1,4\text{-}C_6H_4MeFp)Cr(CO)_3$,[16] $(\eta^6\text{-}C_6H_5((\eta^5\text{-}C_5H_4Me)Fe(CO)_2))Cr(CO)_3$,[16] and $(\eta^6\text{-}C_6H_5((\eta^5\text{-indenyl})Fe(CO)_2))Cr(CO)_3$[16] it can be seen that all of the Fp substituents (where Fp $= (\eta^5\text{-}C_5H_5)Fe(CO)_2)$ and the *ipso*-carbon atoms to which they are attached are bent substantially away from the $Cr(CO)_3$ centers.

21. Li, J.; Hunter, A. D.; Santarsiero, B. D.; Bott, S. G.; Atwood, J. L., unpublished observations.

22. Organometallic fragments such as Fp are reasonably good π-donors,[14b,d] see: (a) Hunter, A. D.; Szigety, A. B. *Organometallics* **1989**, *8*, 2670-2679. (b) Chukwu, R.; Hunter, A. D.; Santarsiero, B. D. *Organometallics* **1991**, *10*,

2141-2152.   (c) Chukwu, R.; Hunter, A. D.; Santarsiero, B. D., Bott, S. G.; Atwood, J. L.; Chassaignac, J. *Organometallics*, in press (accepted: September 18th, 1991).   (d) Stewart, R. P.; Treichel, P. M. *J. Am. Chem. Soc.* **1970**, *92*, 2710-2718.   (e) Bolton, E. S.; Knox, G. R.; Robertson, C. G. *J. Chem. Soc., Chem. Commun.* **1969,** 664.   (f) Nesmeyanov, A. N.; Leshcheva, I. F.; Polovyanyuk, I. V.; Ustynyuk, Y. A. *J. Organomet. Chem.* **1972**, *37*, 159-165.   (g) Butler, I. R.; Lindsell, W. E. *J. Organomet. Chem.* **1984**, *262*, 59-68.   (h) Schilling, B. E. R.; Hoffmann, R.; Lichtenberger, D. L. *J. Am. Chem. Soc.* **1979**, *101*, 585-591.

23. For a detailed discussion of the spectroscopic and especially the electrochemical consequences of adding π-donor and/or π-acceptor substituents to the arene rings of (η^6-arene)Cr(CO)$_3$ complexes and the relationship of this data to our bonding model, For part 2, see: Hunter, A.D.; Mozol, V.; Cai, S. D. *J. Am. Chem. Soc.*, submitted for publication (August 13, 1991).

24. The structures of complexes having transition metal substituents either σ-bonded to the arene (e.g. (η^6-1,4-C$_6$H$_4$MeFp)Cr(CO)$_3$) or as part of the arene substituent (e.g. in (μ_2-η^6,η^6-biphenyl)(Cr(CO)$_3$)$_2$) have the same general structural dependence upon substituent π-donor/π-acceptor character described for the main-group substituents. However, given the added complications of describing their bonding and the possible involvement of direct intermetallic interactions, they will be discussed in detail in a separate manuscript.[21]

25. In *para*-cyclophane complexes, the alkyl groups are observed to bend away from the Cr(CO)$_3$ fragment due to the cyclophane ring strain. This was modelled by distorting the structure of (η^6-1,4-C$_6$H$_4$Me$_2$)Cr(CO)$_3$ towards a boat conformation

which resulted in increased hyperconjugation (i.e. π-donation) to the chromium center.[17b]

26. The spectroscopic and electrochemical studies presented in reference 8b unambiguously demonstrate that a substantial portion of the electron-density transferred by π-symmetry interactions with the substituents becomes localized on the $Cr(CO)_3$ center.

27. For examples of cyclohexadienyl complexes with non-coordinated exocyclic double bonds, see: (a) Lacoste, M.; Rabao, H.; Astruc, D.; Ardoin, N.; Varet, E.; Saillard, J. Y.; Le Beuze, A. *J. Am. Chem. Soc.* **1990**, *112*, 9548-9557. (b) Crocker, L. S.; Mattson, B. M.; Heinekey, D. M. *Organometallics* **1990**, *9*, 1011-1016. (c) Crocker, L. S.; Heinekey, D. M. *J. Am. Chem. Soc.* **1989**, *111*, 405-406. (d) Ceccon, A.; Gambaro, A.; Venzo, A. *J. Chem. Soc., Chem. Commun.* **1985**, 540-542. (e) Ceccon, A.; Gambaro, A.; Venzo, A. *J. Organomet. Chem.* **1984**, *275*, 209-222. (f) Ceccon, A.; Gambaro, A.; Romanin, A. M.; Venzo, A. *J. Organomet. Chem.* **1983**, *254*, 199-205. (g) Lacoste, M.; Varret, F.; Toupet, L.; Astruc, D. *J. Am. Chem. Soc.* **1987**, *109*, 6504-6506. (h) Rieke, R. D.; Henry, W. P.; Arney, J. S. *Inorg. Chem.* **1987**, *26*, 420-427. (i) Milligan, S. N.; Rieke, R. D. *Organometallics* **1983**, *2*, 171-173.

28. In the calculations for these species, the exocyclic double bond was predicted to bend towards $Cr(CO)_3$ by 11 for $[(C_6H_5=CR_2)Cr(CO)_3]^+$ and away from $Cr(CO)_3$ in $[(C_6H_5=CR_2)Cr(CO)_3]^-$, see: (a) Albright, T.A.; Hoffmann, R.; Hofmann, P. *Chem. Ber.* **1978**, *111*, 1591-1602. (b) Hoffmann, R.; Hofmann, P. J. Am. Chem. Soc. 1976, 98, 598-603, and references cited therein. For leading references to

$[(C_6H_5=CR_2)Cr(CO)_3]^+$ complexes and their chemistry, see: (c) Top, S.; Jaouen, G.; Sayer, B. G.; McGlinchey, M. J. *J. Am. Chem. Soc.* **1983**, *105*, 6426-6429, and references cited therein.

29. With a more electron-rich complexes (e.g. (η^6-arene)Cr(PR$_3$)$_3$ and (η^6-arene)$_2$Cr) however, the relative contributions from Resonance Forms II of **Figure 1.4.9** and **Figure 1.4.11** to the overall electronic structure would be expected to increase and decrease, respectively.

30. In practice, the extreme difficulty encountered in synthesizing substituted (η^6-arene)Cr(CO)$_3$ complexes having strongly π-accepting substituents (e.g. NO$_2$),[3] is an additional factor making the *observation* of the structural consequences for π-acceptance interactions in (η^6-arene)Cr(CO)$_3$ complexes more difficult. For part 2, see: Hunter, A.D.; Mozol, V.; Cai, S. D. *J. Am. Chem. Soc.*, submitted for publication (August 13, 1991).

31. Hunter, A. D.; Shilliday, L. *Organometallic,* **1992**, 11, 1550-1560.

32. Hunter, A. D.; Bianconi, L. J.; DiMuzio, S. J.; Braho, D. L. *J. of Chemical Education,* **1998**, 75, 891-983

33. (a) Ebsworth, E. A.; Rankin, D. W.; Cradock, S.; Raymond, K. *Structural Methods in Inorganic Chemistry*; Blackwell Scientific Publications; 1991; 2nd ed.; pp255-303. (b) **Hüfner, S.** *Photoelectron Spectroscopy: Principles and Applications*; Berlin New York: Springer; 2003; 3rd ed.. (c) Eland, J.H.D. *Photoelectron Spectroscopy: An Introduction to Ultraviolet Photoelectron Spectroscopy in the Gas Phase*; London; New York: Butterworths, 1984, 2nd ed.. (d) *Electron Spectroscopy: Theory, Techniques and Applications*; Brundle, C.R.;

Baker, A.D.; London; New York: Academic Press, 1984; 5 Volume Series. (e)

Rabalais, J. W. *Principles of Ultraviolet Photoelectron Spectroscopy*; New York:

Wiley; 1977.

34. Einstein, A. *Ann. Phys.* **1905**, *17*, 549.

35. Koopmans, T. *Physica* **1933**, *1*, 104.

36. Citrin, P. H.; Wertheim, G. K.; Baer, Y. *Phys. Rev. B* **1977**, *16*, 4256.

37. Bancroft, G. M.; Adams, I.; Coatsworth, L. L.; Bennewitz, C. D.; Brown, J.D.;

    Westwood, W. D. *Anal. Chem.* **1975**, *47*, 586.

38. Lichtenberger, D. L.; Copenhaver, A. S. *Journal of Electron Spectroscopy and*

    Related Phenomena **1990**, *50*, 335-352.

39. Atkins, P. W. Friedman, R. S. *Molecular Quuantum Mechanics*; Oxford New

    York; 1997; 3rd ed.; pp276-319.

40. Hohenberg, P.; Kohn, W. *Phys. Rev.* **1964**, *136*, B864-B871.

41. Kohn, W.; Sham, L. J. *Phys. Rev.*, **1965**, *140*, A1133-A1138.

42. Guest, M. F.; Hillier, I. H.; Higginson, B. R.; Lloyd, D. R. *Mol. Phys.* **1975**, *29*,

    113-128.

43. (a) Lipkowitz, K. B.; Peterson, M. A. *Chem. Rev.* **1993**, *93(7)*, 2463-2486. (b)

    Jungwirth, P.; Gerber, R. B. *Chem. Rev.* **1999**, *99(6)*, 1583-1606.

44. March, N. H. *Advan. Phys.* **1957**, *6*, 1.

45. Ziegler, T. *Chem. Rev.* **1991**, *91*, 651.

46. (a) Becke, A. D. *J. Chem. Phys.* **1992**, *96(3)*, 2155-2160. (b) Becke, A. D. *J.*

    Chem. Phys. **1992**, *97(12)*, 9173-9177. (c) Becke, A. D. *J. Chem. Phys.* **1993**,

    98(7), 5648-5652.

47. (a) Hall, M. B.; Fenske, R. F. *Inorganic Chemistry* **1972**, *11(4)*, 768-775. (b) Herman, F.; Skillman, S. "Atomic Structure Calculations" 1963, Prentice-Hall: Englewood Cliffs, N. J. (c) Bursten, B. E.; Fenske, R. F. *J. Chem. Phys.* **1977**, *67*, 3138. (d) Bursten, B. E.; Jensen, R. J.; Fenske, R. F. *J. Chem. Phys.* **1978**, *68*, 3320.

48. Information of procedures in Fenske-Hall are at the following site: http://www.chem.arizona.edu/~dll518/Fenske-Hall/FenskeHall.html

Chapter Two – Experimental

Section One

1.   **Data Collection of the Photoelectron Spectra for (η^6-arene)Cr(CO)$_3$ Complexes**

The gas-phase photoelectron spectra were collected at the center for Gas-phase Electron Spectroscopy at The University of Arizona using a photoelectron spectrometer equipped with a 36 cm hemispherical analyzer, custom designed aluminum sample cell, excitation source, and detection and control electronics that have been described in detail elsewhere.[1,2] All of the spectra were collected using He I photons and were calibrated with the argon $^2P_{3/2}$ ionization (15.759 eV). The resolution was determined by measuring the full-width-at-half-maximum of the argon $^2P_{3/2}$ ionization which was 0.015-0.030 eV during data collection. The spectra are intensity corrected by an experimentally determined instrument analyzer sensitivity function that assumes a linear dependence of analyzer transmission (intensity) to the kinetic energy of the electrons within the energy range of these experiments.[3]

All eight complexes were heated *in vacuo* to achieve sufficient vapor pressure in the gas phase for data collection and there was no sign of thermal decomposition or impurities. The conditions for sublimation were (at about 10^{-4} Torr): (η^6-C$_6$H$_6$)Cr(CO)$_3$ at 70 – 80 °C, (η^6-C$_6$H$_5$NMe$_2$)Cr(CO)$_3$ at 72 – 114 °C, (η^6-C$_6$H$_5$OMe)Cr(CO)$_3$ at 58 – 80 °C, (η^6-C$_6$H$_5$CO$_2$Me)Cr(CO)$_3$ at 64 – 78 °C, (η^6-C$_6$H$_5$CF$_3$)Cr(CO)$_3$ at 30 – 35 °C, (η^6-C$_6$H$_5$F)Cr(CO)$_3$ at 40 – 55 °C, (η^6-C$_6$Me$_6$)Cr(CO)$_3$ at 85 – 110 °C, and (η^6-C$_6$H$_5$Me)Cr(CO)$_3$ at 45 – 60 °C. The temperatures were monitored by a "K" type

thermocouple passed through a vacuum feed through and attached directly to the ionization cell.

The photoelectron spectra for the uncomplexed arenes were also collected. The conditions for sublimation were all samples at about 10^{-4} Torr. Liquid samples of C_6H_5F, $C_6H_5CF_3$, $C_6H_5NMe_2$, C_6H_5OMe, and $C_6H_5CO_2Me$ were volatile at room temperature *in vacuo*. Liquid samples were run from a glass side arm tube attached to the ionization chamber via a length of ¼" stainless steel tubing and sample pressure was controlled by a micro-metering valve. C_6Me_6 is a solid that required heating to 30 - 32 °C.

2.   Data Analysis of Photoelectron Spectra for $(\eta^6\text{-arene})Cr(CO)_3$ Complexes

The spectra of the valance ionization bands are fit with asymmetric Gaussians as previously described.[4,5] Each Gaussian is defined by a position, amplitude, and half-width at the high binding energy side of the peak and the low binding energy side of the peak. The reproducibility of the peak positions and half-widths are about ±0.02 eV (≈3σ level) for Gaussians that are well separated from others. However, the uncertainties are higher when two or more Gaussians are close and their parameters are dependent upon one another. Due to the fact that the metal ionization band had the a_1 and e bands overlapped, the vertical positions and relative energy ordering of the a_1 and e bands can't be determined with certainty. For comparison of metal-based ionization energies within this series of molecules, the onset of ionization was determined by taking the peak position of the lowest energy Gaussian used to define the shape of the metal-based ionization band and subtracting 90% of the half-width at the low binding energy side of the peak. The total half-width of the metal ionization band was determined by fitting the

band with three Gaussians and summing 90% of the half-width at the low binding energy side of first Gaussian, 90% of the half-width at the high binding energy side of third Gaussian, and the difference between the positions of the first and third Gaussian.[6]

3. Theoretical Studies for (η^6-arene)Cr(CO)$_3$ Complexes

Density Functional molecular orbital calculations and geometry optimizations were done on all eight complexes mentioned. The ionization energies were calculated for them from the Density Functional Single Points Energies. The Gaussian 03W (G03W 6.0.0.0v) software package was employed for all DFT calculations.[7] The reported calculations used B3LYP and the 6-31++G** basis set. Fenske-Hall (6.0005v) software was also used to determine the percent composition of the molecular orbitals.[8]

4. Syntheses of (η^6-arene)Cr(CO)$_3$ Complexes

The (η^6-C$_6$H$_6$)Cr(CO)$_3$ complex was purchased from Aldrich Chemical. All other complexes have been previously reported and were synthesized via previously reported methods.[9] In addition, these complexes were provided by the Hunter group.

Section Two

Basics on How to Use the Gaussian 03W Software Package[7]

1.   Background on Gaussian 03W Software Package

The Gaussian 03W software package is primarily a text based molecular modeling and computational program that runs in a Windows® environment. This means that the program uses input files which have the coordinates for the atoms in the molecule and the type of calculation to be run and these are created in simple text input files processing programs (*e.g.*, Notepad®). Similarly, the output files contain all of the final results from the calculations that were performed as text.

This type of program can be quite difficult for a beginner to use quickly and confidently. Graphical interface programs have been written to make software like Gaussian 03W easier to use for the novice. GaussView version 3.09 is such a program which aids in the creation of the input file and in viewing of the results. In the following text, the basic use of the GaussView program to run the Gaussian 03W software will be discussed.

2.   General Guidelines in Using Theoretical Results in Research

There are a few important things one should know before using theoretical results in a research project. First, one should have an idea of the level of errors in the method that one would be choosing for a particular system or set of systems. General Hartree-Fock methods are good for simple organic molecules. Density Functional Theory works well for the more computationally intensive transition metal containing complexes. Semi-

emprical methods are good for preliminary studies for various systems. Finally, Molecular Mechanics coupled with a high level *ab-intio* method about the active sites are good for work with large systems (*i.e.* proteins, dendrimers, and polymers). Density Functional Theory (DFT) and hybrid functionals at a 6-31G basis set has become a common method for computational results.

Next, it is usually a good idea to do a preliminary study of the system at hand. This means that one should run some calculations on the system at basis set that won't take long computational times to acquire a general understanding of the system and to guide how the higher level basis sets will be used. Also higher level basis set calculations should be guided by how the experimental data compared to the calculated results to insure errors in the calculated results are understood.

3.   Operating the Gaussian 03W Software Package

3a.   Drawing the Molecule

The GaussView 3.09 Software is how we run Gaussian 03W. First, open the GaussView 3.09 window. Then, begin to draw your molecule in the window much as you would with Chem Draw®, etc. Use the elemental, ring, R-group, biological, and/or custom fragments in the toolbar to draw your molecule. You can make modifications to the bond lengths and angles with the icons found in the toolbar.

3b.   Setting Point Groups

If you want to set the point group, go to Edit in the toolbar and in this menu click on the Point Group. Then, the Point Group Symmetry window will open and you check

the Enable Point Group Symmetry box. Next, click on the Symmetrize button to implement the point group. You can set the constraints to any point group you would like but it is a good idea to set it to a low symmetry point group (*i.e.*, C_1) because this will allow the molecule the freedom to break out of higher symmetry point groups. However, the lower the symmetry the longer the calculation. If you are running a high level geometry optimization, it might be better if you don't even enable the point group to ensure that there is not any point group constraints to bias the results.

3c.   Creating Checkpoint Files

To make various plots like MO plots you need to create a checkpoint file (*e.g.*, .chk for Gaussian 03). To do this, first open GaussView and create a molecule. Then, go to Edit in the toolbar and then to MOs in the edit menu. Now, the MOs window will open. Title the file in the Checkpoint File box and click generate. Then, the file will be generated by Gaussian 03.

3d.   Running a Calculation

After the molecule and checkpoint file have been generated, go to the toolbar and click on Calculate. Then, in this menu click on Gaussian. Next, a window will appear called Gaussian Calculation Setup. Now, click the tab Job Type. There are many types of calculation (*e.g.*, population analysis, geometry optimization, vibrational frequencies, and NMR data). Choose the calculation you want. [Note: It is important to notice that you need the geometry optimized whether it is from Gaussian 03 or empirical data. It is important because the atom will not be in the correct position otherwise and this will lead

to errors in the analysis. However, you can run non-optimized geometries when you want to look at excited state geometries.] You will need to set the method you wish to use on your system. First, click on the Method tab and choose the method (*e.g.*, Semi-Empirical, Hartee-Fock, or DFT), spin restrictions (*i.e.*, restricted, unrestricted, and restricted-open), basis set, spin multiplicity, and charge.

The other tabs are various settings you can make for the calculation. The Link 0 tab is the tab where you can set the checkpoint file by clicking on the Checkpoint File... button for the molecule that was created. [Note: You will need to create and set the checkpoint file if you want MO plots later. But, if no plots are desired, the checkpoint file is not necessary.] The Title tab is where you can give the job a title. The Solvation tab allows you to set a model to attempt to take solvation effects in to account (although the accuracy of this approach is debatable). The Guess tab is where you can set the method for your calculation's initial guess. One important feature in the Gaussian Calculation Setup window is the Additional Keywords where you can add other specialized commands that are found in the Gaussian 03 User Guide.

After the calculation is ready, click on the submit button. GaussView will ask you to save the input file (*e.g.*, .gjf for Gaussian 03). Name it and save it. Gaussian 03 will begin to run the calculation and when it is complete an output file (*e.g.*, .log for Gaussian 03) will be created. You can view this file with a text editor or with GaussView.

To use GaussView to view the data, open the output file in GaussView and go to Results in the toolbar. In this menu, click on the data you wish to view. To view specific bond lengths and angles, open the menus that allow you to modify the bonds and then highlight the bond angle or length.

3e.   **Creating Plots**

To make various plots (*e.g.*, MO plots), you need to create a checkpoint file (*e.g.*, .chk for Gaussian 03). To do this, first open the <u>checkpoint file</u>. Then, go to <u>Edit</u> in the toolbar and then to <u>MOs</u> in the edit menu. Now, the MOs window will open. It may be necessary to load the checkpoint file in the MOs window if the file didn't load. You can use the <u>New</u> tab to set the type to <u>Read Checkpoint File</u>. Then, type the path and file name in <u>Checkpoint File</u> box and click <u>load</u>. After the file is loaded, go to the <u>Visualization</u> tab and select the MO's that you wanted plotted. Now, click update and Gaussian 03 will plot the MO's in cube files (*e.g.*, .cub for Gaussian 03).

The cube files can be viewed in GaussView by opening the checkpoint file. Now, go to <u>Results</u> in the toolbar, and in this menu click on <u>Surfaces</u> which will open the <u>Surfaces and Cube</u> window. Then, open up the <u>MOs</u> window and have Gaussian 03 plot the cube files. You can then view the files in the <u>Surfaces and Cube</u> window. You can also save the cube file in the window by clicking on the <u>cube action</u> button and then <u>save</u> the file.

While you are in the <u>Surfaces and Cube</u> window, you can create other density plots by going to the cube action button. Then, click on <u>new cube</u> and then select what surface you would like to view (*e.g.*, electrostatic surface potentical). After calculation, you will need to load the plot by clicking on <u>surface action</u> button and then clicking on <u>new surface</u>. You can save them just as with the MO's cube files.

Section Three

Basics on How to Use the Fenske-Hall Software[8,10]

1.   Background on Fenske-Hall Software

Fenske-Hall version 6.0 is another text based molecular orbital calculator.[10] It is a faster method of calculation particularly for large molecules containing up to 99 atoms. It even runs well on older computers that have only a 250 MHz CPU and 64 Mb of RAM. For this program, an input file must created the with a text editor like Notepad[®]. Also, it is very important to know that Fenske-Hall only calculates molecular orbital, percent composition, population analysis, and the other information relevant to these calculations. Most importantly, it will not do geometry optimization. Thus, when creating an input file you must have an appropriate input geometry for the molecule. Otherwise the calculation you did is meaningless. The Fenske-Hall program does not have a viewing program, but the utility program MOPlot creates files that can be viewed with the general viewing program Molekel.[11]

2.   Operating the Fenske-Hall Software

2a.   Fenske-Hall Software

A Fenske-Hall calculation is rather tedious to prepare but is very efficient once it is running. First, to run a Fenske-Hall calculation you must have and/or generate five files in one folder on your computer's hard drive. The first is the fh6.exe file which is the Fenske-Hall program. Next is the mp3.exe file which is the plotter program. Then is the stofxn.dat file which contains all the basis sets for the atoms (this file can be viewed in

notepad). Finally, there is the customized .bat file which is used for executing the Fenske-Hall program and the .fhi file which is the input file.

2b.   Creating an Input File

To create an input file, you need a numerical representation of the positions of the atoms in the molecule. This can be done two ways in Fenske-Hall, either by a simple xyz coordinate system or by a z-matrix. [Note: The location of the atoms for the molecule must be in the optimized positions.] The xyz coordinate system is based on the values for the x-coordinate, y-coordinate, and z-coordinate in a basic three-dimensional Cartesian coordinate system for each atom.

Atoms	X	Y	Z
C	0.702995	-1.227908	-1.629135
C	1.414898	0.005142	-1.629135
C	0.711902	1.222766	-1.629135
C	-0.711902	1.222766	-1.629135
C	-1.414898	0.005142	-1.629135
C	-0.702995	-1.227908	-1.629135
H	1.245519	-2.165447	-1.589604
H	2.498091	0.004072	-1.589604
H	1.252572	2.161374	-1.589604
H	-1.252572	2.161374	-1.589604
H	-2.498091	0.004072	-1.589604
H	-1.245519	-2.165447	-1.589604
CR	0.000000	0.000000	0.111901
C	0.000000	1.515272	1.190229
C	1.312264	-0.757636	1.190229
C	-1.312264	-0.757636	1.190229
O	0.000000	2.480652	1.836530
O	-2.148308	-1.240326	1.836530
O	2.148308	-1.240326	1.836530

Figure 2.3.1 Example of $(\eta^6\text{-}C_6H_6)Cr(CO)_3$ represented in the xyz coordinate system (.xyz file).[7]

A z-matrix representation of the molecule is a bit more complex to set up. It is made by positioning a primary atom then positioning subsequent atoms based on the lengths, angles, and dihedral angles for the previously placed atom(s). The lengths, angles, and dihedral angles are all found in the matrix. The first column of values is the lengths followed by the angles and the dihedral angles. It is important to know that Gaussian z-matrixes are in slightly different format than most z-matrixes, but Fenske-Hall does recognize it as a properly formated z-matrix.

Atoms		Lengths		Angles		Dihedral Angles
C						
C	1	1.42390252				
C	2	1.40606417	1	119.820105		
C	3	1.4238324	2	120.17452583	1	-0.53004013
C	4	1.40610499	3	119.8302556	2	0.50371556
C	1	1.40604948	2	120.17202133	3	0.53436065
H	1	1.08407898	6	119.95754709	5	177.41647761
H	2	1.08377206	1	120.01577568	6	177.91553025
H	3	1.08408017	2	119.97608844	1	177.3465241
H	4	1.08380886	3	120.00670066	2	177.84350013
H	5	1.08410016	4	119.96899617	3	177.41235126
H	6	1.08381343	1	120.0992104	2	-177.88154039
CR	5	2.24258171	4	71.90317749	3	54.56734209
C	13	1.85975322	5	118.99185694	4	45.55188157
C	13	1.85987227	5	151.24607694	4	-136.67322436
C	13	1.85981161	5	89.4238744	4	134.93039985
O	14	1.16169435	13	178.35469523	5	-48.13168211
O	16	1.16168981	13	178.41718395	5	14.68763779
O	15	1.16166881	13	178.37172637	5	47.51382674

Atom Labels

Figure 2.3.2 Example of $(\eta^6\text{-}C_6H_6)Cr(CO)_3$ represented as a z-matrix from Gaussian.[7]

As stated earlier, it is important to have an appropriate geometry because Fenske-Hall doesn't compute geometry optimization. The geometry can be found in the literature

as a solved microwave or crystal structure. Also, an optimized structure can be extracted from a Gaussian 03 output file. It is important to know that when using a Gaussian 03 output file for an optimized structure that a geometry optimization calculation has been run and that the last "Standard orientation" for the XYZ coordinates or last Z-matrix are used for the optimized structure. Also, when using Gaussian 03 to generate an optimized structure, it is important to know that you must have the molecule lying in the correct orientation because Fenske-Hall has rigidly defined coordinates. Thus, the z coordinate is coming out of the plane of the computer screen, and the x and y coordinates are in the plane of the computer screen with x coordinate being horizontal and y coordinate being vertical. If you don't have the correct orientation, you will see odd results for the percent compositions of the orbitals. You can try to fix this by switching the coordinates around to reorient the molecule to the proper axis.

After you have obtained a Z-matrix or a molecule in XYZ coordinates, you can construct the input file. We will first go though the input file with an XYZ coordinate system. I prefer a XYZ coordinate system rather than Z-matrix because XYZ coordinate systems are easier to manipulate. Both type of input files are almost the same but with few differences as seen below (**Figure 2.3.3**).

```
Number of atoms
Name of molecule
XYZ coordinate system or Z-matrix representations of the molecule

charge=?

additional commands

end of input
```

Figure 2.3.3 Generic input file for Fenske-Hall.

To construct the input file with a xyz coordinate system, you first need to open Notepad. Then, on the first line write the number of atoms in the molecule. Next, write the name of the molecule and insert your molecule represented in a xyz coordinate system. [Note: Most elements that have two letter symbols have both of the letters capitalized (*e.g.*, Chromium is Cr, so input CR). You can check the stofxn.dat file for exceptions.] The next line after the molecule was added should be a blank space. In the next line, you enter the charge of the molecule followed by a space for the next line. Then, you can put in additional commands if you want to generate MO plots, transform basis sets, or carry out other commands. You can create MO plots by writing "density" on the next line and then in the following lines you can put the various HOMO's and LUMO's that you want. The final line is always "end of input".

```
19
tricarbonyl(eta6-benzene)chromium
C         0.702995   -1.227908   -1.629135
C         1.414898    0.005142   -1.629135
C         0.711902    1.222766   -1.629135
C        -0.711902    1.222766   -1.629135
C        -1.414898    0.005142   -1.629135
C        -0.702995   -1.227908   -1.629135
H         1.245519   -2.165447   -1.589604
H         2.498091    0.004072   -1.589604
H         1.252572    2.161374   -1.589604
H        -1.252572    2.161374   -1.589604
H        -2.498091    0.004072   -1.589604
H        -1.245519   -2.165447   -1.589604
CR        0.000000    0.000000    0.111901
C         0.000000    1.515272    1.190229
C         1.312264   -0.757636    1.190229
C        -1.312264   -0.757636    1.190229
O         0.000000    2.480652    1.836530
O        -2.148308   -1.240326    1.836530
O         2.148308   -1.240326    1.836530

charge=0

density
homo -1
homo
lumo
lumo +1

end of input
```

Figure 2.3.4 Example of an input file for (η^6-C_6H_6)Cr(CO)$_3$.

You now need to save the file. You can do this by going to Save As in the File menu as you would do with any other program but the unique thing that must be done is defining the file type as .fhi which is the Fenske-Hall input file type. This all can be done by setting the file type as All Files in the Save As window. Then type in the name for the file and end it with .fhi (*i.e.*, (arene)Cr(CO)3.fhi). Then, click <u>save</u> and you have created an input file.

The Z-matrix input file is almost the same but with a few differences. One thing is that on the line with the number of atoms you will need to put the word "zmatrix" to signify that the Z-matrix will be used for the input. The other thing is that you need to put in a Z-matrix instead of xyz coordinate system.

```
19 zmatrix
tricarbonyl(eta6-benzene)chromium
C
C   1   1.42390252
C   2   1.40606417   1   119.820105
C   3   1.4238324    2   120.17452583   1    -0.53004013
C   4   1.40610499   3   119.8302556    2     0.50371556
C   1   1.40604948   2   120.17202133   3     0.53436065
H   1   1.08407898   6   119.95754709   5   177.41647761
H   2   1.08377206   1   120.01577568   6   177.91553025
H   3   1.08408017   2   119.97608844   1   177.3465241
H   4   1.08380886   3   120.00670066   2   177.84350013
H   5   1.08410016   4   119.96899617   3   177.41235126
H   6   1.08381343   1   120.0992104    2  -177.88154039
CR  5   2.24258171   4    71.90317749   3    54.56734209
C  13   1.85975322   5   118.99185694   4    45.55188157
C  13   1.85987227   5   151.24607694   4  -136.67322436
C  13   1.85981161   5    89.4238744    4   134.93039985
O  14   1.16169435  13   178.35469523   5   -48.13168211
O  16   1.16168981  13   178.41718395   5    14.68763779
O  15   1.16166881  13   178.37172637   5    47.51382674

end of file
```

Figure 2.3.5 Example of an input file for (η^6-C_6H_6)Cr(CO)$_3$ with a Z-matrix.

2c.   Creating a Transformed Basis Input File

If you are interested in creating a molecular orbital diagram, then Fenske-Hall can do this with a transformed basis input file and the percent composition. A transformed basis input file is an input file that considers a ligand to be treated like an atom and also

considers the metal center with other possible ligands to be treated like an atom. In this way, you can relatively easily construct the molecular orbital diagram for ligand(s) and metal center(s) to show individual fragment-fragment interaction.

To make a transformed basis input file, first you must run a Fenske-Hall calculation on the ligand and the metal center separately. After those two calculations you will need the .mos file which contains a shorthand for the molecular orbital energies also known as brevity's coefficients. You will construct the input as you did before. However, after assigning the charge you will need to add the commands for a transformed basis set. Enter "lprint 1" and on the second line following this enter "transform." On the next line enter the total number of transformed basis (*e.g.*, total number of ligand(s) and the metal center(s)). On the following line, enter the number of metal centers transformed basis (*e.g.*, total number the metal center(s) in the final complex). Then, on the same line, write by total number of orbitals for a single metal centers transformed basis. This is immediately followed by an M, which means the metal center, and you put the number for the orbital at which you are starting. This would be "1" if it is the first transformed basis you put into the input file. In the following line, enter the name for all the orbitals of the metal centers transformed basis. This can be as simple as just "1 M1" for the first metal orbital or say if metal orbital 16 has mainly d_z^2 character you can put "16 z2." Now, you will need to add the .mos file's brevity's coefficients which will follow the series of "2.00000" that is a small population analysis in the .mos file. You will need to copy and paste all the brevity's coefficients into the input file. You will enter all the information about the ligand(s) as you did for the metal center and copy and paste all the

brevity's coefficients into the input file. On the final line, enter "end of input" and you

have now completed a transformed basis input file.

```
19
tricarbonyl(eta6-benzene)chromium_transform
C        0.702995    -1.227908    -1.629135
C        1.414898     0.005142    -1.629135
C        0.711902     1.222766    -1.629135
C       -0.711902     1.222766    -1.629135
C       -1.414898     0.005142    -1.629135
C       -0.702995    -1.227908    -1.629135
H        1.245519    -2.165447    -1.589604
H        2.498091     0.004072    -1.589604
H        1.252572     2.161374    -1.589604
H       -1.252572     2.161374    -1.589604
H       -2.498091     0.004072    -1.589604
H       -1.245519    -2.165447    -1.589604
CR       0.000000     0.000000     0.111901
C        0.000000     1.515272     1.190229
C        1.312264    -0.757636     1.190229
C       -1.312264    -0.757636     1.190229
O        0.000000     2.480652     1.836530
O       -2.148308    -1.240326     1.836530
O        2.148308    -1.240326     1.836530

charge=0

lprint 1

transform
2
1 33 M 1
1 M1 2 M2 3 M3 4 M4 5 M5 6 M6 7 M7 8 M8 9 M9 10 M10
11 M11 12 M12 13 M13 14 M14 15 M15 16 z2 17 xy 18 x2y2
19 yz 20 xz 21 M21 22 M22 23 M23 24 M24 25 M25 26 M26
27 M27 28 M28 29 M29 30 M30 31 M31 32 M32 33 M33
    -0.00036    0.00000    0.00000    0.00000    0.00000    0.02579    0.00000    0.00001
     0.05097   -0.20128    0.00000   -0.09712   -0.06674   -0.20124   -0.08409    0.04855
    -0.06673   -0.20121    0.08407    0.04854   -0.06672   -0.39672    0.00000    0.05237
     0.03496   -0.39657   -0.04534   -0.02618    0.03495   -0.39663    0.04535   -0.02618
     0.03495
(There are only 2 of 33 brevity's coefficients shown)
     0.00000    0.06329   -0.00207    0.00344   -0.10521   -0.00002    0.00921   -0.28161
    -0.00001   -0.63098   -0.00097   -0.87611   -0.61648    0.33334    0.41340   -0.20965
     0.32568    0.29759   -0.37090   -0.18400    0.29076    0.96912    0.00036   -0.55093
    -0.35887   -0.45708   -0.22012   -0.13842    0.16926   -0.51197    0.24733   -0.15371
     0.18959
1 30 L 34
1 L1 2 L2 3 L3 4 L4 5 L5 6 L6 7 L7 8 L8 9 L9 10 L10 11 pi1 12 L12 13 L13
14 pi2 15 pi3 16 pi4 17 pi5 18 pi6 19 L19 20 L20 21 L21 22 L22 23 L23
24 L24 25 L25 26 L26 27 L27 28 L28 29 L29 30 L30
     0.26197   -0.01646    0.02463   -0.00001    0.26199   -0.02957    0.00195   -0.00001
     0.26200   -0.01311   -0.02658   -0.00001    0.26202    0.01310   -0.02659   -0.00001
     0.26203    0.02958    0.00195   -0.00001    0.26199    0.01646    0.02464   -0.00001
     0.03203    0.03204    0.03204    0.03204    0.03204    0.03203
(There are only 2 of 30 brevity's coefficients shown)
    -0.80546    0.34243   -0.49204    0.00224    0.80547   -0.59733    0.05054   -0.00224
    -0.80546    0.25489    0.54258    0.00224    0.80546    0.25489   -0.54258   -0.00224
    -0.80547   -0.59733   -0.05054    0.00224    0.80546    0.34242    0.49204   -0.00224
    -0.05831    0.05831   -0.05831    0.05831   -0.05831    0.05831

end of input
```

Figure 2.3.6 Example of an transformed basis input file for $(\eta^6\text{-}C_6H_6)Cr(CO)_3$.

2d.   Running a Fenske-Hall Calculation

After you have created the input file, you will want to run the calculation. You will need to have the five essential files in one folder on the hard drive and those five files are the fh6.exe, mp3.exe, stofxn.dat, and "your" .fhi and .bat files. The only thing you will need to create at this point is the .bat file. This can be done be copying a previous .bat file. Then, open the copy in Notepad® and change all of the old names in the file and the name the file to the name of "your" input file. After you have completed "your".bat file, double click on the .bat file with all the other files in the same folder. Now, the Fenske-Hall program should be running and will be complete in few moments. When it is done you should have new files in the folder. These new files are: .fho, which is the output file, .xyz, which is a file of the molecule, .mos, which contains the data for transformed basis, and, if you run MO plots, they will be there too. The MO plots will be .t41 files and the name of the file will state what orbital that it is. The .t41 file format is the standard cube text file format used by the Amsterdam Density Functional (ADF) package.

3.   Using Molekel

To view the MO plots, you will need to use the viewing program Molekel. Open Molekel and, in the black window, right click which should cause a menu to appear. Go to the first option which is Load. In this new menu, click on xyz and in the xyz format window, click Ok when you have set the first check (%s %f %f %f). Now, find the .xyz file for the molecule you want to view and accept it. Again right click on the black window and go to Surface in the menu that appears. In the first big box of the surface

window, set file type to adf tape41 and then click on load. Find the MO plot you want to load and accept it. In the surface window in the second big box, click add surface and both signs, set the cutoff (0.02), and finally click on the create surface button. Now, you should be able to view the plot. You can remove the plot by going back to the surface window and click on the delete surface button. [Note: Molekel can view many other file types from different programs not just Fenske-Hall.]

Honda, O. Kitao, H. Nakai, M. Klene, X. Li, J. E. Knox, H. P. Hratchian, J. B. Cross, C. Adamo, J. Jaramillo, R. Gomperts, R. E. Stratmann, O. Yazyev, A. J. Austin, R. Cammi, C. Pomelli, J. W. Ochterski, P. Y. Ayala, K. Morokuma, G. A. Voth, P. Salvador, J. J. Dannenberg, V. G. Zakrzewski, S. Dapprich, A. D. Daniels, M. C. Strain, O. Farkas, D. K. Malick, A. D. Rabuck, K. Raghavachari, J. B. Foresman, J. V. Ortiz, Q. Cui, A. G. Baboul, S. Clifford, J. Cioslowski, B. B. Stefanov, G. Liu, A. Liashenko, P. Piskorz, I. Komaromi, R. L. Martin, D. J. Fox, T. Keith, M. A. Al-Laham, C. Y. Peng, A. Nanayakkara, M. Challacombe, P. M. W. Gill, B. Johnson, W. Chen, M. W. Wong, C. Gonzalez, and J. A. Pople, Gaussian, Inc., Pittsburgh PA, 2003. (b) Hohenberg, P.; Kohn, W. *Phys. Rev.* **1964**, *136*, B864-B871. (c) Kohn, W.; Sham, L. J. *Phys. Rev.* **1965**, *140*, A1133-A1138. (d) *The Challenge of d and f Electrons*, Ed. Salahub, D. R.; Zerner, M. C. ACS, Washington, D.C.; 1989. (e) Parr, R. G.; Yang, W. *Density-functional theory of atoms and molecules* Oxford Univ. Press, Oxford; 1989. (f) Becke, A. D. *J. Chem. Phys.* **1992**, *96(3)*, 2155-2160. (g) Becke, A. D. *J. Chem. Phys.* **1992**, *97(12)*, 9173-9177. (h) Becke, A. D. *J. Chem. Phys.* **1993**, *98(7)*, 5648-5652.

8. Hall, M. B.; Fenske, R. F. *Inorganic Chemistry* **1972**, *11(4)*, 768-775.

9. (a) Hunter, A. D.; Mozol, V.; Tsai, S. D. *Organometallics* **1992**, *11*, 2251-2262.

   (b) Hunter, A. D.; Shilliday, L. *Organometallics* **1992**, *11*, 1550-1560.

10. Additional information on the internet at the following site and link there in: http://www.chem.arizona.edu/~dll518/Fenske-Hall/FenskeHall.html

11. Flukier, P.; Luthi, H. P.; Portmann, S.; Weber, J. *Molekel 4.1*; Swiss Center for Scientific Computing: Manno, Switzerland, 2000-2001.

Section Four

References

1. Lichtenberger, D. L.; Kellogg, G. E.; Kristofzski, J. G.; Page, D.; Turner, S.; Klinger, G.; Lorenzen, J. *Rev. Sci. Instrum.* **1986**, 57, 2366.

2. Siegbahn, K.; Nordling, C.; Fahlman, A.; Nordberg, R.; Hamrin. ESCA: Atomic, *Molecular and Solid State Structure Studied by Means of Electron Spectroscopy*; Almqvist & Wiksells: Uppsala; 1967.

3. Westcott, B. L.; Gruhn, N. E.; Enemark, J. H., "Evaluation of Molybdenum – Sulfur Interaction in Molybdoenzyme Model Complexes by Gas-Phase Photoelectron Spectroscopy. The 'Electronic Buffer' Effect." *J. Am. Chem. Soc.* **1998**, 120, 3382-3386.

4. Lichtenberger, D. L.; Copenhaver, A. S. *J. Electron Spectrosc. Relat. Phenom.* **1990**, 50, 335.

5. Westcott, B. L.; Gruhn, N. E.; Enemark, J. H. *J. Am. Chem. Soc.* **1998**, *120*, 3382-3386 and references therein.

6. Cotton, F. A.; Gruhn, N. E.; Gu, J.; Huang, P.; Lichtenberger, D. L.; Murillo, C. A.; Van Dorn, L. O.; Wilkinson, C. C. *Science* **2002**, *298*, 1971.

7. (a) Gaussian 03, Revision B.04, M. J. Frisch, G. W. Trucks, H. B. Schlegel, G. E. Scuseria, M. A. Robb, J. R. Cheeseman, J. A. Montgomery, Jr., T. Vreven, K. N. Kudin, J. C. Burant, J. M. Millam, S. S. Iyengar, J. Tomasi, V. Barone, B. Mennucci, M. Cossi, G. Scalmani, N. Rega, G. A. Petersson, H. Nakatsuji, M. Hada, M. Ehara, K. Toyota, R. Fukuda, J. Hasegawa, M. Ishida, T. Nakajima, Y.

Chapter Three – Results and Discussion

Theoretical and Spectroscopic Studies of the Structure-Property Relationships in the Mono-substituted (η^6-arene)Cr(CO)$_3$ Complexes

1.   Theoretical Studies of the Mono-substituted (η^6-arene)Cr(CO)$_3$ Complexes

1a.   Overview

Hybrid functional (B3LYP) studies were done on the eight (η^6-arene)Cr(CO)$_3$ complexes having arene = C_6H_6, C_6Me_6, and C_6H_5X where X = CF$_3$, F, CO$_2$Me, Me, OMe, NMe$_2$. These studies were mainly conducted to give some added insight to the structural-property relationship[1] in the complexes and to aid in the assignments in the photoelectron spectra.

In the past, there have been multiple computational studies done on the parent complex, benzenechromiumtricarbonyl.[2,3] These studies were broadly comparable to each other yet they did differ in the assignment of the HOMO. The *ab intio* study reported e orbital as the HOMO[3] while the extended Hückel study reported a$_1$ orbital as the HOMO.[2] Howell *et al.*, who followed extended Hückel study by Albright *et al.*, seem to believe that the a$_1$ is the HOMO because of the correlation between the oxidation potentials of the (η^6-arene)Cr(CO)$_3$ complexes and the free arenes.[4] They noted that the slope for the line on the plot of these two potential was small implying that there was not much of an influence of the arene's structure on the bonding of the complex. Since the calculated a$_1$ orbital is almost all on the Cr(CO)$_3$ fragment with little overlap from the arene, the a$_1$ orbital has a probability of being the HOMO. They seem to fail to consider that the e orbital as well has a 88%[5] Cr(CO)$_3$ fragment character. Even so, the implication

that the arene doesn't dramatically affect the e and a_1 orbitals seems to hold true because in the first ionization band, which contain both the e and a_1 ionzation bands, we only see a broadening of the band based on the π-donor/acceptor ability of the arene, which will be discussed later.

Even though there has been ambiguity some of the molecular orbital calculations in the past, I have a degree of trust in the study that was conducted here because these molecular orbital calculations seem to fit the photoelectron spectra within reason and the calculated structures, expect for the complexes containing π-accepting substituents, were very consistent with the reported X-ray structures.[1b-f] Complexes containing π-accepting substituents did not follow the observed distortion in the arene on the reported X-ray structures as well the π-donor substituents complexes. This difficuly with the calculated structures was seen in past computational studies.[6]

1b.   B3LYP Molecular Orbital Calculations

The molecular orbital calculations done on the eight complexes showed that the frontier molecular orbitals are closely related to those of the parent complex, benzenechromiumtricarbonyl. There are some exceptions in some mono-substituted complexes where the bulk character of the orbital is from the substituent in the HOMO-3 of the NMe_2 substituent and in the HOMO-3 and HOMO-4 of the CO_2Me and where there is a split in the e orbitals.

The frontier molecular orbitals for the benzenechromiumtricarbonyl were as expected. The HOMO and HOMO-1 was calculated to be of e symmetry which has substantial character from the chromium's d_{xy} and $d_{x^2-y^2}$ orbitals and some character from

the arene's π^* LUMO. The next occupied orbital, HOMO-2, is of a_1 symmetry which is predominantly on the $Cr(CO)_3$ fragment with character from the chromium's d_z^2, p_z, s orbitals and very little overlap from the arene. This is followed by another set of e orbitals, which are mainly of the arene's π HOMO character with some chromium d_{xz} and d_{yz} character. The LUMO is an δ anti-bond between the chromium's d_{xy} and $d_{x^2-y^2}$ orbitals and the arene's π^* LUMO.
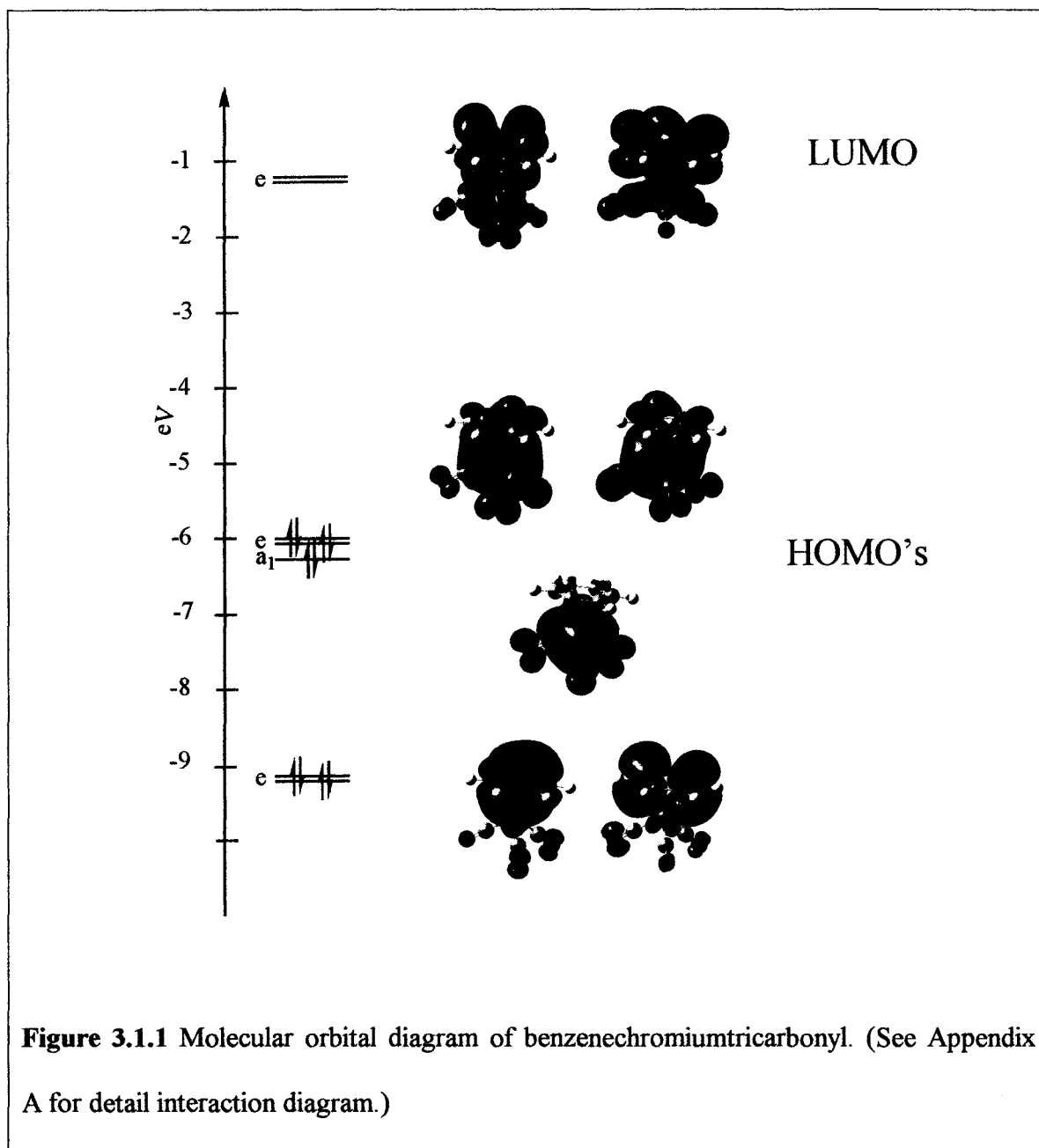
Figure 3.1.1 Molecular orbital diagram of benzenechromiumtricarbonyl. (See Appendix A for detail interaction diagram.)

The other seven complexes generally follow this model closely for the displayed molecular orbitals. The six mono-substituted complexes have split their e orbitals into lower symmetry a' and a" orbitals because of the reduction in symmetry of the complexes to C_s from C_{3v}. [Note: The $(C_6H_5OMe)Cr(CO)_3$ and $(C_6H_5CO_2Me)Cr(CO)_3$ complexes are technically C_1 symmetry. However for our purposes, we can consider them C_s

symmetry.] The $(C_6H_5NMe_2)Cr(CO)_3$ and $(C_6H_5CO_2Me)Cr(CO)_3$ complexes have the bulk character of the orbitals that are mainly from the substituent. The $(C_6H_5NMe_2)Cr(CO)_3$ complex has an a' orbital, HOMO -3, which correlates with the nitrogen atom's lone pair of electrons. The $(C_6H_5CO_2Me)Cr(CO)_3$ complex has two orbitals, HOMO -3 and HOMO -4, that consist of the π system about the carbonyl in the substituent.

B3LYP / 6-31++G**	LUMO +1	LUMO	HOMO	HOMO -1	HOMO -2
$(C_6H_5CF_3)Cr(CO)_3$	-1.706	-1.941	-6.277	-6.293	-6.449
$(C_6H_5CO_2Me)Cr(CO)_3$	-1.454	-2.168	-6.103	-6.112	-6.268
$(C_6H_5F)Cr(CO)_3$	-1.405	-1.623	-6.064	-6.096	-6.277
$(C_6H_5Me)Cr(CO)_3$	-1.258	-1.316	-5.828	-5.852	-6.015
$(C_6H_5OMe)Cr(CO)_3$	-1.044	-1.351	-5.745	-5.828	-5.975
$(C_6H_5NMe_2)Cr(CO)_3$	-0.813	-1.148	-5.476	-5.619	-5.736
$(C_6H_6)Cr(CO)_3$	-1.365	-1.366	-5.920	-5.921	-6.087
$(C_6Me_6)Cr(CO)_3$	-0.901	-0.904	-5.461	-5.464	-5.708
	HOMO -3	HOMO -4	HOMO -5	HOMO -6	HOMO -7
$(C_6H_5CF_3)Cr(CO)_3$	-9.431	-9.441	-10.998	-11.105	-11.182
$(C_6H_5CO_2Me)Cr(CO)_3$	-8.289	-8.887	-9.087	-9.217	-10.343
$(C_6H_5F)Cr(CO)_3$	-8.914	-9.325	-10.837	-10.924	-11.070
$(C_6H_5Me)Cr(CO)_3$	-8.655	-8.973	-10.481	-10.541	-10.622
$(C_6H_5OMe)Cr(CO)_3$	-7.883	-9.021	-9.937	-10.101	-10.793
$(C_6H_5NMe_2)Cr(CO)_3$	-6.769	-8.788	-9.306	-10.264	-10.550
$(C_6H_6)Cr(CO)_3$	-9.055	-9.056	-10.726	-10.726	-10.844
$(C_6Me_6)Cr(CO)_3$	-7.846	-7.851	-9.601	-9.686	-9.687

Table 3.1.1 Eigenvalues of the orbitals. (in eV)

B3LYP / 6-31++G**	LUMO +1	LUMO	HOMO	HOMO -1	HOMO -2
$(C_6H_5CF_3)Cr(CO)_3$	a"	a'	a"	a'	a'
$(C_6H_5CO_2Me)Cr(CO)_3$	a"	a'	a"	a'	a'
$(C_6H_5F)Cr(CO)_3$	a'	a"	a'	a"	a'
$(C_6H_5Me)Cr(CO)_3$	a'	a"	a'	a"	a'
$(C_6H_5OMe)Cr(CO)_3$	a'	a"	a'	a"	a'
$(C_6H_5NMe_2)Cr(CO)_3$	a'	a"	a'	a"	a'
$(C_6H_6)Cr(CO)_3$	e		e		a_1
$(C_6Me_6)Cr(CO)_3$	e		e		a_1

	HOMO -3	HOMO -4	HOMO -5	HOMO -6	HOMO -7
$(C_6H_5CF_3)Cr(CO)_3$	a'	a"	a'	a"	a'
$(C_6H_5CO_2Me)Cr(CO)_3$	(a)	(a)	a'	a"	(a)
$(C_6H_5F)Cr(CO)_3$	a'	a"	a"	a'	a'
$(C_6H_5Me)Cr(CO)_3$	a'	a"	a"	a'	a'
$(C_6H_5OMe)Cr(CO)_3$	a'	a"	(a)	(a)	(a)
$(C_6H_5NMe_2)Cr(CO)_3$	a'	a"	a'	a"	a"
$(C_6H_6)Cr(CO)_3$	e		e		a_1
$(C_6Me_6)Cr(CO)_3$	e		a_1	e	

Table 3.1.2 Symmetry of the orbitals. ((a) are orbital that cannot be fitted to C_s.)

1c.   Structure-Property Relationships

The observed structural distortions in the $(\eta^6\text{-arene})Cr(CO)_3$ complexes have been noted in experimental and theoretical studies and seem to be related to the π-donor/acceptor ability of the arene's substituent(s). [1a-b,6] This is consistent with our results. We used $\Delta\pi$ parameter as a direct measurement of the substituent π-donor/acceptor ability[1a,12] and the ionization energies was indirect measurements of the complexes' electron richness. [Note: See below (pp. 111-112) for a more detailed definition of the $\Delta\pi$ parameter.] These two types of parameters are well correlated (see pp. 104, 112) and demonstrate that the π-donor/acceptor ability of the arene affects the electron density about the chromium.
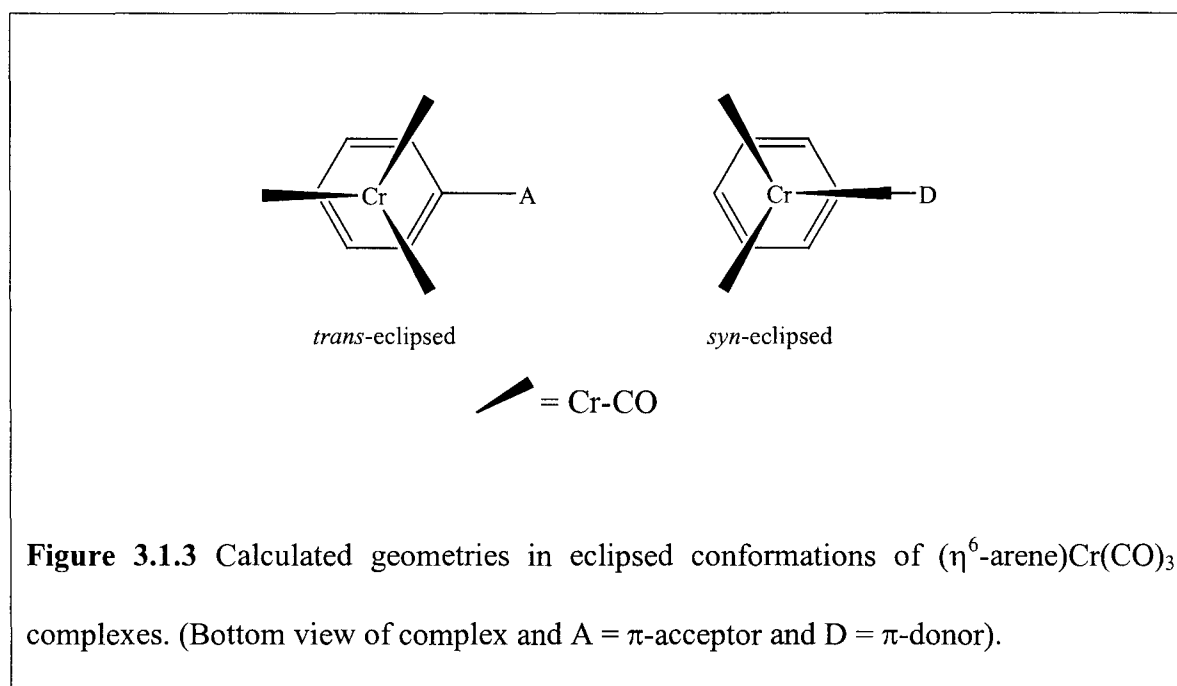
The magnitude of the e splitting was dependant on the magnitude of the π-donor/acceptor ability. When this calculated e splitting (i.e., $\varepsilon_{HOMO-1} - \varepsilon_{HOMO}$) for the HOMO was compared to the onset of ionization a good correlation was found (i.e., correlation coefficient (corr) = 0.91). Also, when the $\Delta\pi$ parameters were plotted against the calculated e splitting another good correlation was observed (i.e., corr = 0.90). These correlations show that the π-donor substituent complexes have a larger e splitting than do the π-acceptor complexes. The carbomethoxy substitute had an unexpectedly small e splitting. The reason for this is not apparent but is consistent with the fact that this compound is an "outlier" in all our studies.

The difference between the eigenvalues for HOMO and HOMO -2 orbitals, e and a_1, also is to be influenced by the π-donor/acceptor ability of the arene's substituent(s). This calculated splitting had a good correlation to $\Delta\pi$ and to the onset of ionization (i.e., corr = 0.98 and 0.83 for $\Delta\pi$ and onset of ionization, respectively).

Figure 3.1.2 Molecular orbital diagrams of the HOMO's for the mono-substituted complexes.
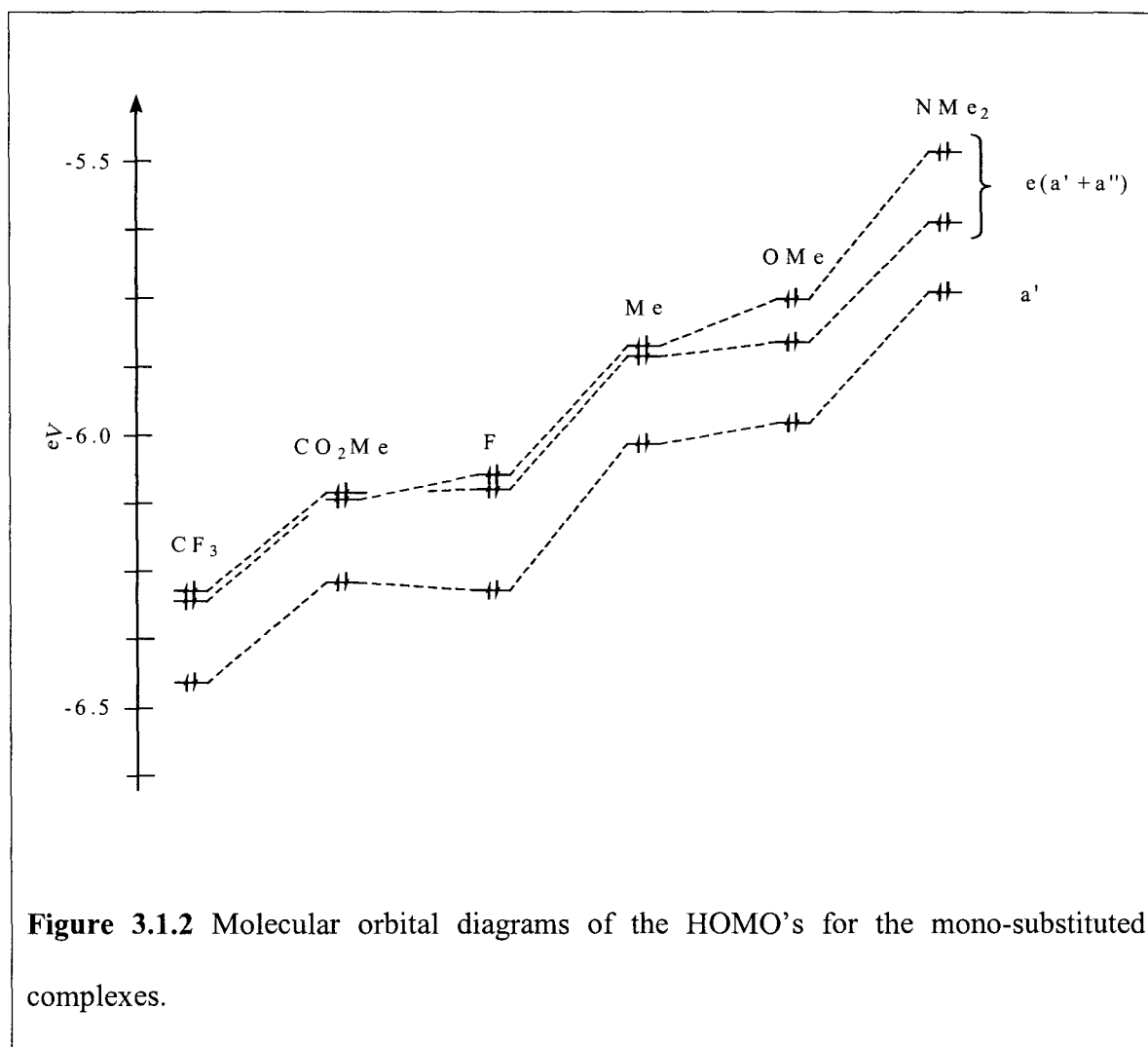
Another interesting structure-property relationship was found in the conformation of the carbonyl ligands relative to the arenes. The carbonyl ligands are observed to be influenced by the π-donor/acceptor ability of the arenes' substituent where a π-donor substituent leads to a *syn*-eclipsed geometry and a π-acceptor has a staggered geometry, as observed in the X-ray structure.[1b-f] In our theoretical study of the mono-substituted complexes, the calculated geometries did have the π-donor substituents exhibiting *syn*-eclipsed geometries (*i.e.*, with a carbonyl ligand under the substituent) and the π-acceptor substituents exhibiting *trans*-eclipsed geometries (*i.e.*, the carbonyl ligand not under the

substituent). There is a slight discrepancy for the π-acceptor complexes between the observed X-ray structures and calculated geometries. The calculated geometries are *trans*-eclipsed while the X-ray structures are reported as staggered. This discrepancy is likely due to solid-state effects on the solved X-ray structure. In particular, the calculations were done on isolated molecules (*i.e.*, in the gas phase) and any packing forces were not taken into account.

trans-eclipsed   syn-eclipsed

$\diagup$ = Cr-CO

Figure 3.1.3 Calculated geometries in eclipsed conformations of $(\eta^6$-arene)Cr(CO)$_3$ complexes. (Bottom view of complex and A = π-acceptor and D = π-donor).

It interesting to note that in the calculation the symmetries of the HOMO and HOMO -1 flip when the substituents' π-donor/acceptor ability changes. The symmetry ordering for π-donor substituents is a' > a" and for π-acceptor substituents it is a" > a' for the HOMO and HOMO −1, respectively. These orbitals are interesting because the a' is symmetric about the mirror plane in the molecule and has a probability of electron density about that mirror plane. While the a" is asymmetric about the mirror plane and

has zero probability of electron density about that mirror plane. Further investigation of this could lead the underlying reason for the two different conformations.

2. Photoelectron Spectra of the (η^6-arene)Cr(CO)$_3$ Complexes

2a. Assignment of the PES Bands

The photoelectron spectra were fitted with multiple bands as described below to show all ionizations that were expected from the theoretical studies. Thus, the first ionization band is expected to contain three metal base ionizations.[3,4] There followed additional arene and subtituent based ionizations between 9.5 to 12 eV (*i.e.*, in the window of the collected spectrum) In earlier PES studies of the parent complex, a single band was observed for the e and a$_1$ metal base ionizations. Hittier *et al.*[4] initially expected two resolved bands when only one is observed. Their expectation may be incorrect because their Hartee-Fock calculation didn't properly take into account the electron correlation effects. After considering the ^{2}E and ^{2}A$_1$ spin states, they determined that the ionizations from the e and a$_1$ symmetry orbitals should overlap each other resulting in the single band that is observed for the different ionizations.[3]

The curve fitting we did on the first ionization band, which will be referred to as the metal band because of the high metal character of the ionization, was done with three gaussian peaks representing the three ionizations. This curve fitting was used to get a better measurement of the total of the metal band width at half height and not, primarily, to find the position of the peaks. It must be strongly stressed that the position of these peaks has a relatively high level of error because of the lack of definition for the band. In this regard, the first and third gaussian are the most reliable and are the most reliable and

are fairly reproducible to about ± 0.05 eV. However, the second gaussian can be fit over a broader region between the first and third gaussians. The second gaussian was therefore assigned a position based on our expectation from the theoretical studies. As a result, argument will not be based on its position.

Because of this level of uncertainty in the positions of the peaks, we have used the onset of ionization,[7] rather than the position of the first peaks, for our correlation studies. Using the onset of ionization reduces the error to about ± 0.02 eV, but there are limitations to this approach as well. For example, using the position of the gaussian peaks and the predicted first ionization from calculations one finds that the hexamethyl substituted complex has a lower first ionization potential than the dimethylamine substituted complex while the onset of ionization has the dimethylamine substituent at the lower potential. Both techinques are reasonable but we are observing some discrepancy between the two because the two complexes have extremely close first ionizations (*i.e.*, predicted and observed,) and experimentally because of the relatively broad gaussian fits for the dimethylamine complex. However, this discrepancy is not unreasonable because it can be agued that any difference is within experimental error and the other complexes do not have this problem because they are widely spaced. Thus, we have chosen to use the onset of ionization as an index for the HOMO energies and our primary arguments because it has less uncertainty than using the position of the first Gaussian peak.

All of the complexes should experience Jahn-Teller distortion upon ionization. For this reason, we have fitted the e bands, even for the C_6H_6 and C_6Me_6, C_{3v} symmetry complexes with two gaussians to represent the Jahn-Tell distortion induced split. This

distortion should be small and constant though all of the complexes and is not expected to influence the results of out arguments.

Figure 3.1.4 Photoelectron spectra of mono-substituted complexes.
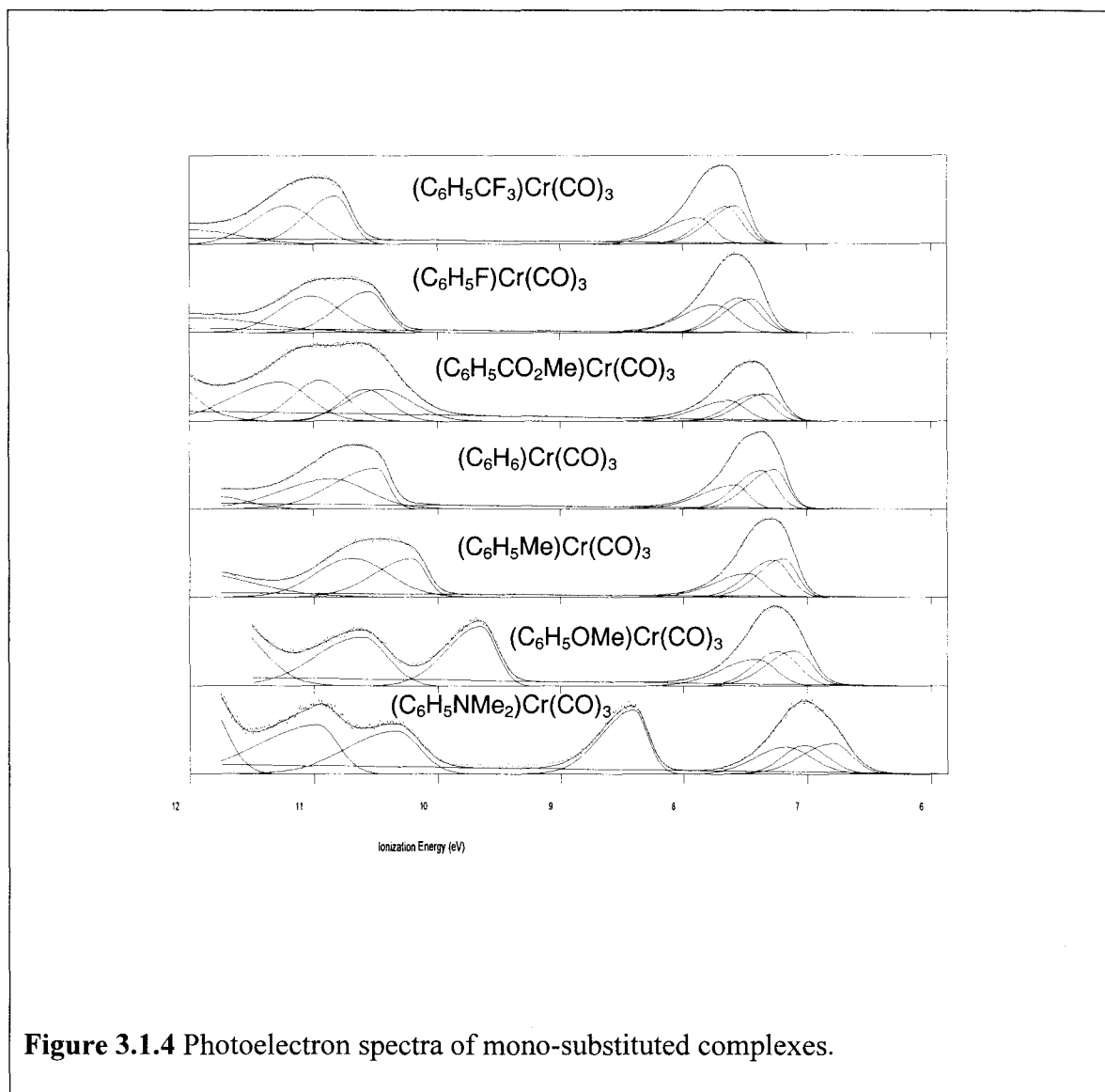
Molecule	Onset	Peak 1	Peak 2	Peak 3	Peak 4	Peak 5	Peak 6	Peak 7
$(C_6H_5CF_3)Cr(CO)_3$	7.35	7.57	7.65	7.87	10.82	11.22	-	-
$(C_6H_5F)Cr(CO)_3$	7.18	7.41	7.51	7.72	10.55	11.03	-	-
$(C_6H_5CO_2Me)Cr(CO)_3$	7.09	7.33	7.40	7.62	10.47	10.58	10.95	11.27
$(C_6H_6)Cr(CO)_3$	7.06	7.29	7.35	7.58	10.49	10.87	-	-
$(C_6H_5Me)Cr(CO)_3$	6.96	7.18	7.27	7.49	10.21	10.69	-	-
$(C_6H_5OMe)Cr(CO)_3$	6.82	7.10	7.24	7.39	9.65	10.61	-	-
$(C_6H_5NMe_2)Cr(CO)_3$	6.47	6.79	7.01	7.19	8.41	10.33	10.97	-
$(C_6Me_6)Cr(CO)_3$	6.50	6.72	6.84	6.99	9.30	9.66	-	-

Table 3.1.3 Table of peak positions and the onset of ionizations, eV. (Peaks are labeled numerically increasing form right to left in the spectra.)

2b. Metal Band Width in the PES

The total width at half height of the metal band, "total width", is an interesting parameter because it can give us information on the experimental values of the e splitting and the e and a_1 split, both in term of their magnitudes and especially their trends. However, the total width is a combination of the e splitting and the e and a_1 split. While it is true that a larger e and a_1 split would widen this band, it would also be expected to show a marked change to the feature in the band's shape (*i.e.*, a valley in the middle of the peak). Thus, we believe the trends found here are mainly from the e splitting. These splittings are correlated with the π-donor/acceptor ability of the arenes' substituent(s) as

shown also in our calculations. Finally, the total width of the metal band can give us some insight as to the origin of the complexed arenes' distortions.

The total width was compared to both the onset of ionization and $\Delta\pi$ parameter to demonstrate that the "total width" is related to the π-donor/acceptor ability of the arenes' substituent. A reasonable correlation was found (*i.e.*, *corrl.* = 0.80 and 0.91 for both the onset of ionization and $\Delta\pi$ plots, respectively) indicating that the total width was influenced by the π-donor/acceptor ability as observed in the calculations. Also, the total width was compared to the inductive parameter, σ_i,[8] and no substantial correlation was found (*i.e.*, *corrl.* = 0.29). This indicates that the total width is not significantly influenced by inductive effects transmitted by σ bonds.

Molecule	$\Delta\pi$ (ppm)	σ_i	Onset of Ionization (eV)	Total Metal Band Width (eV)
$(C_6H_5CF_3)Cr(CO)_3$	5.51	0.41	7.35	1.03
$(C_6H_5F)Cr(CO)_3$	-6.67	0.52	7.18	1.08
$(C_6H_5CO_2Me)Cr(CO)_3$	4.99	0.30	7.09	1.03
$(C_6H_6)Cr(CO)_3$	0.00	-	7.06	1.06
$(C_6H_5Me)Cr(CO)_3$	-2.94	-0.05	6.96	1.06
$(C_6H_5OMe)Cr(CO)_3$	-10.04	0.25	6.82	1.22
$(C_6H_5NMe_2)Cr(CO)_3$	-16.13	0.10	6.47	1.23

Table 3.1.4 Table of the total metal bands' width, $\Delta\pi$, σ_i, and Onset of IE's. (Taft's inductive parameter for uncomplexed arene.[8])
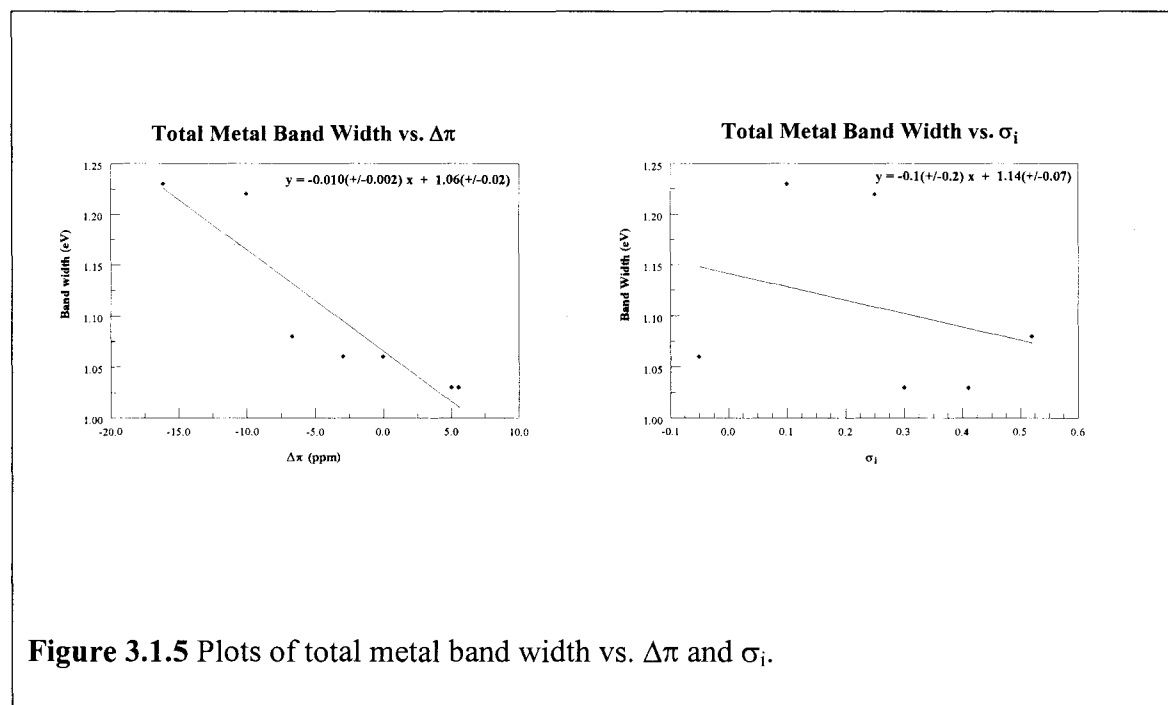

Figure 3.1.5 Plots of total metal band width vs. $\Delta\pi$ and σ_i.

Looking at the band positions and shapes more closely, we observed that we should first separate our complexes into two groups, the C_{3v} and C_s symmetry complexes. This must be done because the reduction of symmetry from C_{3v} to C_s increases the magnitude of the e split. However, this symmetry induced splitting should be relatively small and constant with in a point group. Looking at the two C_{3v} symmetry complexes, we observe that $(C_6H_6)Cr(CO)_3$ complex has a significantly smaller metal band width than does $(C_6Me_6)Cr(CO)_3$ complex and that the band is at a much higher potential. The fact that the metal band width is larger for $(C_6Me_6)Cr(CO)_3$ is constituent with the expected greater π-donor character of the Me verses H. The observation that the $(C_6Me_6)Cr(CO)_3$ complex's metal band position is shifted to a lower potential than $(C_6H_6)Cr(CO)_3$ is interpreted as being due to the δ bond between the chromium and the arene being slightly destabilized for $(C_6Me_6)Cr(CO)_3$ relative to $(C_6H_6)Cr(CO)_3$. In turn, because the δ bond has been destabilized and weakened the arene is allowed to move away for the chromium. Although, in this case, all of the subtiteunts are the same on the arene and thus no major distortion in arene planarity is observed when we apply this idea to the mono-substituted complexes we do see some interesting trends.
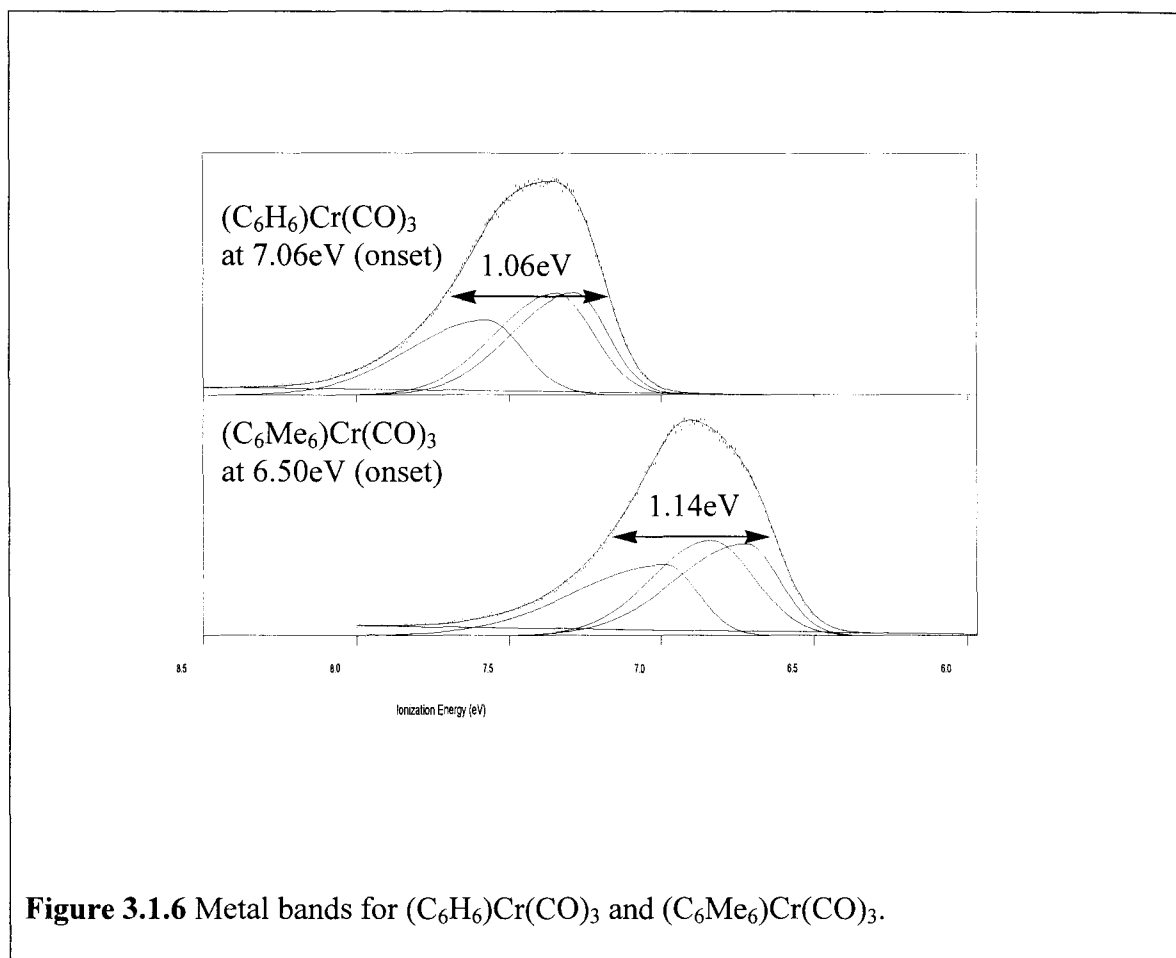
Figure 3.1.6 Metal bands for $(C_6H_6)Cr(CO)_3$ and $(C_6Me_6)Cr(CO)_3$.

If we look at the mono-substituted complexes with the same idea in mind, we observe some interesting events. First, looking at the π-donor substituents (*i.e.*, Me, OMe, and NMe_2) and using $(C_6H_6)Cr(CO)_3$ as the point of reference, it is observed that the stronger the π-donor the lower the potential of the band and the wider the bands' metal band width. Again using the argument stated above, we must conclude that a strong π-donor substutient results in a weaker chromium-arene bond. Weakening of the bond allows the arene to deform from full η^6 coordination to wards η^5 coordination as was proposed in the resounces structures and, concomitantly, has the substituent and its *ipso*-carbon moving away from the chromium. The strength of the π-donor substituent does

effect the magnitude of the distortion because the π-donor character effects the strength of the chromium-arene bond. Thus, as shown by X-ray structural data, strong π-donors there is a relatively large distortion while with weaker π-donors there is less distortion which is consistent with experimental observations.[1]

The π-acceptors substituted complexes (*i.e.*, CF_3 and CO_2Me) on the other hand, shift to higher potentials and have smaller total widths than the π-donor substituted complexes and the parent complex. The total widths for the CF_3 and CO_2Me substituents are the same at 1.03 eV within experimental error. This was not unexpected because the Δπ values for the two substituents are relatively close at 5.51 and 4.99 ppm, respectively. The shift to a higher potential for the metal bands of these π-acceptor complexes compared to the parent complex would indicate that the chromium-arene bond is strengthened for the π-acceptors substituents.

At first glance, this analysis of the fluoro substituent complex seems to fail. However, when considering that the fluoro substituents are known to have the strongest inductive withdrawing effects and to be only a moderate π-donor, we realize that there are two competing forces. From the argument above, the inductive withdrawal is causing the shift to higher potentials from the parent complex while the π-donation should cause a destabilization of the chromium-arene bond. Thus, the two forces should tend to cancel each other out, and we should observe for the fluoro substituent complex a near planar arene. Looking at the reported X-ray structure the fluoro substituent complex has the substituent and its *ipso*-carbon slightly away from the chromium. When the magnitude of this distortion is compared to a weaker π-donor such as methyl substituted complex, the

fluoro substituted complexes' distortion is found to be relatively smaller than if the fluoro

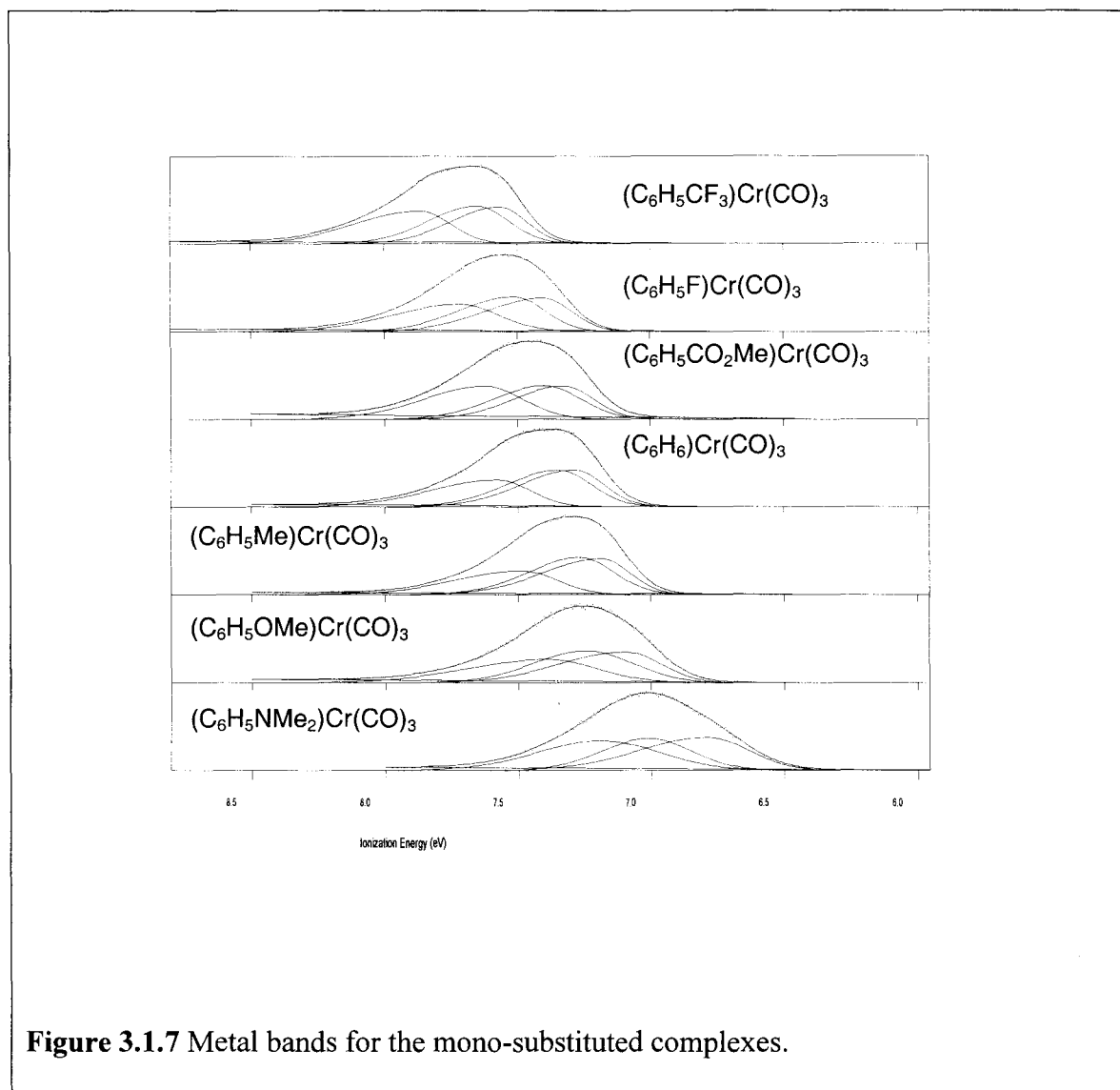substituted complex had only the π-donation effect occurring.

Figure 3.1.7 Metal bands for the mono-substituted complexes.

## 3. Spectroscopic Correlations to the Photoelectron Data

3a. Overview

All correlations were plotted as a function of the various ionization energies. Linear correlations were assumed and statistical analysis and plot were done using PSI Plot (32-bit edition, version 6.0). All of the spectroscopic data except for the PES and computed data were from previously reported sources.[1] Expanded scale plots and table of values are available in Appendix B.

x	y	COD	*Corrl*	Slope	y-int.
IE (onset)	$E^{o'}$	0.93	0.97	0.53($\pm$0.05)	-2.8($\pm$0.4)
IE (onset)	ν_{CO} (E)	0.92	0.96	58($\pm$7)	1490($\pm$50)
IE (e)	ν_{CO} (E)	0.93	0.97	65($\pm$7)	1420($\pm$50)
IE (onset)	ν_{CO} (A$_1$)	0.90	0.95	43($\pm$6)	1670($\pm$40)
IE (a$_1$)	ν_{CO} (A$_1$)	0.94	0.97	48($\pm$5)	1610($\pm$40)
IE (onset)	K^i_{CO}	0.76	0.87	-0.06($\pm$0.01)	0.8($\pm$0.1)
IE (onset)	K_{CO}	0.92	0.96	0.8($\pm$0.1)	9.1($\pm$0.7)
IE (onset)	δ_{ipso}	0.25	0.50	-40($\pm$30)	400($\pm$200)
IE (onset)	δ_{ortho}	0.33	0.57	20($\pm$10)	-30($\pm$80)
IE (onset)	δ_{meta}	0.72	0.85	-8($\pm$2)	150($\pm$20)
IE (onset)	δ_{para}	0.69	0.83	16($\pm$5)	-20($\pm$30)
IE (onset)	δ_{CO}	0.85	0.92	-4.6($\pm$0.8)	266($\pm$6)
IE (onset)	$\Delta\pi$	0.72	0.85	24($\pm$7)	-169($\pm$50)
IE (onset)	d_{Cr-CO} (X-Ray)	0.38	0.62	0.02($\pm$0.01)	1.70($\pm$0.07)
IE (onset)	d_{CrC-O} (X-Ray)	0.40	0.63	-0.008($\pm$0.004)	1.21($\pm$0.03)
IE (onset)	d_{Cr-CO} (DFT)	0.92	0.96	0.022($\pm$0.003)	1.70($\pm$0.02)
IE (onset)	d_{CrC-O} (DFT)	0.93	0.97	-0.0075($\pm$0.0008)	1.214($\pm$0.006)

Table 3.1.5 Correlation data.

3b.   Electrochemical vs. Photoelectron Data

One can usefully compare electrochemical potentials to ionization energies since both measure the energy for removing one electron from a system albeit in solution and the gas phase, respectively. Thus there should be a good correlation if the solvation effects are comparable between the two measurements. [Note: This has been demonstrated to be the case for many series of related compounds.][9] When the eight chromium complexes' previously reported formal redox potentials[1a] were plotted against the onset of ionization a linear correlation is observed with a slope of 0.53, and a correlation coefficient of 0.97. This coefficient is high enough to say there is a very strong correlation between the formal redox potentials and the onsets of ionization.

Electrochemical Data vs. The Onset of Ionizations

Figure 3.1.8 Plot of the Electrochemical Data vs. The Onset of Ionizations.
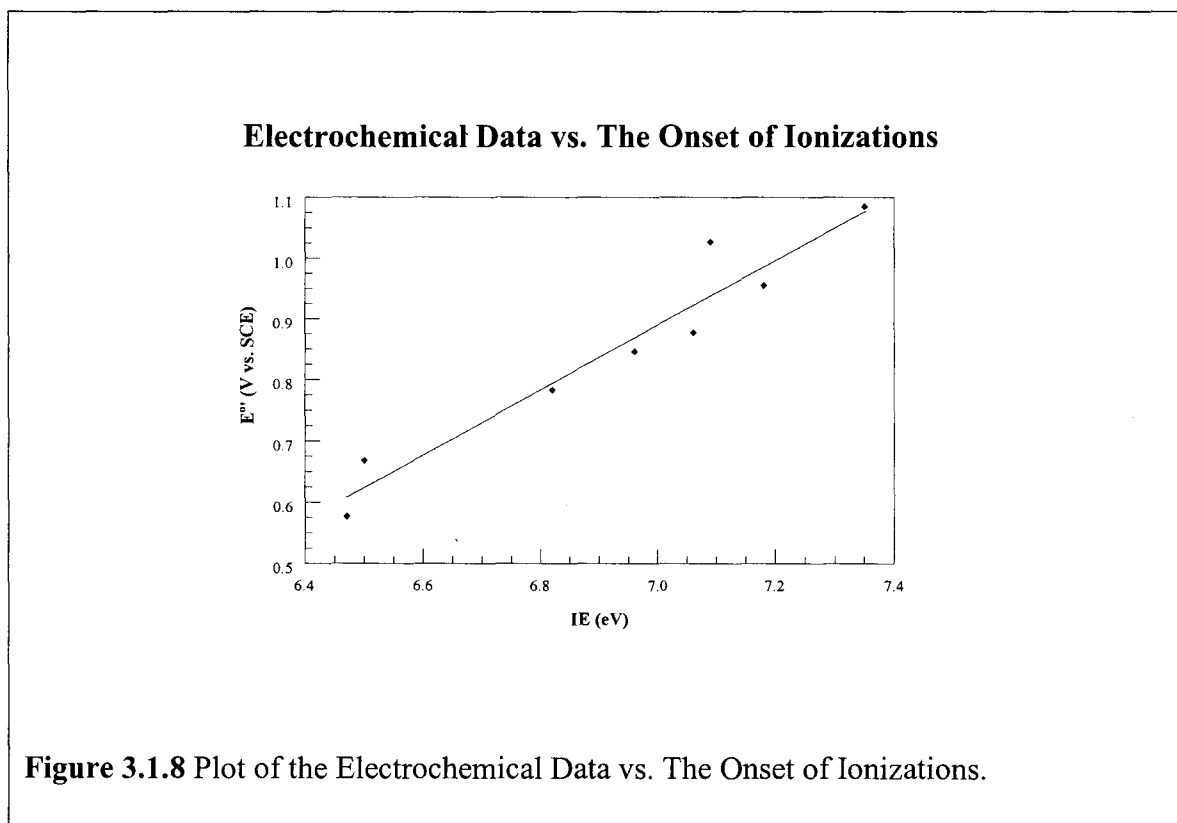
There are several issues arising from this graph that merit additional comments. Firstly, the two points for the dimethylamine and hexamethyl complexes are one area that has an outlying point. In the PES measurements, the onset of ionization are 6.47 eV and 6.50 eV for dimethylamine and hexamethyl complexes, respectively. Since ± 0.02 eV is a reasonable estimate of the error in the results, the two ionizations are roughly equivalent according to the PES data. These nearly equivalent ionizations are also observed in the DFT calculations where the difference in the ionization energies of two complexes is calculated to be 0.09 ± 0.05 eV with having the $(C_6Me_6)Cr(CO)_3$ complex being at the lower potential. The difference in the calculated HOMO energies was 0.02 ± 0.05 eV with again having $(C_6Me_6)Cr(CO)_3$ complex being at the lower potential. In spite of this similarity in their gas phase oxidations, the formal redox potentials for these complexes in CH_2Cl_2 were reported as 0.577 V and .668 V (V vs. SCE) for the dimethylamine and hexamethyl complexes, respectfully. The difference in the two potentials is $0.091 \pm 0.004V$, which would be considered a moderate to large difference for the reported potentials, and their order is also reversed.

Comparing this moderately large difference in formal redox potentials in solution to the small differences found from the PES data and DFT calculation in the gas phase, it seems likely that there is a solvent effect causing this discrepancy.[10] In particular, the dimethylamine substituent would, in one resonance form, have localized partial charges on the nitrogen and chromium atom. Thus, it is plausible that the solvent molecules arrange about the complex differently than they do for the hexamethyl species. Therefore, it is not unexpected that the solvent reorginization energy which contributes to the redox

potentials and is not seen in the PES data is significantly different between the two species.

The issue related to the carbomethoxy complex which might also be related to a solvent effect. However, the carbomethoxy complex is an outlying point in other correlations as well (*i.e.*, IR, NMR and structural data). Given these problems it is not clear if a solvent effect or some other unique effect occurring for the complex.
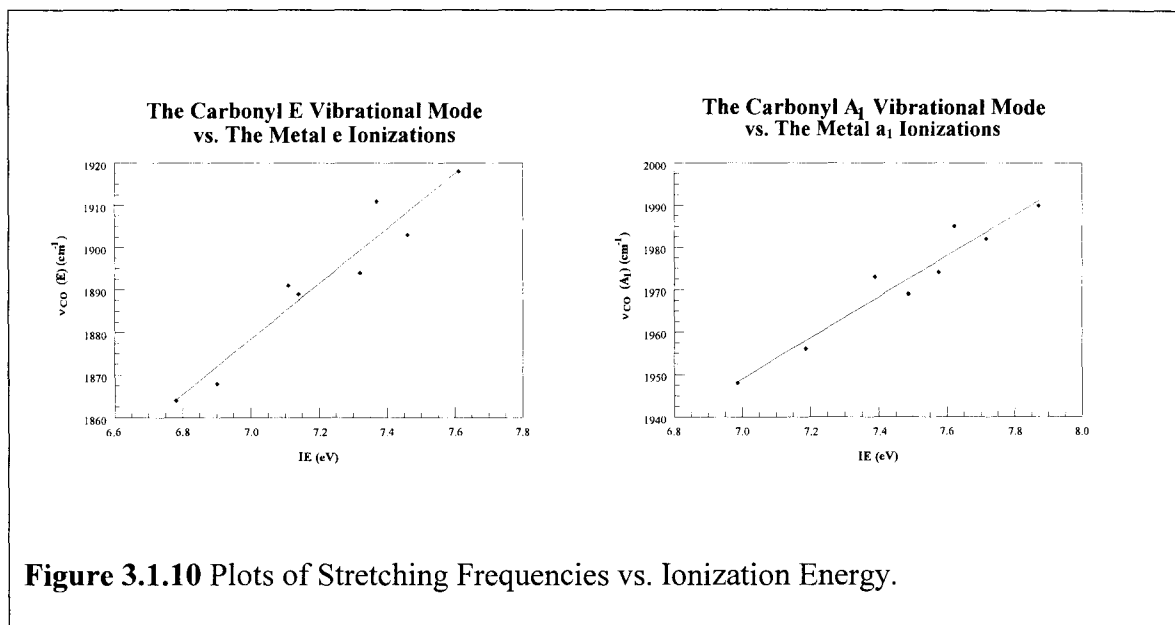
3c.   Infrared vs. Photoelectron Data

The photoelectron spectra were also correlated to previously reported infrared data for the carbonyl ligands.[1a] We have compared this data because the carbonyls' stretching frequencies are related to the electron density about the chromium atom.[1a] We have compared data for the two different types of carbonyl stretching frequencies, v_{CO} A_1 and v_{CO} E, the stretching force constant, K_{CO}, and the interaction stretching force constant, K^i_{CO}, to the onset of ionization of the metal ionization bands. It should be noted that there is a relatively large level of uncertainty in the position of the individual guassians of the metal bands which was addressed earlier.

The two different carbonyl stretching frequencies were plotted them against the onset of ionization. We found that these frequencies had good correlation coefficients of 0.96 and 0.95 for v_{CO} E and v_{CO} A_1, respectively. If one plots the individual types of frequencies with the onset of ionization, one gets an indication that the e ionizations are the first ionizations (*i.e.*, because the correlation for the v_{CO} E is slightly better than for v_{CO} A_1 against the onset of ionization.)

Figure 3.1.9 Plot of the Stretching Frequencies vs. The Onset of Ionizations.
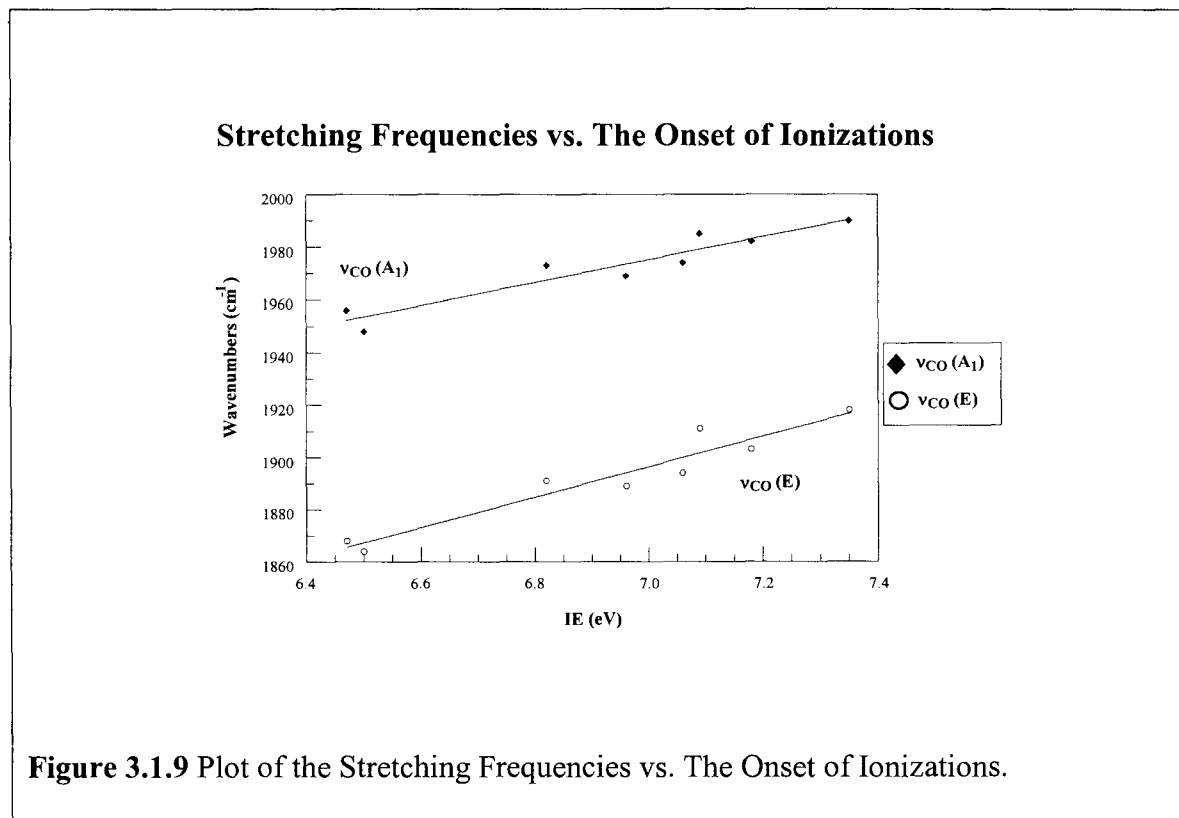
When we took the two different types of carbonyl stretching frequencies and plotted them against the proper type of ionization a better correlation was found for both plots. The A_1 bands plot had a correlation coefficient of 0.97. This moderate increase in the correlation could be an indication that we are assigning the a_1 type ionizations correctly. The E type bands were treated a bit differently in that the plot was constructed against the midpoint of position for the two metal e type ionizations because of the e splitting. The E type bands were fitted and had a correlation coefficient of 0.98. Again, this moderate increase in the correlation could are consistent with us assigning the e ionizations correctly.

**The Carbonyl E Vibrational Mode
vs. The Metal e Ionizations**

**The Carbonyl A₁ Vibrational Mode
vs. The Metal a₁ Ionizations**

Figure 3.1.10 Plots of Stretching Frequencies vs. Ionization Energy.

The two force constants were also plotted against the onset of ionization. The two

stretching force constants are a direct measure of the strength of the M-CO interaction

and thus they would be expected to show some correlation with the photoelectron spectra.

$$K_{CO} = 0.1346(v^2_{A1} + 2v^2_{E})$$

$$K^i_{CO} = 0.1346(v^2_{A1} - v^2_{E})$$

Equation 3.1.1 Definition of force constants, in units of 10^5 dyn cm^{-1}.[11]

The K^i_{CO} was found to have a correlation coefficient of 0.87, and the K_{CO} plot had a correlation coefficient of 0.96, with respect to the onset of ionization. This was not too surprising because the stretching frequencies used to derive the force constants where correlated to the onset of ionization.


Figure 3.1.11 Plot of the Stretching Frequency Force Constants vs. The Onset of Ionizations.
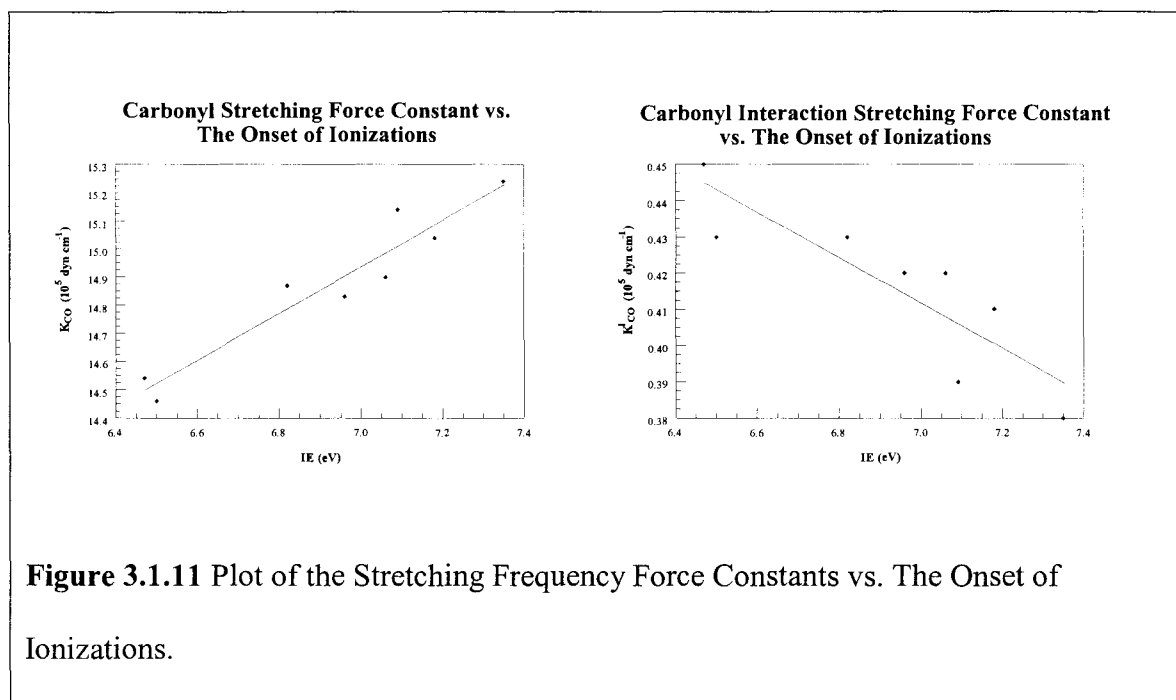
3d.   Nuclear Magnetic Resonance vs. Photoelectron Data

Nuclear magnetic resonance spectroscopic data was compared to the photoelectron spectra of the mono-substituted complexes. This was done because the chemical shift of particular carbons should give insight to π-donating and π-accepting effects in the arene and to the electron density about the metal center.[11]

When the previously reported chemical shifts for the carbonyl carbons were plotted against the onset of ionization, a good linear correlation was observed with a

correlation coefficient of 0.92. The slope of the line was negative. This was expected because high chemical shift and the low onset of ionization both imply high electron density about the metal and hence strong backbonding to carbonyl and vise versa for the low electron density case. The chemical shifts of the *ipso*, *ortho*, *meta* and *para*-carbons of the arene were also was plotted against the onset of ionization. The *ipso* and *ortho*-carbons did not have a very significant correlation to the onset of ionization (*i.e.*, correlation coefficient = 0.50 and 0.57, respectively), but the *meta* and *para*-carbons did have a correlation coefficient of 0.85 and 0.83, respectively.

Figure 3.1.12 Plot of the ^{13}C NMR Data vs. The Onset of Ionizations. (See Appendix B for *ipso*, *ortho*, *meta*, and *para*-carbons plots.)
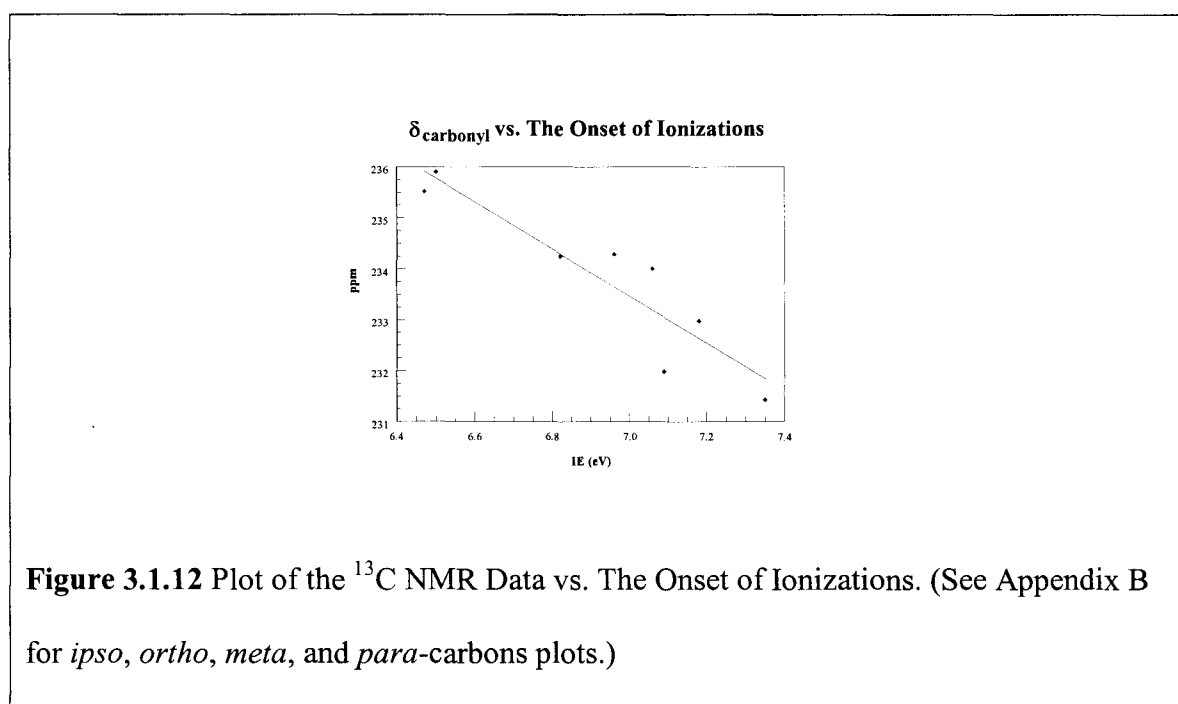
The $\Delta\pi$ parameters were also plotted against the onset of ionizations. The $\Delta\pi$ parameter is defined as the difference between the chemical shift values for the *para*-carbons and *meta*-carbons, and the $\Delta\pi$ parameter is associated with only the π-electron

donating/accepting ability of the substituent. Thus, it is expected that the π-donors have lower onsets potentials and acceptors raise the onset potentials.[11,12] The observed correlation coefficient is 0.85. The point for the fluoro substitutent was the major outlying point. This is not unexpected because fluoro substitutents are modrate π-donors but are the strongest inductive electron withdrawing groups. If the fluoro substitutent is removed from the plot, the correlation increases to an correlation coefficient of 0.95. The correlation has a positive slope which means as $\Delta\pi$ increases the ionization energies increase as expected.

Figure 3.1.13 Plot of $\Delta\pi$ vs. The Onset of Ionizations.
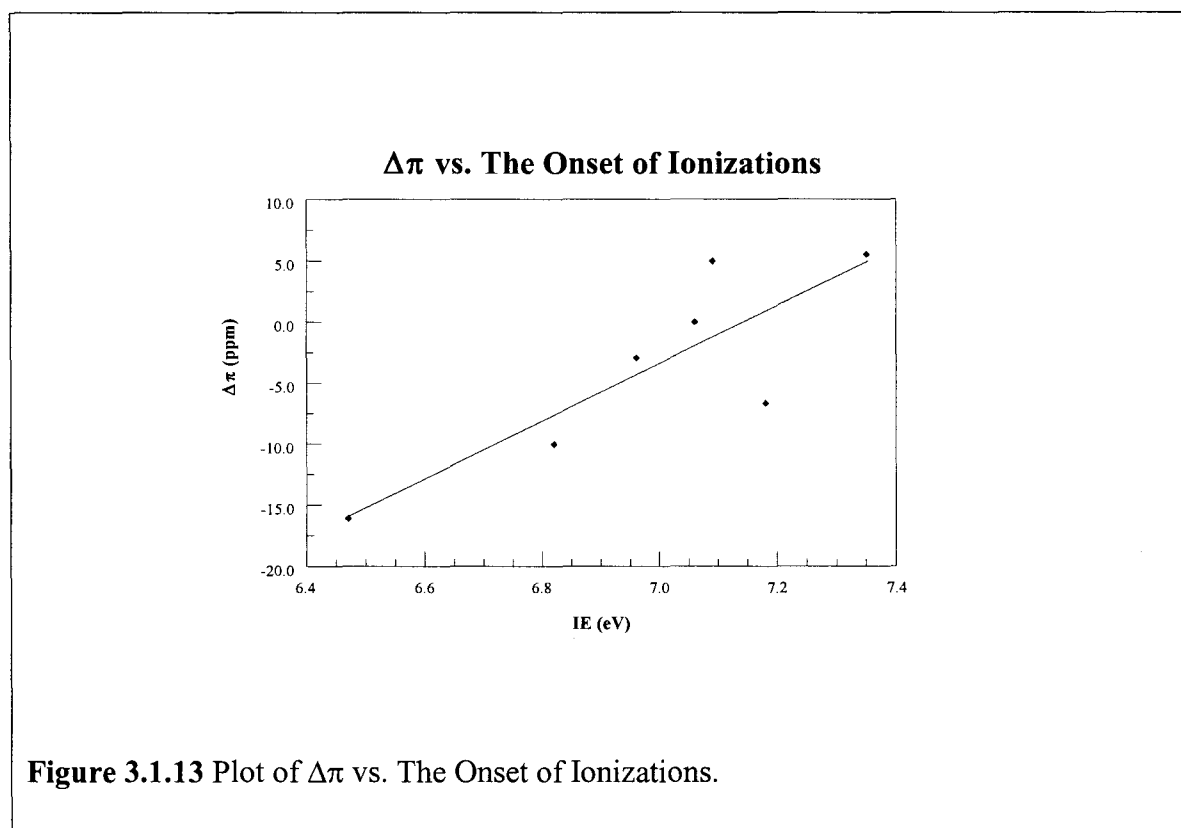
3e.   Structural Data vs. Photoelectron Data

We have also compared various structural properties of the eight complexes with the photoelectron spectra. We looked at the bonds between the metal and carbonyl carbon and the carbon and oxygen atoms in the carbonyl. These bonds were examined because the bonds about the carbonyl should be strongly effected by the metal center's electron density due primarily to backbonding effects. If the metal center has low electron density, it should cause the bond between the metal and carbonyl to reduce in bond order which will lead to the metal and carbonyl bond increasing in length. On the other hand, low electron density should increase the bond order between the carbon and oxygen atoms in the carbonyl which will lead to carbon and oxygen bond being shorter. A high electron density about the metal center should have an opposite effect where the bond order increases between the metal and the carbonyl and reduces between the carbon and oxygen atoms. Thus leading to a shorter bond between the metal and carbonyl and a longer carbon-oxygen bond.[11]

When plots were made of previously reported X-ray structural data against (some collected because of the requirements of this thesis) the onset of ionization, only a weak correlation is observed. The correlation coefficient for the metal-carbonyl bond length was 0.62 and for the carbon-oxygen bond length was 0.63. These are obviously weak correlations, yet, when considering that the reported X-ray structures data was collected at different temperatures, at multiple levels of accuracy, and the possibility of solid-state effects, this low correlation is acceptable. That is, it may be due to the error in the crystallographic data as well as packing effects. A systematic study of X-ray or

microwave structures (at constant temperature and in the gas phase, respectively) would

be warranted.

Figure 3.1.14 Plot of the X-ray Structural Data vs. The Onset of Ionizations.
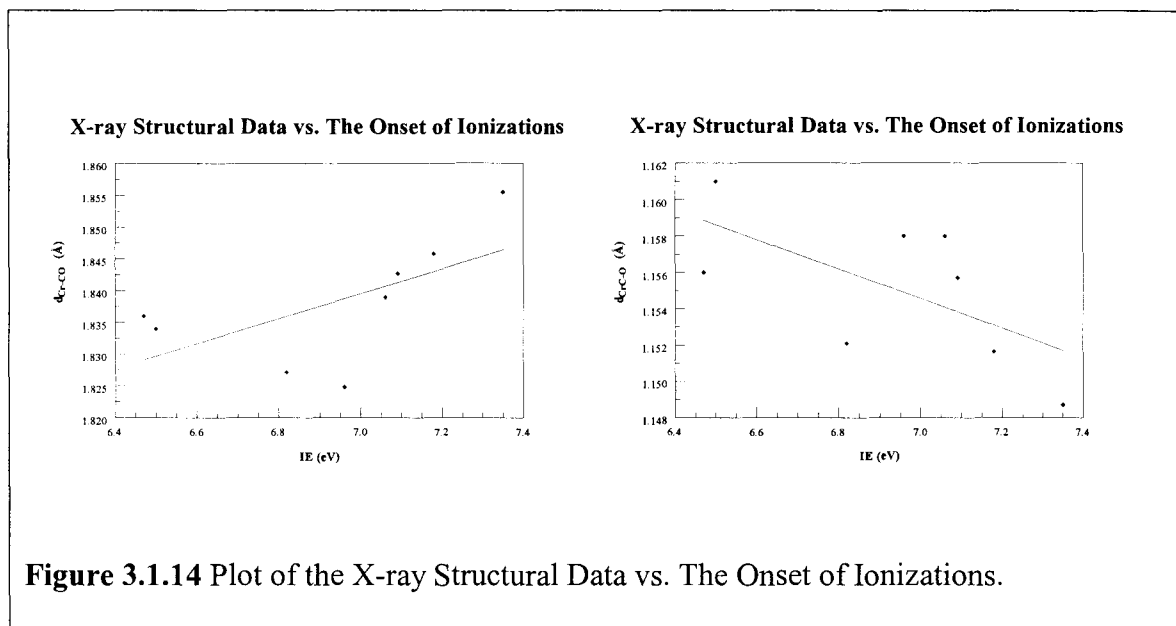
When the bond lengths from the calculated structures were plotted against the

onset of ionization a stronger correlation was observed. For the calculated bond lengths,

the correlation coefficients were 0.96 and 0.97 for the metal-carbonyl and carbon-oxygen

bond lengths, respectively. These are good enough to say there is a correlation between

the calculated bond lengths and the onset of ionization and reflects the fact that the

calculations were done for isolated gas phase molecules as opposed to the solid state data

discussed above.

Figure 3.1.15 Plots of the Calculated Structural Data vs. The Onset of Ionizations.
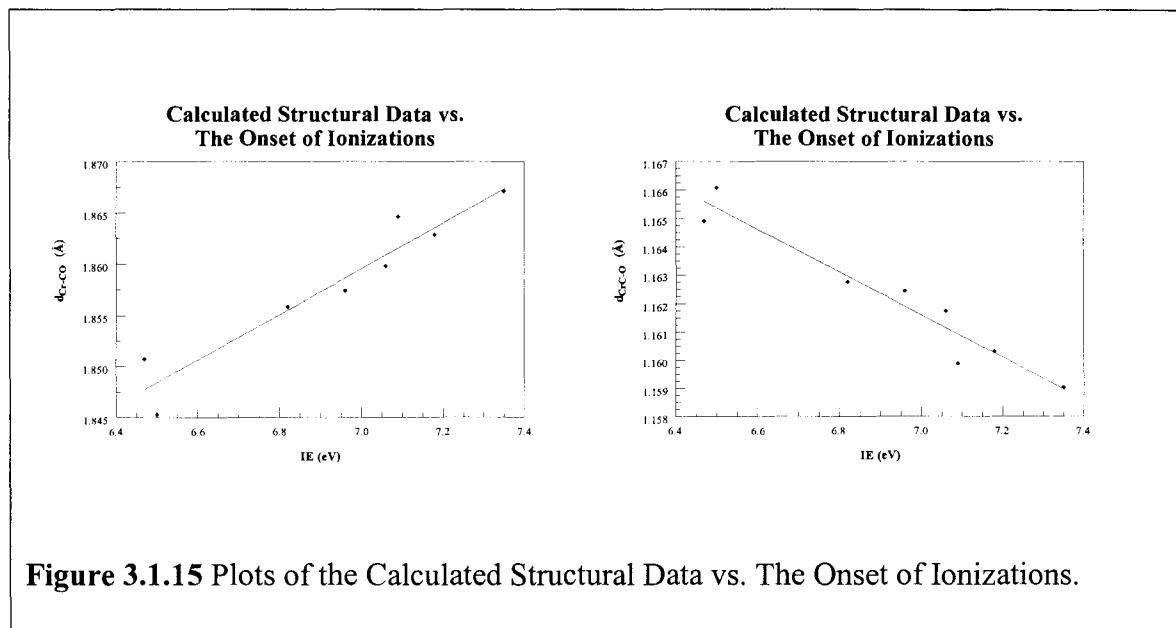
When we examine the plots for the two bond lengths against the onset of ionization, we observe that the slopes for the lines of the metal-carbonyl bond length and carbon-oxygen bond length are as expected. Thus, the metal-carbonyl bond length has a positive slope which implies that more electron density about the metal will result in a shorter metal-carbonyl bond. Similarly, carbon-oxygen plot has a negative slope which implies that more electron density about the metal will result in a longer carbon-oxygen bond.

References

1. (a) Hunter, A. D.; Mozol, V.; Tsai, S. D. *Organometallics* **1992**, *11*, 2251-2262.

    (b) Hunter, A. D.; Shilliday, L. *Organometallics* **1992**, *11*, 1550-1560. (c) Zeller,

    M.; Hunter, A. D.; Perrine, C. L.; Payton, J. *Acta Cryst.* **2004**, *E60*, m650-m651.

    (d) Zeller, M.; Hunter, A. D.; Perrine, C. L.; Payton, J. *Acta Cryst.* **2004**, *E60*,

    m668-m669. (e) Pfletschinger, A.; Dargel, T. K.; Bats, J. W.; Schmalz, H. G.;

    Koch, W. *Chem.-Eur. J.* **1999**, *5*, 537. (f) Le Magueres, P.; Lindeman, S. V.;

    Kochi, J. K. *Organometallics* **2001**, *20*, 115.

2. Muetterties, E. L.; Bleeke, J. R.; Wucherer, E. J.; Albright, T. *Chem. Rev.* **1982**,

    82, 499-525.

3. Guest, M. F.; Hillier, I. H.; Higginson, B. R.; Lloyd, D. R. *Mol. Phys.* **1975**, *29*,

    113-128.

4. Howell, J. O.; Goncalves, J. M.; Amatore, C.; Klasinc, L.; Wightman, R. M.;

    Kochi, J. K. *J. Am. Chem. Soc.* **1984**, *106*, 3968-3976.

5. Hall, M. B.; Fenske, R. F. *Inorganic Chemistry* **1972**, *11(4)*, 768-775.

6. Suresh, C. H.; Koga, N.; Gadre, S. R. *Orgonmetallics* **2000**, *19*, 3008-3015.

7. Cotton, F. A.; Gruhn, N. E.; Gu, J.; Huang, P.; Lichtenberger, D. L.; Murillo, C.

    A.; Van Dorn, L. O.; Wilkinson, C. C. *Science* **2002**, *298*, 1971.

8. (a)Katritzky, A. R.; Topeom, R. D. *Angew. Chem. Int. Ed. Engl.* **1970**, *9*, 87-100.

    (b) Exner, O. In *Advances in Linear Free Energy Relationships*; Chapman, N. B.,

   Shorter, J., Ed.; Plenum Press: New York, **1972**; pp 1-69.

9. (a) Chang, C. S. J.; Rai-Chaudhuri, A.; Lichtenberger, D. L.; Enemark, J. H. "He I Valence Photoelectron Spectra of Oxomolybdenum(V) Complexes Containing Diolato or Alkoxide Ligands." *Polyhedron* **1990**, *9*, 1965-1973. (b) Hu, Yong-Feng; Bancroft, G. Michael; Liu, Zhifeng; Tan, Kim H. "Comprehensive high resolution photoelectron spectra of metal carbonyls using synchrotron radiation" *Inorg. Chem.* **1995**, *34*, 3716-3723.

10. Graff, J. N.; McElhaney, A. E.; Basu, P.; Gruhn, N. E.; Chang, C.-S. J.; Enemark, J. H. "Electrochemistry and Photoelectron Spectroscopy of Oxomolybdenum(V) Complexes with Phenoxide Ligands: Effect of Para Substituents on Redox Potentials, Heterogeneous Electron Transfer Rates, and Ionization Energies " *Inorg. Chem.* **2002**, *41*, 2642-2647.

11. Tsai, S. D. *Long-Range Electron Transfer*; University of Alberta; **1995**; pp 1-144.

12. (a) Bodner, G. M.; Todd, L. J. *Inorg. Chem.* **1974**, *13*, 360-363. (b) Maciel, G. E.; Natterstad, J. J. *J. Chem. Phys.* **1965**, *42*, 2427-2435.

Chapter Four – Conclusion

Though out our studies of the $(\eta^6\text{-arene})Cr(CO)_3$ complexes, we have observed similar structure–property relationships to those previously reported. In general, our results were in agreement with these reports where the planarity of the substituted arenes in the complexes is strongly correlated to the π-donor/acceptor ability of the substituent(s). Also, the delta-symmetry HOMO component of the arene-chromium bond seems to be strengthened by π-acceptors and weakened by π-donors which is in agreement with the elementary valence bond arguments. We have also noted areas that warrant further study, for example, the conformation of the carbonyl ligands from our theoretical studies, the more systematic study of the bond lengths about the carbonyl ligands for the correlation, and the possible need for the collection of the He II photoelectron spectra.

Appendix A

MO Interaction Diagram of Benzenechromiumtricarbonyl
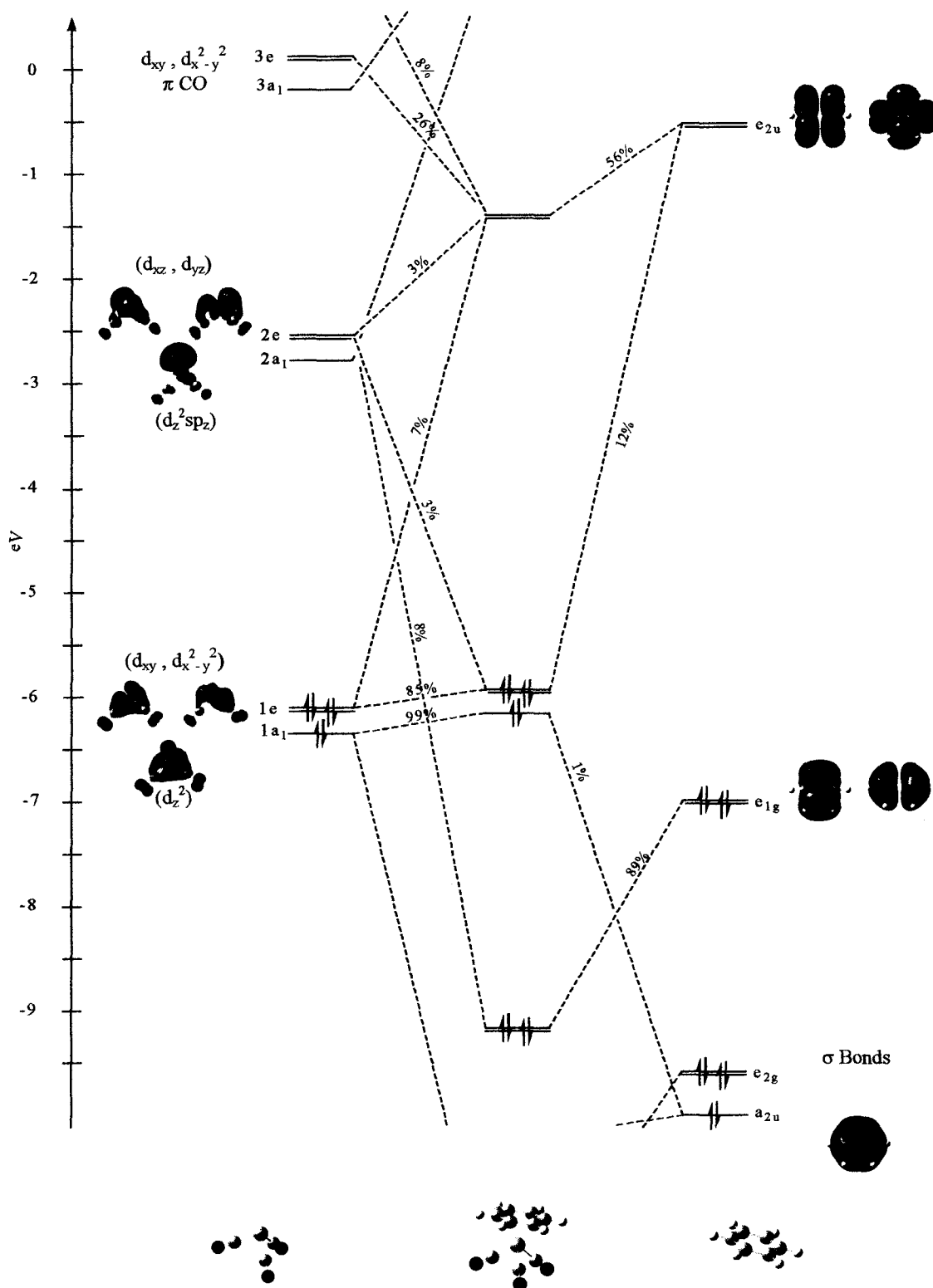
Molecule	PES			DFT (B3LYP)		Echem
	IE (eV) (On Set)	IE (eV) (Average of Metal e's)	IE (eV) (Metal a_1)	IE (eV)	HOMO Energies (eV)	$E^{o\prime}$ (V vs SCE)
$(C_6H_5CF_3)Cr(CO)_3$	7.35	7.61	7.87	7.771	6.277	1.085
$(C_6H_5F)Cr(CO)_3$	7.18	7.46	7.72	7.630	6.064	0.955
$(C_6H_5CO_2Me)Cr(CO)_3$	7.09	7.37	7.62	7.551	6.103	1.027
$(C_6H_6)Cr(CO)_3$	7.06	7.32	7.58	7.456	5.922	0.877
$(C_6H_5Me)Cr(CO)_3$	6.96	7.14	7.49	7.353	5.828	0.846
$(C_6H_5OMe)Cr(CO)_3$	6.82	7.11	7.39	7.301	5.745	0.783
$(C_6H_5NMe_2)Cr(CO)_3$	6.47	6.90	7.19	7.030	5.477	0.577
$(C_6Me_6)Cr(CO)_3$	6.50	6.78	6.99	6.940	5.461	0.668

Electrochemical Data vs. The Onset of Ionizations

Molecule	PES			IR Data				
	IE (eV) (On Set)	IE (eV) (Average of Metal e's)	IE (eV) (Metal a_1)	$\nu_{CO} A_1$ (cm^{-1})	$\nu_{CO} E$ (cm^{-1})	$\Delta\nu^{1/2d}$	$10^5 K^i_{CO}$ (dyn cm^{-1})	$10^5 K_{CO}$ (dyn cm^{-1})
$(C_6H_5CF_3)Cr(CO)_3$	7.35	7.61	7.87	1990	1918	2.2	0.38	15.24
$(C_6H_5F)Cr(CO)_3$	7.18	7.46	7.72	1982	1903	2.0	0.41	15.04
$(C_6H_5CO_2Me)Cr(CO)_3$	7.09	7.37	7.62	1985	1911	2.3	0.39	15.14
$(C_6H_6)Cr(CO)_3$	7.06	7.32	7.58	1974	1894	2.4	0.42	14.90
$(C_6H_5Me)Cr(CO)_3$	6.96	7.14	7.49	1969	1889	2.2	0.42	14.83
$(C_6H_5OMe)Cr(CO)_3$	6.82	7.11	7.39	1973	1891	2.5	0.43	14.87
$(C_6H_5NMe_2)Cr(CO)_3$	6.47	6.90	7.19	1956	1868	2.7	0.45	14.54
$(C_6Me_6)Cr(CO)_3$	6.50	6.78	6.99	1948	1864	2.4	0.43	14.46

Stretching Frequencies vs. The Onset of Ionizations
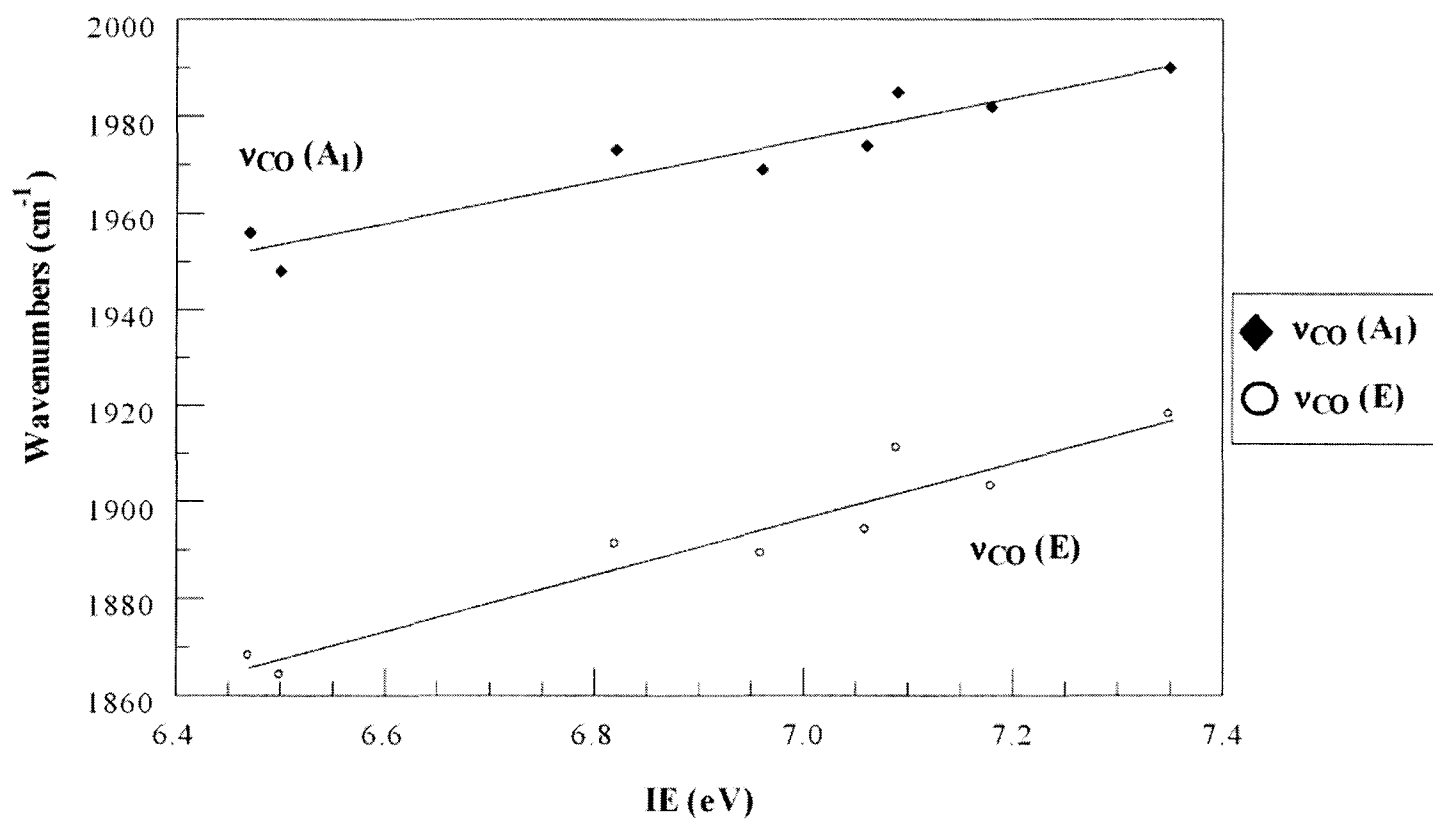
The Carbonyl E Vibrational Mode
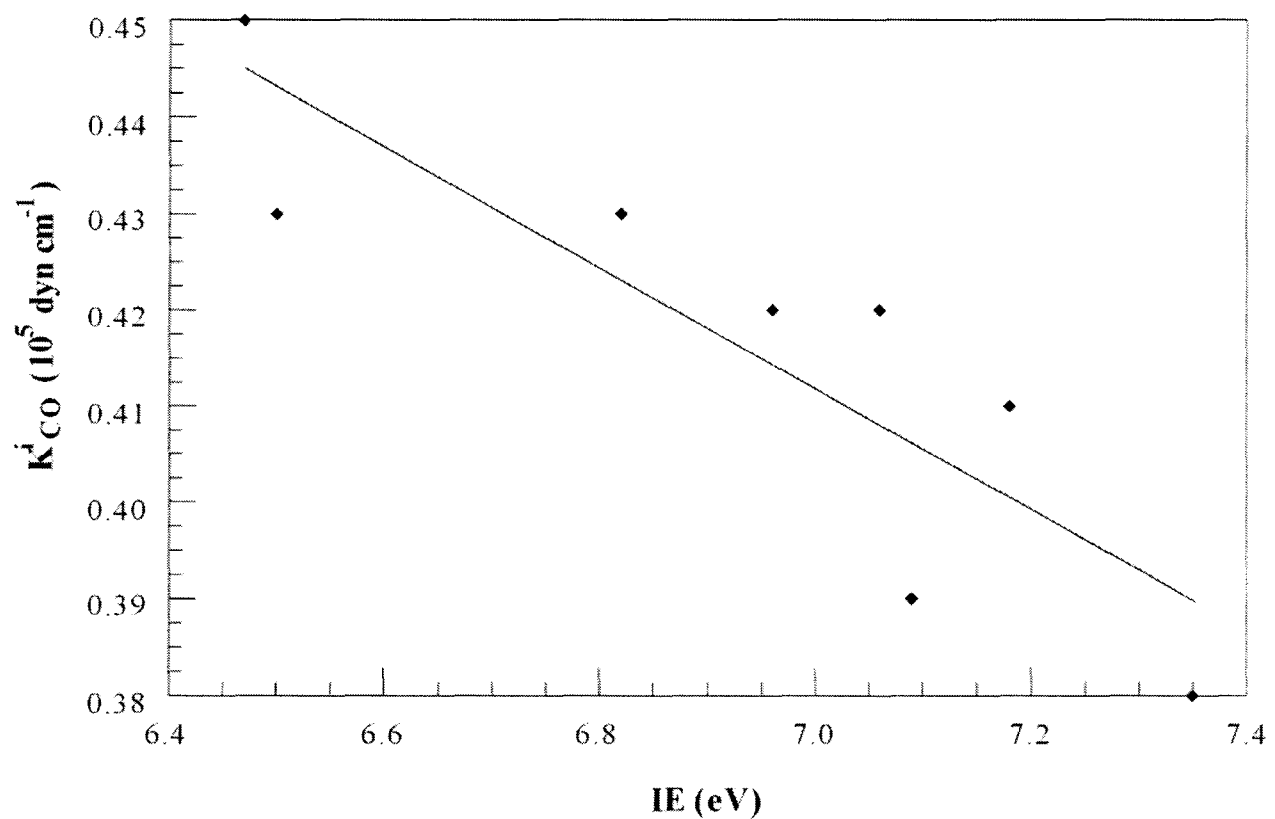# vs. The Metal e Ionizations
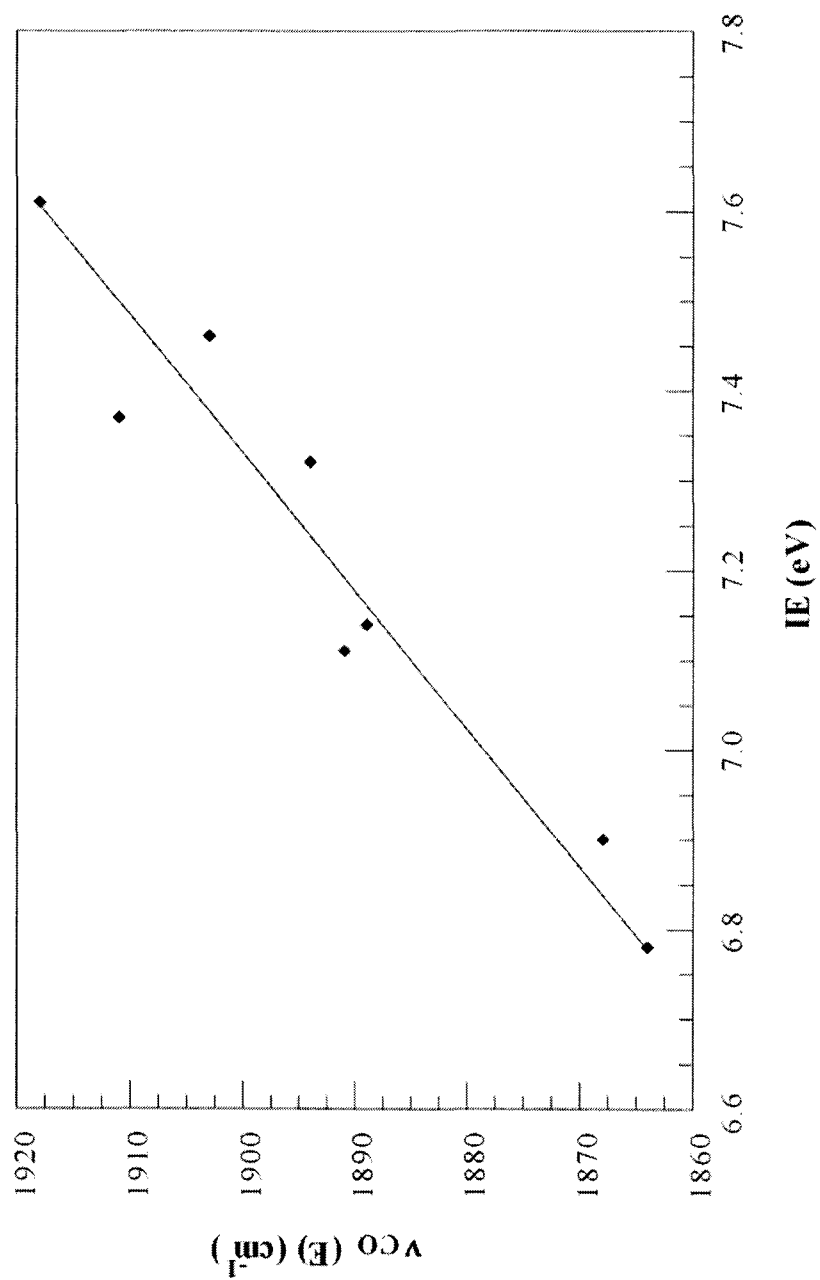
The Carbonyl A_1 Vibrational Mode
vs. The Metal a_1 Ionizations
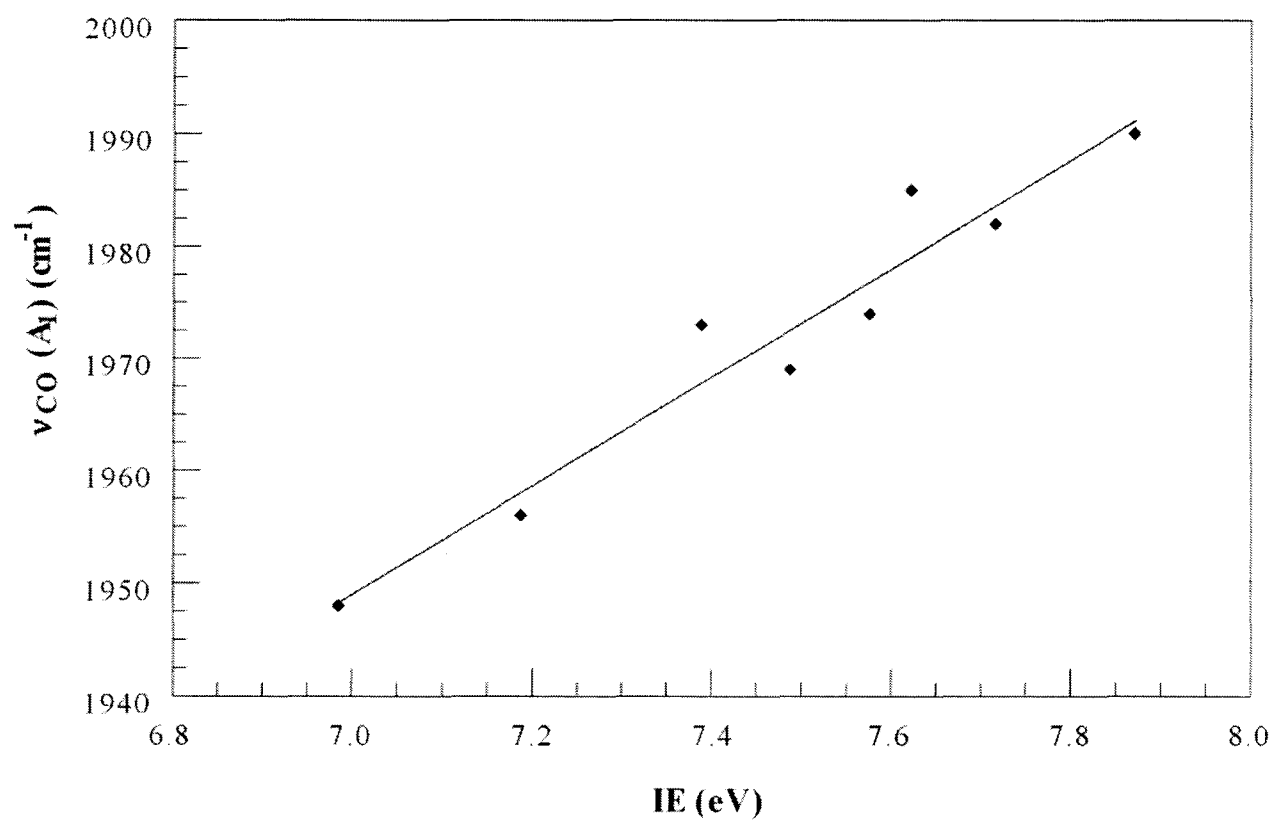
# Carbonyl Stretching Force Constant vs. The Onset of Ionizations
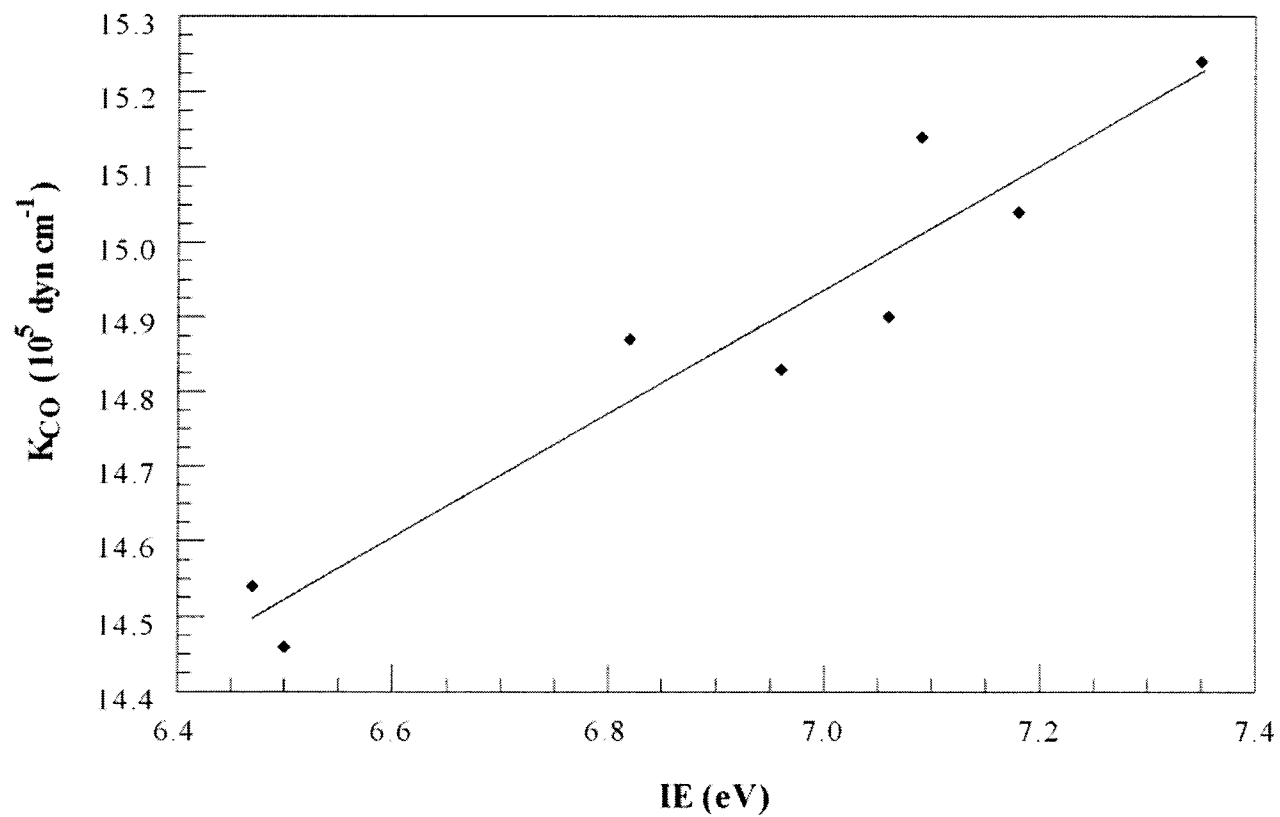
# Carbonyl Interaction Stretching Force Constant vs. The Onset of Ionizations

Molecule	PES		^{13}C NMR Data (ppm)					
	IE (eV) (On Set)	Total Metal Band Width (eV)	δ_{ipso} (C1)	δ_{ortho} (C2)	δ_{meta} (C3)	δ_{para} (C4)	δ_{CO}	$\Delta\pi$ (C4 - C3)
$(C_6H_5CF_3)Cr(CO)_3$	7.35	1.03	96.16	92.17	91.43	96.94	231.43	5.51
$(C_6H_5F)Cr(CO)_3$	7.18	1.08	146.82	81.65	96.09	89.42	232.98	-6.67
$(C_6H_5CO_2Me)Cr(CO)_3$	7.09	1.03	91.05	96.04	92.47	97.46	231.98	4.99
$(C_6H_6)Cr(CO)_3$	7.06	1.06	95.15	95.15	95.15	95.15	234.00	0.00
$(C_6H_5Me)Cr(CO)_3$	6.96	1.06	111.71	96.62	94.79	91.85	234.29	-2.94
$(C_6H_5OMe)Cr(CO)_3$	6.82	1.22	144.15	80.28	97.48	87.44	234.25	-10.04
$(C_6H_5NMe_2)Cr(CO)_3$	6.47	1.23	137.09	77.57	99.09	82.96	235.52	-16.13
$(C_6Me_6)Cr(CO)_3$	6.50	1.14	107.63	107.63	107.63	107.63	235.90	-

| Molecule	Arene Substituents					
	X1	X2	X3	X4	X5	X6
$(C_6H_5CF_3)Cr(CO)_3$	CF_3	H	H	H	H	H
$(C_6H_5F)Cr(CO)_3$	F	H	H	H	H	H
$(C_6H_5CO_2Me)Cr(CO)_3$	CO_2Me	H	H	H	H	H
$(C_6H_6)Cr(CO)_3$	H	H	H	H	H	H
$(C_6H_5Me)Cr(CO)_3$	Me	H	H	H	H	H
$(C_6H_5OMe)Cr(CO)_3$	OMe	H	H	H	H	H
$(C_6H_5NMe_2)Cr(CO)_3$	NMe_2	H	H	H	H	H
$(C_6Me_6)Cr(CO)_3$	Me	Me	Me	Me	Me	Me

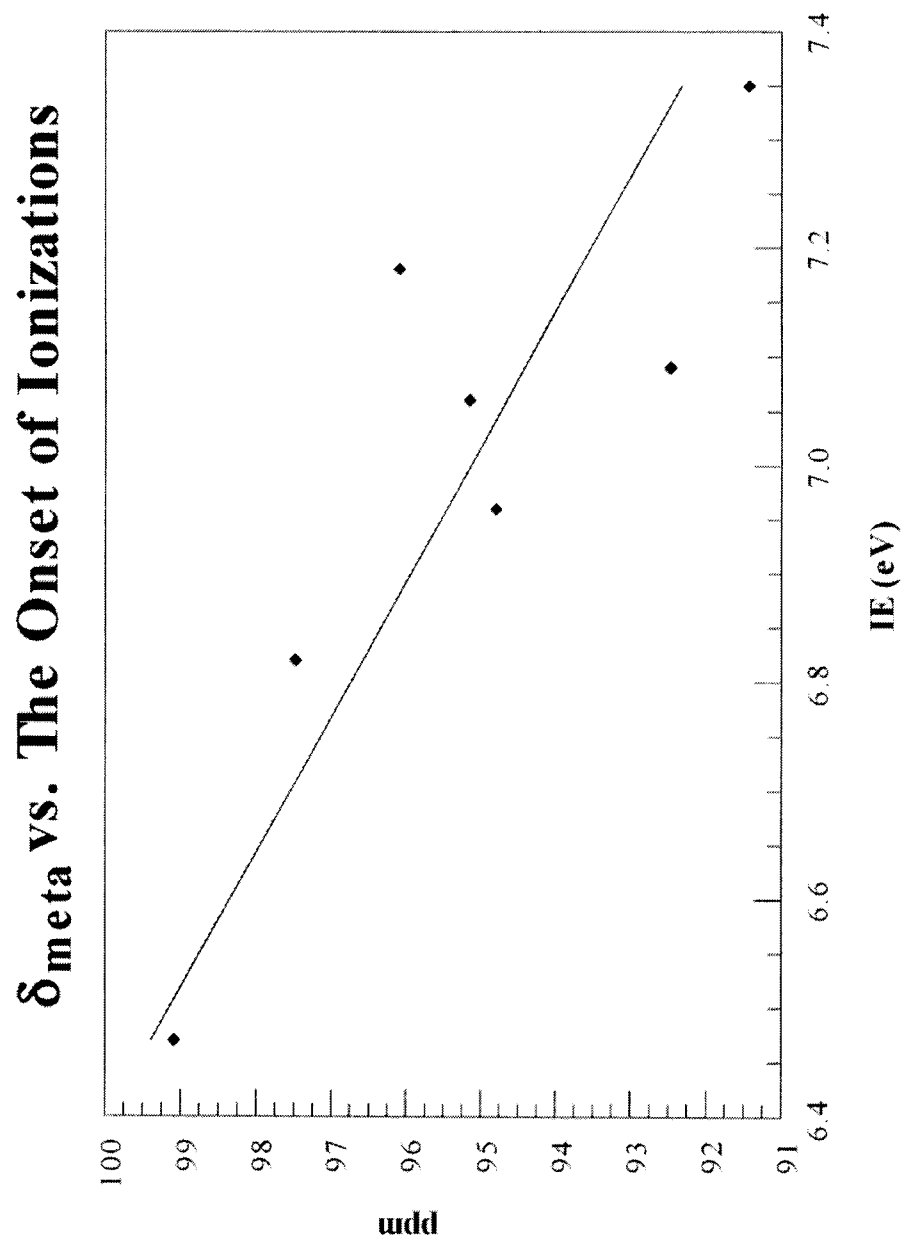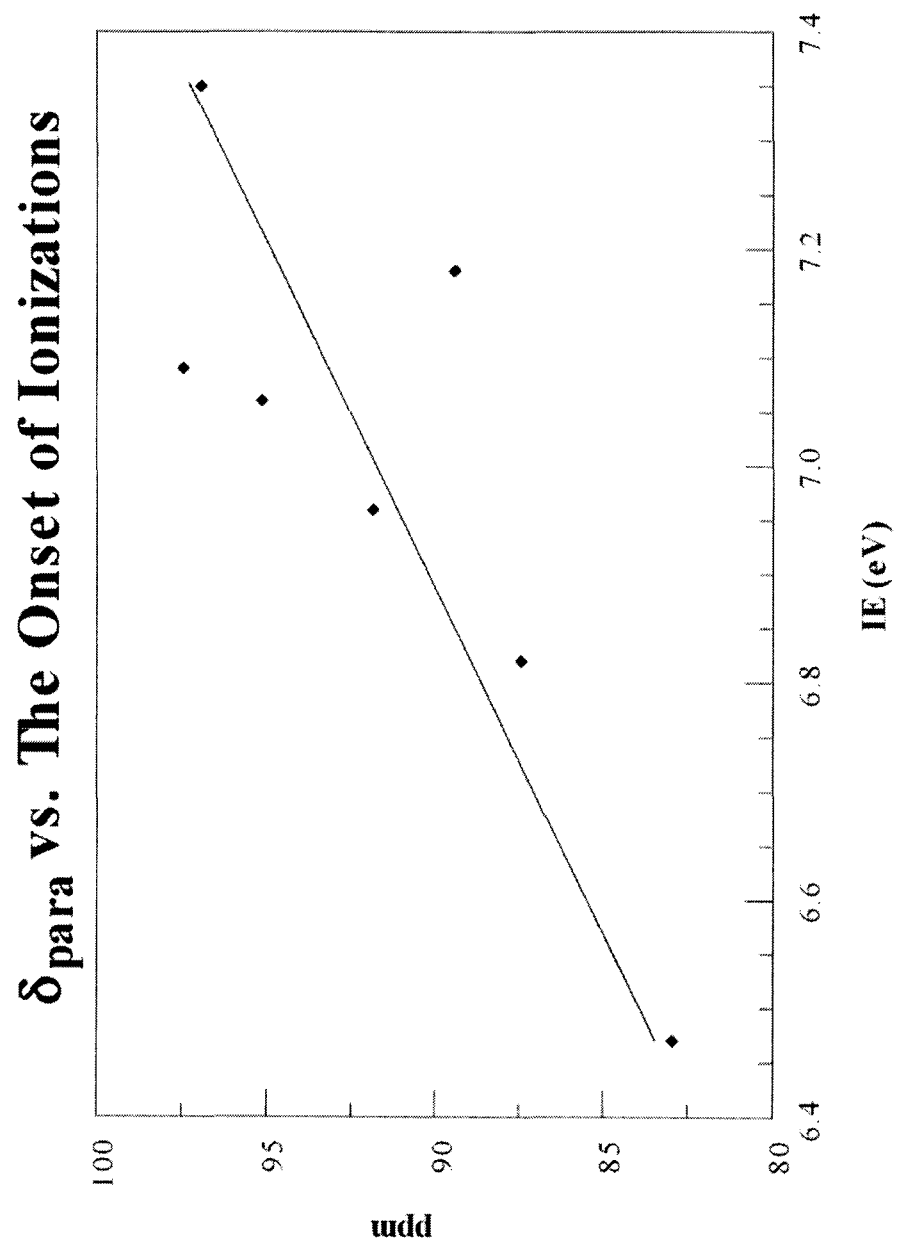$\delta_{carbonyl}$ vs. The Onset of Ionizations
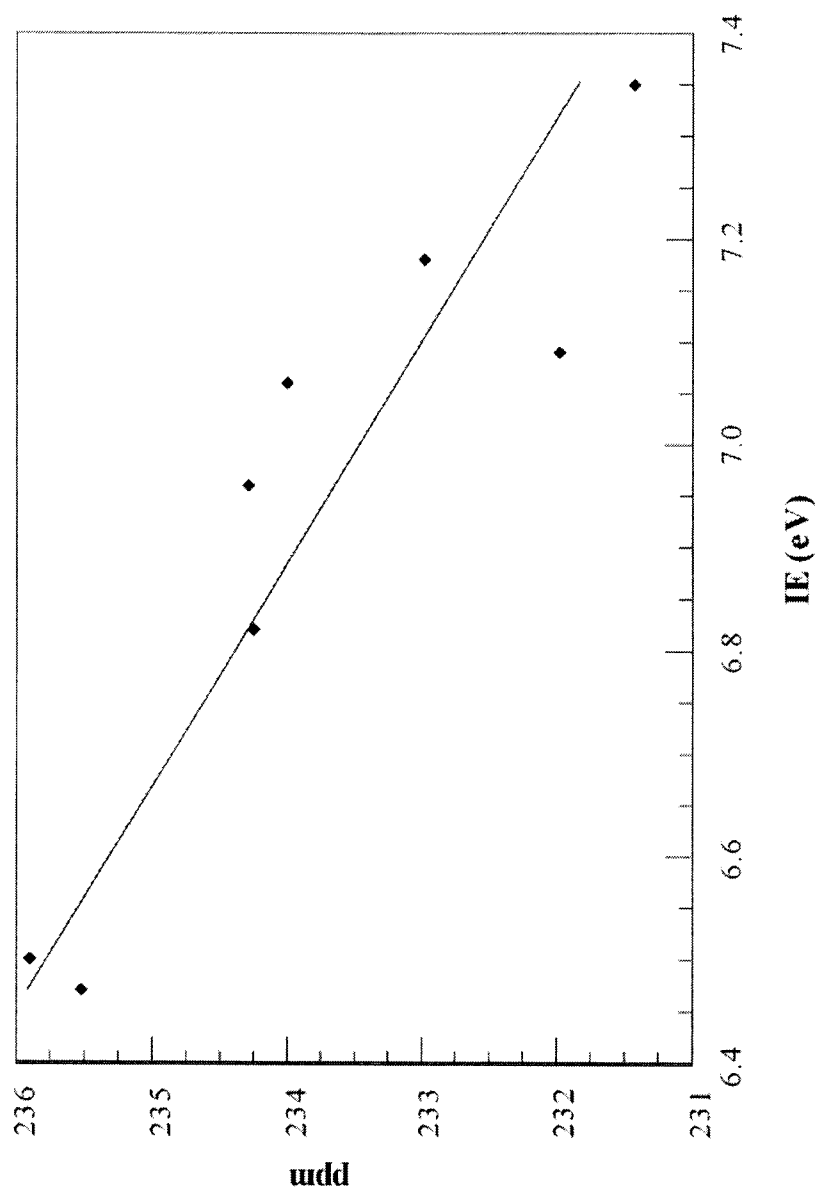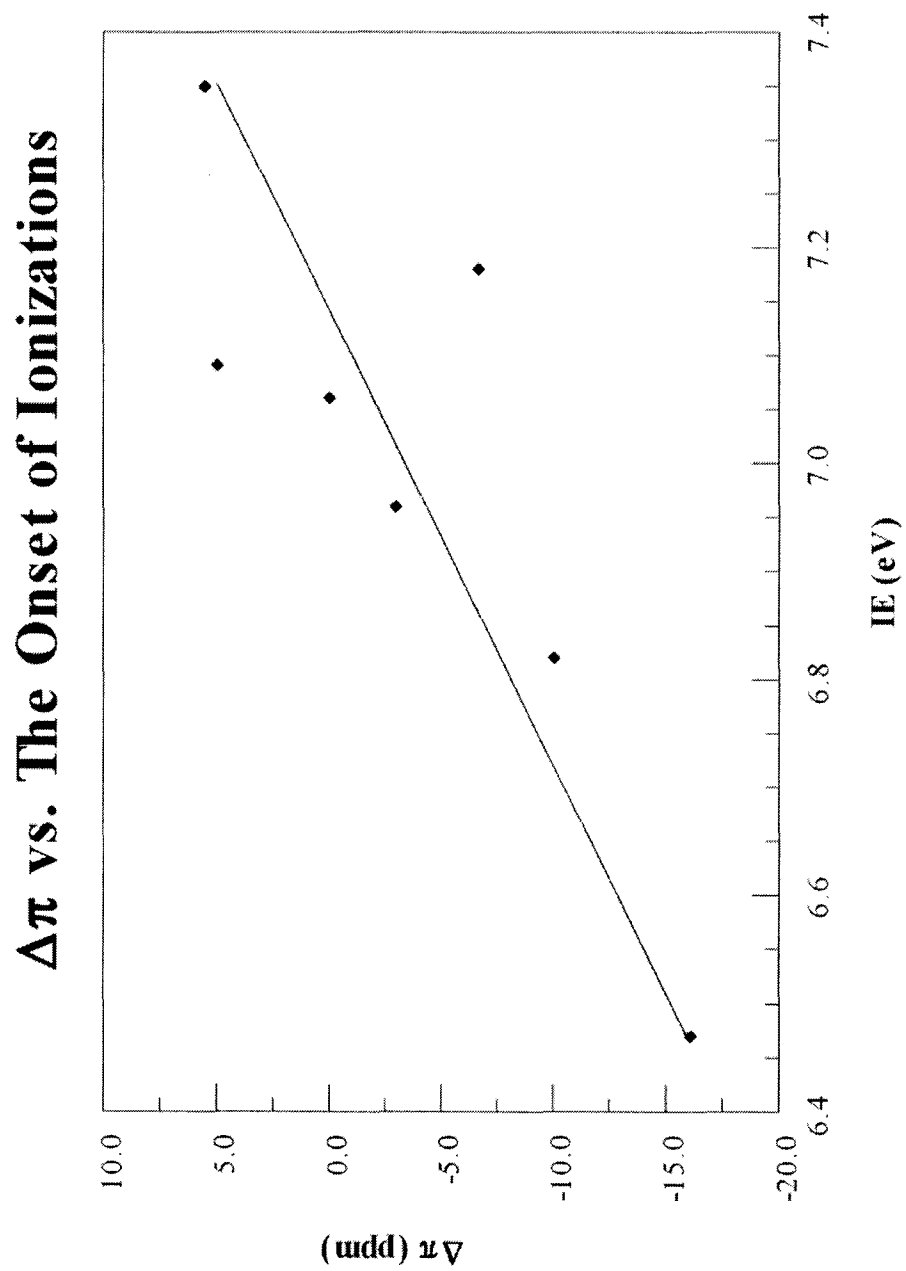
δ_{ipso} vs. The Onset of Ionizations
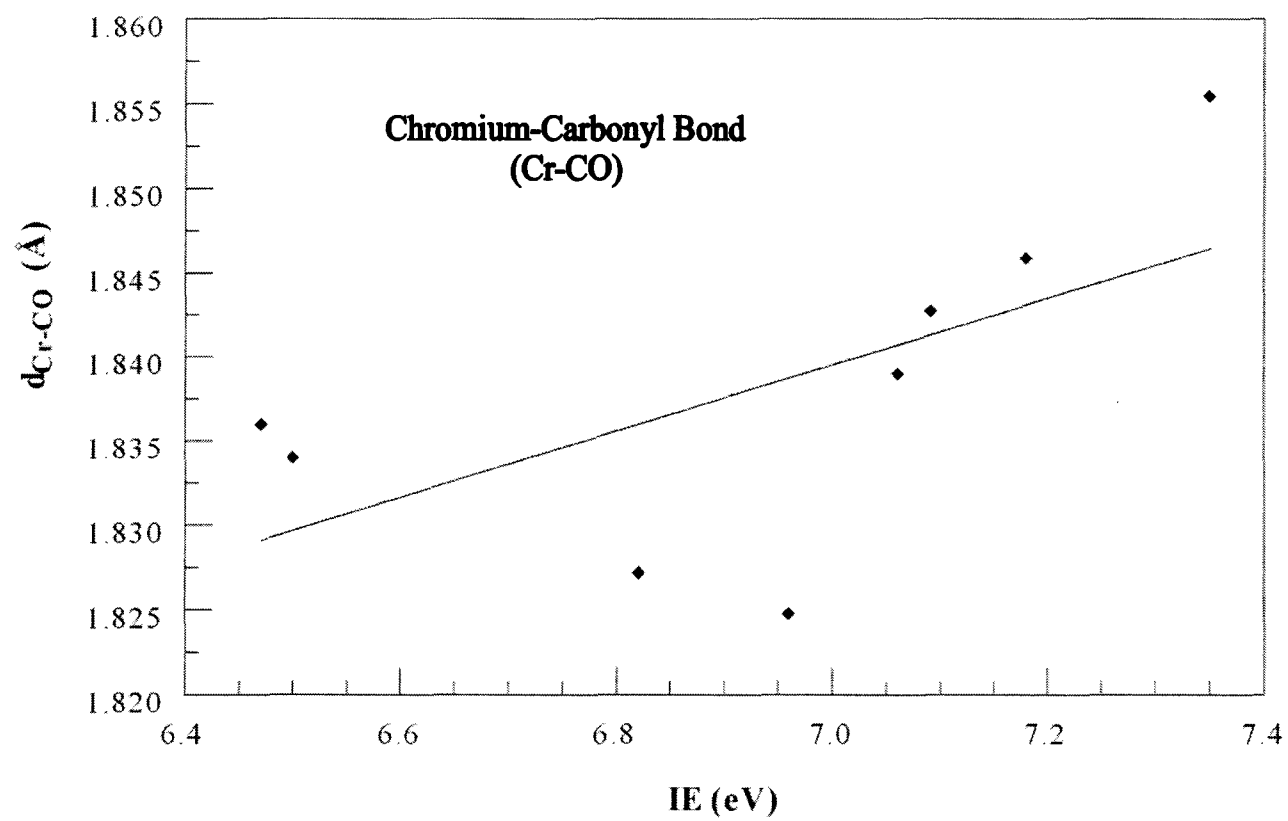
δ_{ortho} vs. The Onset of Ionizations

δ_{meta} vs. The Onset of Ionizations

δ_{para} vs. The Onset of Ionizations
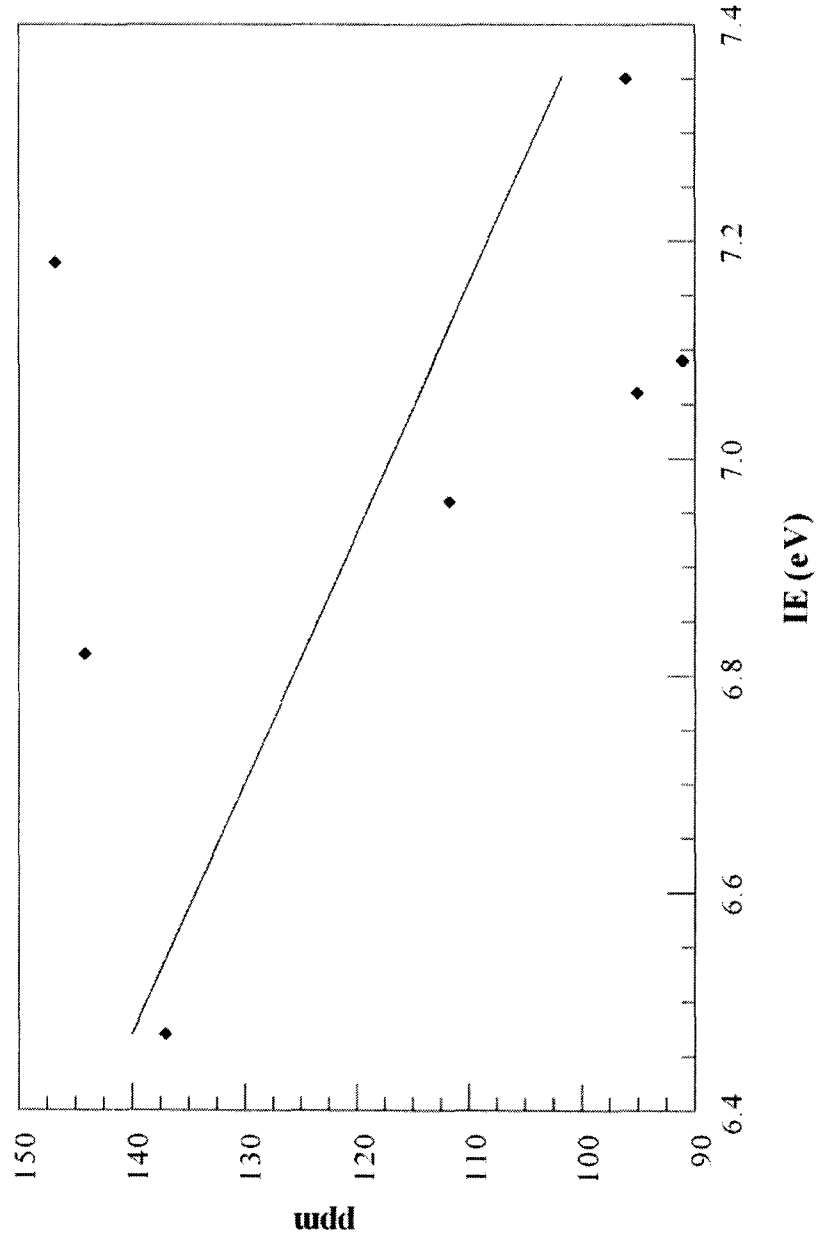
Δπ vs. The Onset of Ionizations
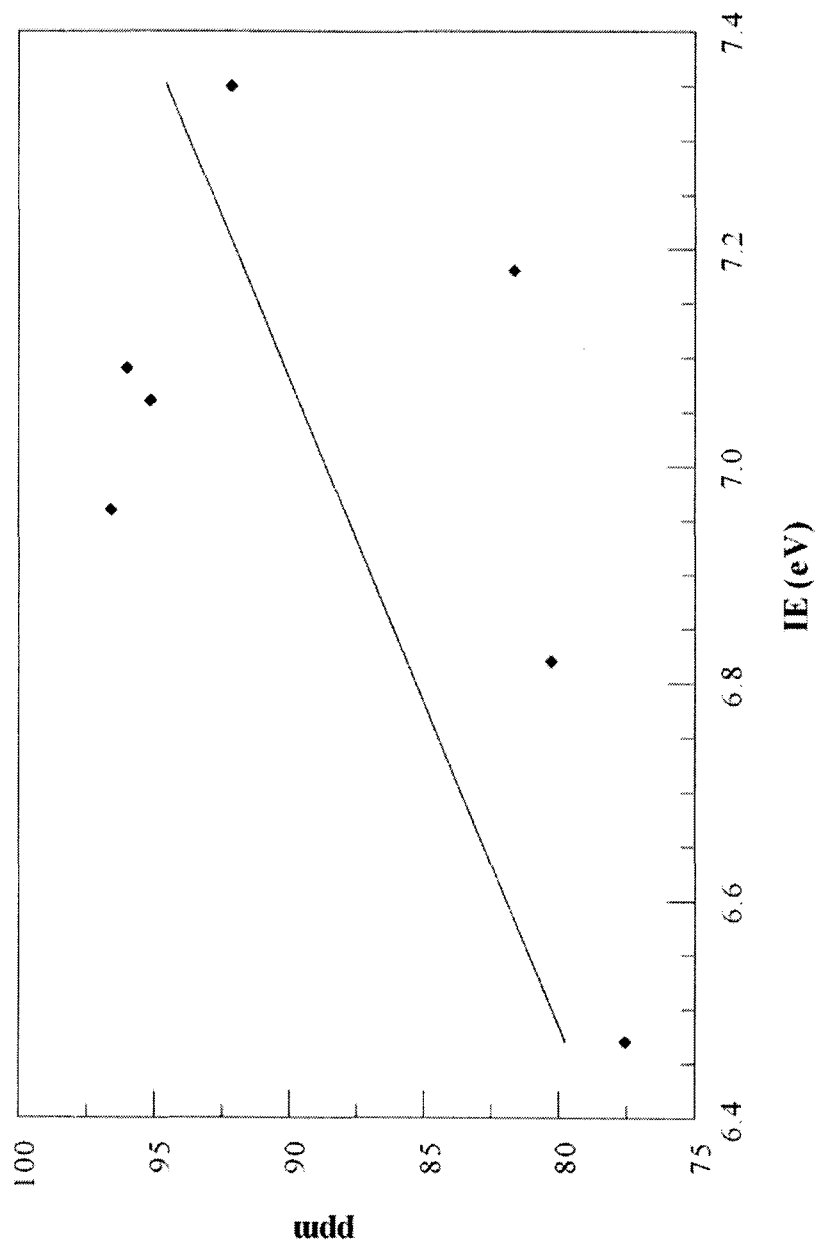
Molecule	PES	X-ray Structrual Data		DFT Structrual Data	
	IE (eV) (On Set)	d_{Cr-CO} (Å)	d_{CrC-O} (Å)	d_{Cr-CO} (Å)	d_{CrC-O} (Å)
$(C_6H_5CF_3)Cr(CO)_3$	7.35	1.855	1.149	1.867	1.159
$(C_6H_5F)Cr(CO)_3$	7.18	1.846	1.152	1.863	1.160
$(C_6H_5CO_2Me)Cr(CO)_3$	7.09	1.843	1.156	1.865	1.160
$(C_6H_6)Cr(CO)_3$	7.06	1.839	1.158	1.860	1.162
$(C_6H_5Me)Cr(CO)_3$	6.96	1.825	1.158	1.857	1.162
$(C_6H_5OMe)Cr(CO)_3$	6.82	1.827	1.152	1.856	1.163
$(C_6H_5NMe_2)Cr(CO)_3$	6.47	1.836	1.156	1.851	1.165
$(C_6Me_6)Cr(CO)_3$	6.50	1.834	1.161	1.845	1.166

X-ray Structural Data vs. The Onset of Ionizations

Chromium-Carbonyl Bond
(Cr-CO)
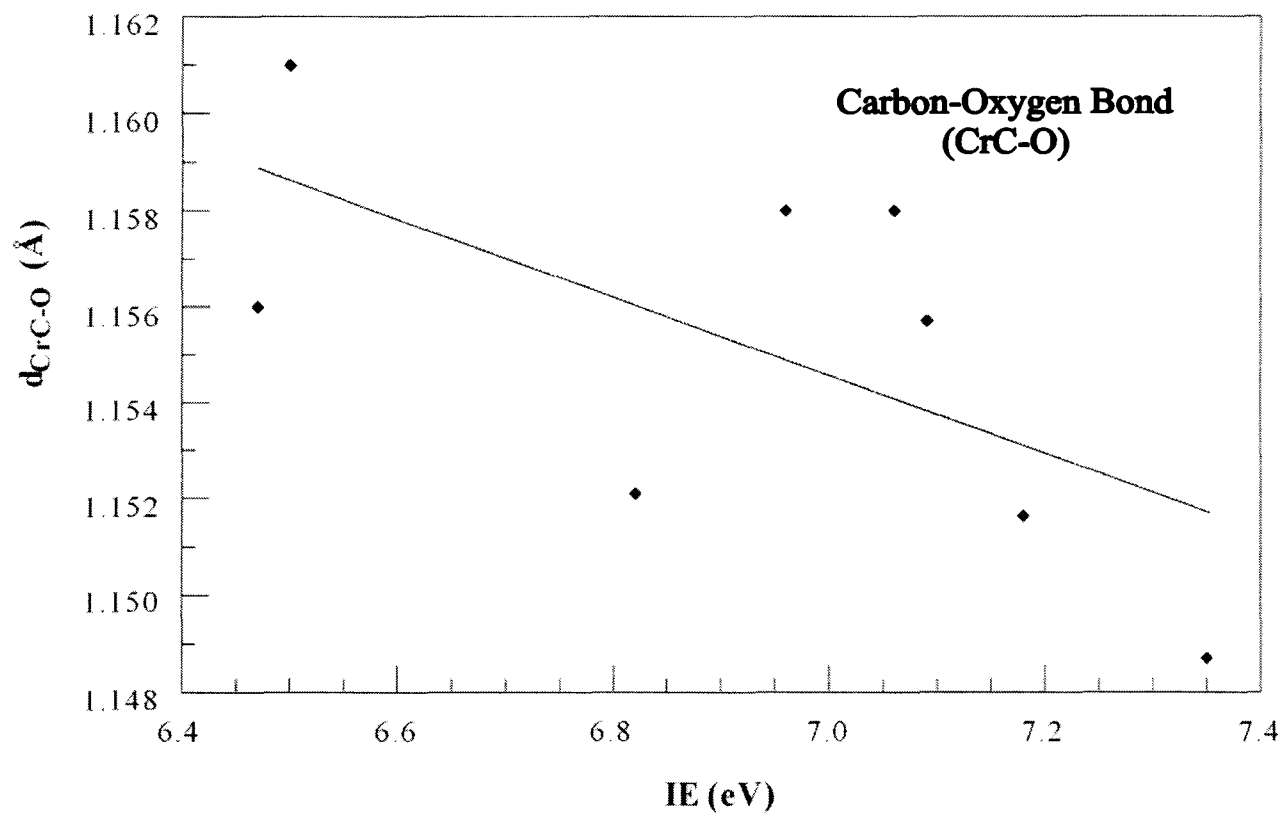
X-ray Structural Data vs. The Onset of Ionizations

Calculated Structural Data vs.
The Onset of Ionizations

Chromium-Carbonyl Bond
(Cr-CO)

d_{Cr-CO} (Å)

IE (eV)

Calculated Structural Data vs.
The Onset of Ionizations